DOE/PC/89652--T13

INNOVATIVE CLEAN COAL TECHNOLOGY (ICCT)

DEMONSTRATION OF SELECTIVE CATALYTIC REDUCTION (SCR) TECHNOLOGY FOR THE CONTROL OF NITROGEN OXIDE (NOx) EMISSIONS FROM HIGH-SULFUR COAL-FIRED BOILERS

Technical Progress Report
Second & Third Quarters, 1993

DOE Contract
DE-FC22-90PC89652

SCS Contract
C-91-000026

Prepared by:

Southern Company Services, Inc.
800 Shades Creek Parkway
Birmingham, Alabama 35209

Cleared by DOE Patent Council on May 31, 1994

DISCLAIMER

Portions of this document may be illegible in electronic image products. Images are produced from the best available original document.

LEGAL NOTICE

This report was prepared by Southern Company Services, Inc. pursuant to a cooperative agreement partially funded by the U. S. Department of Energy and neither Southern Company Services, Inc. nor any of its subcontractors nor the U. S. Department of Energy, nor any person acting on behalf of either:

(a) Makes any warranty or representation, express or implied with respect to the accuracy, completeness, or usefulness of the information contained in this report, or that the use of any information, apparatus, method, or process disclosed in this report may not infringe privately-owned rights; or

(b) Assumes any liabilities with respect to the use of, or for damages resulting from the use of, any information, apparatus, method or process disclosed in this report.

Reference herein to any specific commercial product, process, or service by trade name, trademark, manufacturer, or otherwise, does not necessarily constitute or imply its endorsement, recommendation, or favoring by the U. S. Department of Energy. The views and opinion of authors expressed herein do not necessarily state or reflect those of the U. S. Department of Energy.

Section 1

SUMMARY

The objective of this project is to demonstrate and evaluate commercially available Selective Catalytic Reduction (SCR) catalysts from U. S., Japanese and European catalyst suppliers on a high-sulfur U. S. coal-fired boiler. SCR is a post-combustion nitrogen oxide (NOx) control technology that involves injecting ammonia into the flue gas generated from coal combustion in an electric utility boiler. The flue gas containing ammonia is then passed through a reactor that contains a specialized catalyst. In the presence of the catalyst, the ammonia reacts with NOx to convert it to nitrogen and water vapor.

Although SCR is widely practiced in Japan and Europe on gas-, oil-, and low-sulfur coal-fired boilers, there are several technical uncertainties associated with applying SCR to U. S. coals. These uncertainties include:

(1) potential catalyst deactivation due to poisoning by trace metal species present in U. S. coals that are not present in other fuels.

(2) performance of the technology and effects on the balance-of-plant equipment in the presence of high amounts of SO_2 and SO_3.

(3) performance of a wide variety of SCR catalyst compositions, geometries and methods of manufacture under typical high-sulfur coal-fired utility operating conditions.

These uncertainties are being explored by constructing and operating a series of small-scale SCR reactors and simultaneously exposing different SCR catalysts to flue gas derived from the combustion of high sulfur U. S. coal.

The demonstration is being performed at Gulf Power Company's Plant Crist Unit No. 5 (75 MW capacity) near Pensacola, Florida. The project is funded by the U. S. Department of Energy (DOE), Southern Company Services, Inc. (SCS on behalf of the entire Southern electric system), the Electric Power Research Institute (EPRI), and Ontario Hydro. SCS is the participant responsible for managing all aspects of this project.

The project is being conducted in the following three phases:

Phase I - Permitting, Environmental Monitoring Plan and Preliminary Engineering
Phase II - Detailed Design Engineering and Construction
Phase III - Operation, Testing, Disposition and Final Report

The start-up and shakedown of equipment continued and was completed during the second quarter of 1993, as was commissioning testing without catalysts. The SCR demonstration facility was taken off line the for over two weeks in April as a result of a boiler outage and so needed modifications were made to the SCR facility during this outage. Modifications included installation of a damper on the gas-side ductwork returning flue gas from the facility to the host plant duct. Sootblowing capability was added at the electric heaters and for the bypass gas heat exchangers. Changes were made to the main inlet scoop ductwork and small reactor take-off to resolve a maldistribution problem of particulate between the small and large reactors. These changes included reducing the slot size of the small reactor, adding a mixing device and flow straightening grid prior to the split between the small and large reactors. Some instrumentation was also relocated or replaced.

The major issues experienced during start-up included sulfate and ash deposition. While the ammonia injection system was being completed, the installed injectors presented a low flow area that sulfates diffused into and precipitated out, plugging almost every injection system. The nozzles and injection header were cleaned and some portions of the feed piping had to be replaced. The air fan for ammonia dilution was since placed in service and will be used to supply a continuous air flow to act as a purge to prevent recurrence of the plugging. The bypass heat exchangers were easily plugged by ash and sulfate deposits. Work to develop another means to cool the flue gas while bypassing the air preheaters remained underway at the end of this reporting period.

The commissioning tests without catalyst were completed by the middle of June 1993 and the loading of the catalysts into the reactors began on June 14 and was finished on June 22, 1993. Long-term testing and parametric evaluations were commenced afterwards. Immediately after catalyst loading, all reactors were operated with ammonia briefly to obtain fly ash samples for the Toxicity Characteristics Leaching Procedure (TCLP) analysis. The TCLP results indicated no detectable amounts or change in constituents between baseline ash samples and ash samples from the SCR process outlet.

During July - September, 1993, Reactors A - C were the primary reactors operated with ammonia and the first set of parametric tests were completed for these reactors. The parametric tests for

reactors D - F were just underway at the completion of the third quarter. The total number of operating hours with exposure to flue gas ranged from 4 hours for reactor J to 2033 hours for reactor B.

There were several issues experienced with the continuous gas analysis system including accuracy of NOx outlet data with ammonia injection, coordinating the shared analyzers, and communicating with the test facility data collection system. All these problems with the gas sampling/analysis system were addressed or were in the process of being addressed at the end of the third quarter.

Precision mass flow control valves supplied by Sierra Instrumentation were installed to control the ammonia vapor flow rates for injection into the reactors. These controllers were affected by liquid in the flow stream, pressure variations, trash in the line, and also the orientation of the controller itself. Although initial results indicated accurate flow control, subsequent measurements indicated that actual ammonia flow was 10 to 25 percent higher than the controllers were indicating. Action to correct this situation included installing coalescent filters, reorienting the controllers, replacing the header pressure regulator, cleaning each controller, and recalibrating and verifying with other instruments.

After only a few hours of operation during its first start-up after catalyst loading, the low-dust reactor experienced severe plugging of the first catalyst layer. During start-up an unusually large amount of solid material may have been introduced to the low-dust reactor. The first layer catalyst element was returned to the catalyst vendor for examination and a study undertaken to evaluate solutions to prevent recurrence of this problem. The resulting design changes to prevent recurrence of the plugging problem on the low dust reactor included the following: the reactor isolation and purge dampers should be relocated to minimize the deadleg; and the reactor heater capacity should be uprated and the heater moved to just downstream of the isolation damper so the piping could be slowly warmed while drawing flue gas. These changes were to be installed in the field during the fourth quarter of 1993.

In commissioning, baseline concentrations of flue gas constituents were measured for Unit 5 hot-side ESP inlet and outlet ducts for high and low loads. In addition, the continuous gas analysis system was used to verify baseline flue gas constituents (NOx, O_2, CO_2, CO, SO_2). One major goal was to demonstrate that each of the high-dust reactors was receiving fly ash with similar concentration and particle size as that of fly ash at the inlet to the ESP. As referred to earlier, initial measurements of mass concentration indicated a large disparity among the eight reactors.

After modifications to the inlet transition were completed, repeat measurements indicated much improved results. Particle size distributions for the reactor inlets agreed well with the size distributions taken at the main inlet. Data have also been collected for fly ash and coal chemistry, ammonia/NOx ratios, flue gas temperatures, air heater performance data, and catalyst specific performance parameters (reactor pressure drop, NOx reduction, ammonia slip, and SO_2 oxidation). (Please see Task 1.3.2 - Process Evaluation under PROJECT STATUS).

Papers describing the status of the project and design issues were presented at (1) the 86th Annual Meeting of the Air and Waste Management Association in Denver in June 1993, and (2) the Second Annual Clean Coal Technology Conference sponsored by DOE during September 7-9 in Atlanta, Georgia.

Section 2
INTRODUCTION

The Innovative Clean Coal Technology (ICCT) Program is designed to demonstrate clean coal technologies that are capable of retrofitting or repowering existing facilities to achieve significant reduction in sulfur dioxide (SO_2) and/or nitrogen oxides (NOx) emissions. The technologies selected for demonstration are capable of being commercialized in the 1990s and are expected to be more cost effective than current technologies.

This ICCT project is jointly funded by the U. S. Department of Energy, the Electric Power Research Institute (EPRI), Ontario Hydro, and by Southern Company Services (SCS) on behalf of the entire Southern electric system. The project's objective is to demonstrate the selective catalytic reduction (SCR) process that removes nitrogen oxides (NOx) from the flue gas of boilers that burn U.S. high-sulfur coal. The SCR technology involves the injection of NH_3 into the flue gas and the subsequent catalytic reduction of NOx by NH_3 to produce molecular nitrogen (N_2) and water vapor.

A simplified SCR process flow diagram with major equipment is shown in Figure 1. Specifically, hot flue gas leaving the economizer section of the boiler is ducted to the SCR reactor. Prior to entering the reactor, NH_3 is injected into the flue gas at a sufficient distance upstream of the reactor to provide for complete mixing of the NH_3 and flue gas. The quantity of NH_3 can be adjusted and it reacts with the NO_X from the flue gas. The flue gas leaving the catalytic reactor enters the air preheater where it transfers heat to the incoming combustion air. Provisions are made for ash removal from the bottom of the reactor since some fallout of fly ash is expected. Duct work is also provided to bypass some flue gas around the economizer during periods when the boiler is operating at reduced load. This is done to maintain the temperature of the flue gas entering the catalytic reactor at the proper reaction temperature of about 700°F. The flue gas leaving the air preheater goes to the electrostatic precipitator (ESP) where fly ash is removed. The ESP is part of the existing plant and is generally unaffected by the SCR system except as higher SO_3 content affects the electrical resistivity of the fly ash or if NH_4HSO_4 co-precipitates with the fly ash.

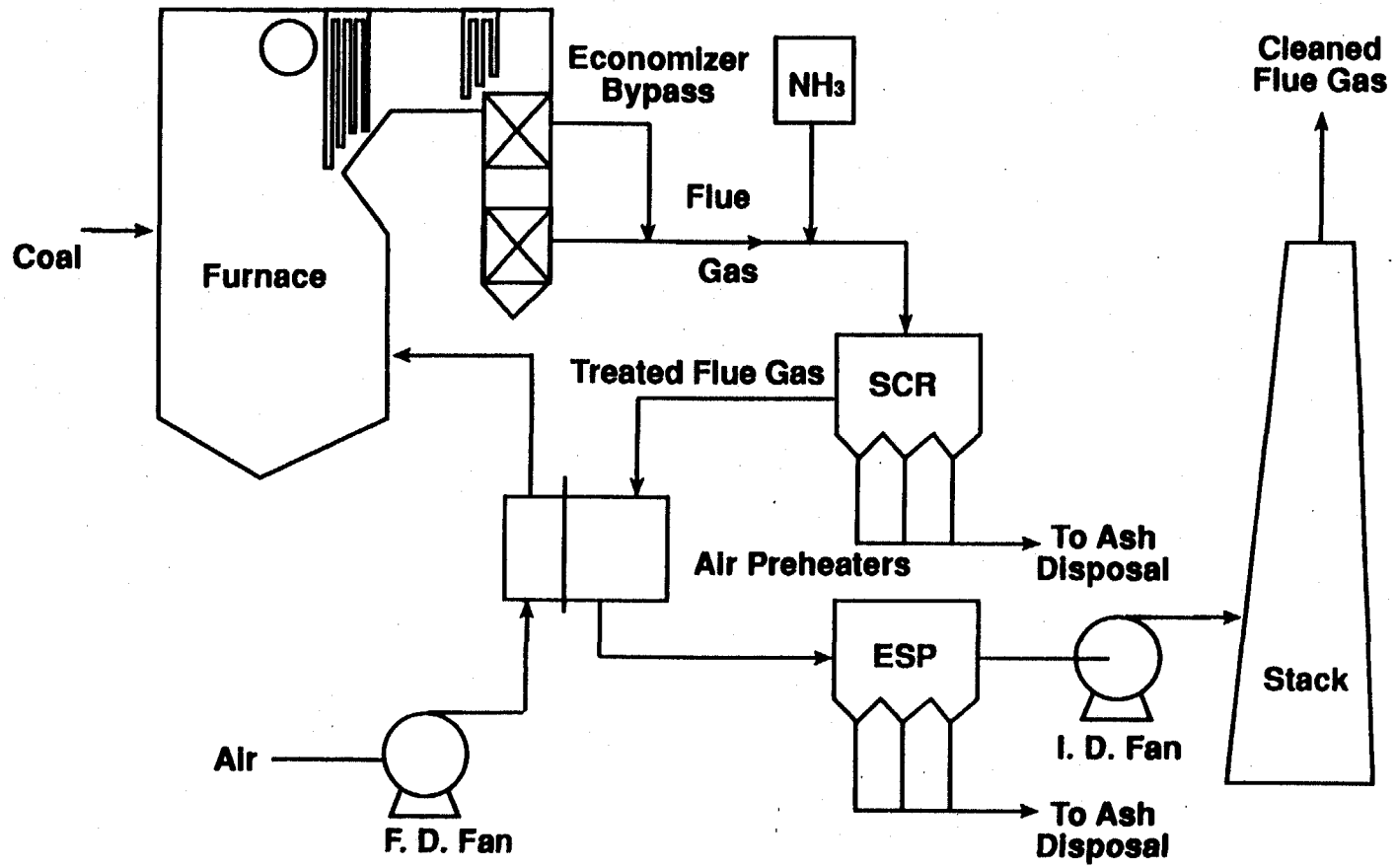

Figure 1. Flow Diagram Of Typical SCR Installation

The SCR technology is in commercial use in Japan and western Europe on gas-, oil-, and on low-sulfur, coal-fired power plants. The first utility applications of SCR catalyst technology started in Japan in 1977 for oil- and gas-fired boilers and subsequently in 1979 for coal-fired boilers. As of 1986, ninety utility boilers in Japan had been equipped with SCR catalyst technology including twenty-two coal-fired boilers. These coal-fired boilers represent a combined capacity in excess of 6500 MWe and are typically fired with a low-ash, low-sulfur coal.

In addition to Japanese experience, several countries in western Europe (most notably Germany and Austria) have passed stringent NO_X emission regulations that have all but mandated the installation of SCR. Prior to commercial SCR installations in Germany, utility companies demonstrated several types of SCR facilities in prototype demonstration programs similar to this ICCT project. Over 50 SCR pilot plants were built and operated in western Europe. These pilot plants ranged from 19 to 6200 SCFM and provided the data base that led to commercialization of the SCR technology in western Europe.

Previously completed U. S. work with the SCR process on utility boilers consists of three projects which were carried out in the late 1970s and early 1980s. One of these was carried out on a natural gas fired boiler by Southern California Edison. Another project consisted of a pilot test conducted for the EPA at Georgia Power's Plant Mitchell. This pilot plant treated a 1000 ACFM (0.5 MWe) slip stream of flue gas resulting from the combustion of low- to medium-sulfur coal. A third pilot-scale project, carried out at the Public Service Company of Colorado's Arapaho Station treated a 5000 ACFM (2.5 MWe) slip stream of flue gas resulting from the combustion of U. S. low-sulfur coal.

Although SCR is widely practiced in Japan and Europe, there are numerous technical uncertainties associated with applying SCR to U. S. coals. These uncertainties include:

(1) potential catalyst deactivation due to poisoning by trace metal species present in U. S. coals that are not present in other fuels.

(2) performance of the technology and effects on the balance-of-plant equipment in the presence of high amounts of SO_2 and SO_3.

(3) performance of a wide variety of SCR catalyst compositions, geometries and methods of manufacture under typical high-sulfur coal-fired utility operating conditions.

These uncertainties will be explored by constructing a series of small-scale SCR reactors and simultaneously exposing different SCR catalysts to flue gas derived from the combustion of high sulfur U. S. coal.

The first uncertainty above will be handled by evaluating SCR catalyst performance for two years under realistic operating conditions found in U. S. pulverized coal utility boilers. The deactivation rates for the catalysts exposed to flue gas from high sulfur U. S. coal will be documented to determine accurate catalyst life, and thus, accurate process economics.

The second uncertainty above will be explored by performing parametric testing and through the installation/operation of air preheaters downstream of the larger reactors. During parametric testing, operating conditions will be adjusted above and below design values to observe deNOx performance and ammonia slip as functions of the change in operating conditions. Air preheater performance will be observed to evaluate effects from SCR operation upon heat transfer, and therefore, upon boiler efficiency.

The third uncertainty is being handled by using honeycomb- and plate-type SCR catalysts from U. S., Japan and Europe of various commercial composition. Results from the tests with these catalysts will expand our knowledge of performance on a variety of SCR catalysts under U. S. utility operating conditions with high-sulfur coal.

The intent of this project is to demonstrate commercial catalyst performance, proper operating conditions, and catalyst life for the SCR process. This project will also demonstrate the technical and economic viability of SCR while reducing NO_X emissions by at least 80%.

The project is being conducted at Gulf Power Company's Plant Crist Unit 5, a commercially operating 75 MW unit, located in Pensacola, Florida, on U. S. coals with a sulfur content near 3.0%. Unit 5 is a tangentially-fired, dry bottom boiler, with hot and cold side ESPs for particulate control. The SCR process used in this demonstration is designed to treat a slip-stream of flue gas and features multiple reactors installed in parallel. With all reactors in operation, the maximum amount of combustion flue gas that can be treated is 17,400 standard cubic feet per minute (scfm) which is roughly equivalent to 8.7 MWe.

The SCS facility is a slip-stream SCR test facility consisting of three 2.5 MWe (5000SCFM) SCR reactors and six 0.20 MWe (400SCFM) reactors that operate in parallel for side-by-side comparisons of commercially available SCR catalyst technologies obtained from vendors

throughout the world. Figure 2 presents a simplified process flow diagram for the proposed facility. The large (2.5 MWe) SCR reactors contain commercially available SCR catalysts as offered by SCR catalyst suppliers. These reactors are coupled with small-scale air preheaters to evaluate the long-term effects of SCR reaction chemistry on air preheater deposit formation and the deposits' effects on air preheater. The small reactors are used to test additional commercially available catalysts. This demonstration facility size is adequate to develop performance data to evaluate SCR capabilities and costs that are applicable to boilers using high-sulfur U. S. coals.

The demonstration project is organized into three phases: (1) Phase I - Permitting, Environmental Monitoring Plan and Preliminary Engineering; (2) Phase II - Detail Design Engineering and Construction; and (3) Phase III - Operation, Testing, Disposition, and Final Report. The cooperative agreement was signed June 14, 1990, and the project completion date is now projected to be at the end of 1995. The original total estimated project costs were $15.6 million but project growth increased the expected total cost to $23 million. The co-funders are SCS ($10 million), DOE ($9.4 million), EPRI ($2.9 million) and Ontario Hydro ($0.75 million).

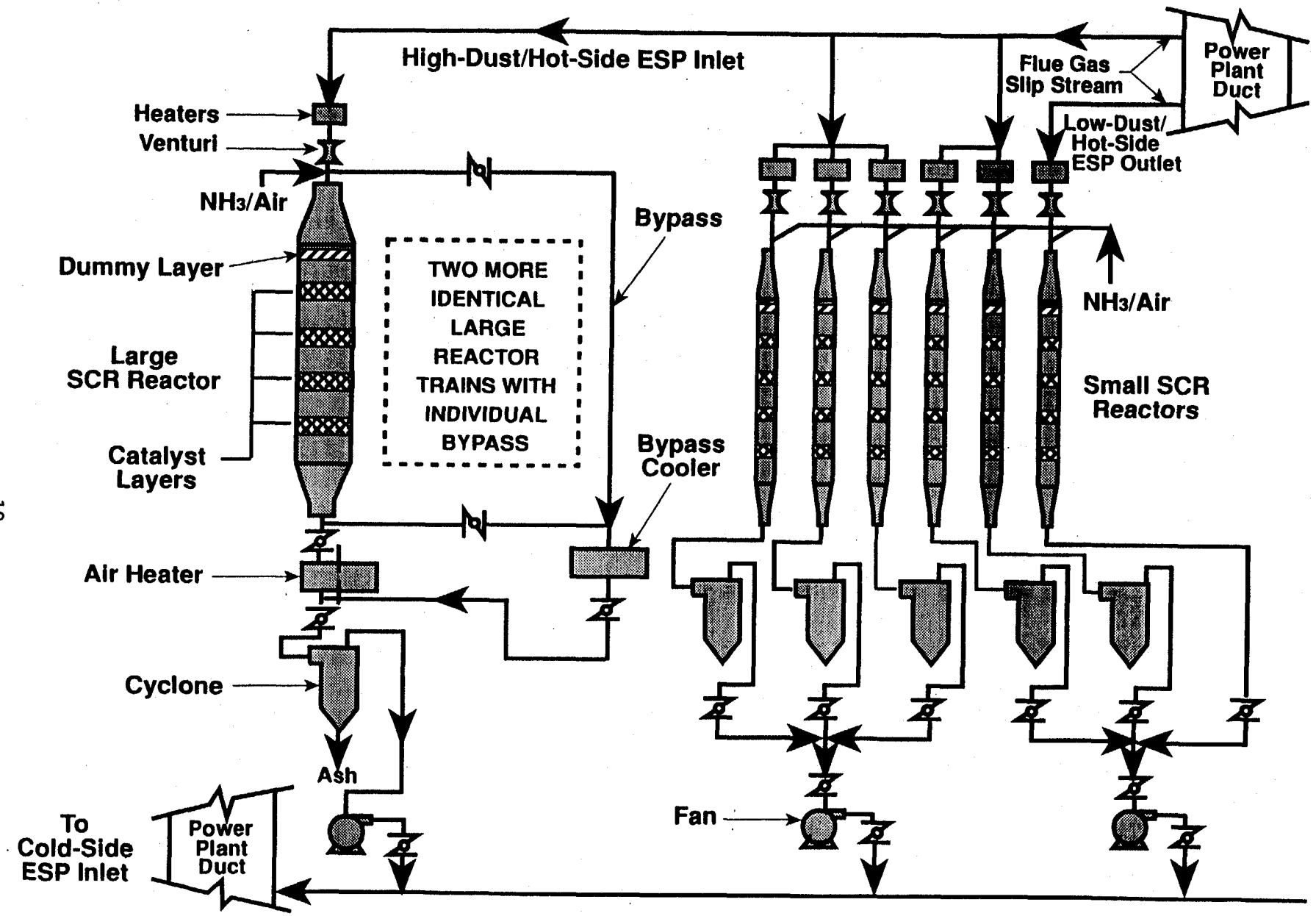

Figure 2. Prototype SCR Demonstration Facility-Process Flow Diagram.

Section 3

PROJECT DESCRIPTION

Within the three phases of the project, the following tasks are to be conducted to effectively demonstrate the SCR process:

Phase I - Permitting, Environmental Monitoring Plan and Preliminary Engineering

Task 1.1.1 - Prototype Plant Permitting Activities
Task 1.1.2 - Develop Environmental Monitoring Program
Task 1.1.3 - Preliminary Engineering
Task 1.1.4 - Engineering and Construction Contracts Scope Development
Task 1.1.5 - Project Management and Reporting

Phase II - Detail Design Engineering and Construction

Task 1.2.1 - Detailed Design Engineering
Task 1.2.2 - Construction
Task 1.2.3 - Operation Staff Training
Task 1.2.4 - Planning for Detailed Testing
Task 1.2.5 - Start-Up/Shakedown
Task 1.2.6 - Project Management and Reporting

Phase III - Operations, Testing, Disposition and Final Report

Task 1.3.1 - SCR Demonstration Facility Operations and Maintenance
Task 1.3.2 - Process Evaluation
Task 1.3.3 - Environmental Data Management and Reporting
Task 1.3.4 - Economic Evaluation
Task 1.3.5 - Dismantling/Disposition
Task 1.3.6 - Project Management and Reporting

Section 4
PROJECT STATUS

Progress during April - September, 1993, is summarized below for each of the on-going tasks in the Scope of Work.

PHASE II - DETAIL DESIGN ENGINEERING AND CONSTRUCTION

Task 1.2.3 - Operations Staff Training

Although the basic operator training was previously concluded, operators continued to gain experience in operating the control system and equipment during the start-up/shakedown period. The operators revised the operating procedures to reflect their experience with the test facility. and coordinated with Unit 5 boiler operators on achieving specific conditions from the boiler which were required during commissioning.

Task 1.2.5 - Start-up/Shakedown

The start-up and shakedown of equipment continued during the second quarter of 1993 as was commissioning testing without catalysts. The SCR demonstration facility was taken off line the first weekend in April as a result of a boiler outage. While off line for over two weeks, necessary construction modifications were made to the SCR facility. These modifications included installation of a damper on the gas-side ductwork returning flue gas from the facility to the host plant duct. The inlet vanes on all fans were modified to resolve a freezing problem with the vanes. Sootblowing capability was added at the electric heaters and for the bypass gas heat exchangers because of concerns with fly ash deposits. The most significant modification included changes to the main inlet scoop ductwork and small reactor take-off. To resolve a maldistribution problem of particulate between the small and large reactors, the slot size of the small reactor take-off was reduced, and a mixing device and flow straightening grid were installed just prior to the split between the small and large reactors. Additional construction modifications included installation of more platforms and walkways for access to equipment and instrumentation and for testing purposes. Some instrumentation was also relocated or replaced. Contracts for instrumentation and controls maintenance were awarded upon completion of bid evaluations. The process for acquiring mechanical maintenance was established.

Some configurational changes with the Bailey control system were made and checked out and acceptance of the gas analysis system continued. (See more details about the gas analysis system in the Phase III, Task 1.3.1 section.)

Near the end of the second quarter, the ammonia flow controllers were repaired and cleaned by the service representatives and the controllers tested accurately against calibrated standards. Sootblowing appeared to be effective on the hot-side of the air preheaters since essentially no fouling was observed when inspected in June. After installing sootblowing capability at the electric heaters in April, by June sootblowing seemed to be controlling the ash fouling problem at the electric heaters.

The commissioning tests without catalysts were completed by the middle of June 1993. The results are reported in the Task 1.3.2 section (Process Evaluation) under Phase III.

The loading of the catalysts into the reactors began on June 14 and was finished on June 22, 1993. The catalyst vendor, assigned reactor, and the catalyst vendor representatives on site for their catalyst loading were as follows:

Catalyst supplier	Reactor designation	Representatives on site for catalyst loading
W. R. Grace	A(large)/D(small)	Mohit Uberoi
Nippon Shokubai	B(large)	Montonobu Kobayashi, Noboru Sugishima, Taka Yatagai
Siemens	C(large)	Ralf Sigling
Cormetech	E(small)	Chris DiFrancesco, Johnny Yamaguchi
Haldor Topsoe	F(small)	John Holst
Hitachi Zosen	G(small)	-
Engelhard	H(small)/J(small)	Ed Balko, Howard Furbeck

Some of the major issues experienced during start-up are highlighted below:

- Sulfate Deposition

There were problems with plugging in ductwork/piping areas without continuous flow because of the high sulfur concentrations in the fuel and the flue gas. While the ammonia injection system was being completed, the installed injectors presented one such low flow area that sulfates diffused into and precipitated out, plugging almost every injection system. The nozzles and injection header were cleaned and some portions of the feed piping had to be replaced. The air fan for ammonia dilution has since been placed in service and will be used to supply a continuous air flow to act as a purge to prevent recurrence of the plugging. The horizontal sections of the large reactor bypass lines accumulated a large amount of sulfate formation that blocked operation of several dampers. These dampers are being exercised on a weekly basis to prevent the blockage from binding the dampers again.

- Bypass Heat Exchangers

The bypass heat exchangers, which were included for use during the parametric testing on the large reactors to minimize effects of high ammonia slip upon the long term evaluation of the air preheaters, were easily plugged by ash and sulfate deposits. Cleaning with either air or water has not been a satisfactory solution. Work to develop another means to cool the flue gas while bypassing the air preheaters remained underway at the end of this reporting period.

- Ash Accumulation

During start-up, especially during low flows, ash build-ups were found in several areas of the ductwork including the main scoop area, the electric flue gas heaters, and the bypass heat exchangers. Extra access ports for sootblowing were added to clean these areas.

Task 1.2.6 - Project Management and Reporting

The Management Information System, developed for tracking overall budget and schedule information, was used to monitor budget and schedule and to help fulfill DOE reporting requirements. Monthly progress reports were submitted to DOE.

A paper describing the status of the project and design issues was presented at the 86th Annual Meeting of the Air and Waste Management Association in Denver in June 1993.

PHASE III - OPERATIONS, TESTING, DISPOSITION, AND FINAL REPORT

Task 1.3.1 - SCR Demonstration Facility Operations and Maintenance

Upon completion of commissioning tests without catalyst, catalyst loading was completed in late June 1993. Long-term testing and parametric evaluations were commenced afterwards, and July 1 is considered the beginning of operation phase of the project with catalysts. Immediately after catalyst loading, all reactors were operated with ammonia briefly to obtain fly ash samples for the Toxicity Characteristics Leaching Procedure (TCLP) analysis. The TCLP results indicated no detectable amounts or change in constituents between baseline ash samples and ash samples from the SCR process outlet.

During July - September, 1993, Reactors A - C were the primary reactors operated with ammonia and the first set of parametric tests were completed for these reactors. The parametric tests for reactors D - F were just underway at the completion of the quarter. The total number of operating hours with exposure to flue gas for each reactor by the end of the quarter is as follows:

Reactor A	-	1111 hours	Reactor E	-	399 hours
Reactor B	-	2033 hours	Reactor F	-	399 hours
Reactor C	-	2009 hours	Reactor G	-	42 hours
Reactor D	-	399 hours	Reactor H	-	42 hours
			Reactor J	-	4 hours

During the third quarter of 1993, there was a brief outage over the July 4th holiday to allow final tie-in of fire protection piping. In August, one bypass heat exchanger developed a water leak that led to the plugging of the reactor cyclone. The cyclone was cleaned without taking the reactor off-line, but further cleaning was reserved until the next outage in September. Also, a large reactor fan caused a brief outage when ash build-up caused an imbalance that vibrated the bearing pedestal bolts loose. After ash removal, bearing inspection, and acceptable balance testing, the fan was returned to service. There were two outages in September. The first outage was scheduled over the Labor Day holiday to inspect and clean the cyclone hoppers which were plugged, inspect the air preheaters, and clean two of the large reactor fans. These efforts restored flow rates above the maximum rates needed during parametric testing. The second outage was unscheduled and resulted from a bearing failure on the host boiler's forced draft fan.

As may be normally expected, there have been several issues encountered during operation, some of which are not associated with the SCR process per se. The major experiences are highlighted below.

- Dilution/Extraction Gas Sampling/Monitoring System

The SCR test facility uses a Lear Seigler dilution/extraction sampling system for measurement of NOx, SO2, CO_2, and CO in the flue gas. This sampling method uses dry air as a dilution medium, with typical air/sample dilution ratios ranging from 30 to 250, to minimize the problems associated with the transport and measurement of these gases as compared to other available methods. There have been several issues with this system including accuracy of NOx outlet data with ammonia injection, coordinating the shared analyzers, and communicating with the test facility's data collection system.

Problems were experienced with NO_X measurements in the presence of ammonia, apparently with catalytic reactions proceeding in the sampling system, thus reducing NOx before the sample reaches the analyzers. There has been a series of traps and filters installed in sample line to capture the ash, water vapor and acid condensate in order to improve the accuracy of the analyzer system and work is underway to investigate a probe with different material of construction.

For the nine reactors, there are three NOx analyzers for the reactor outlet measurements. Each of these analyzers operate on a time-shared basis serving three specific reactors. These systems use a complex system of pumps and valves to direct the sample that is continuously extracted to the analyzer. Problems occurred with erroneous data being transmitted for the two points which are supposedly holding their previous values while the third reactor sampling point is active.

The gas analyzer system has a dedicated programmable controller that collects the data from all the analyzers and then sends them to the test facility's control and data collection system. Because these are different systems, the communication protocol had to be worked out during start-up. Although many of the communication problems were solved during the start-up of the test facility, there were still some communication failures occurring. All these problems with the gas sampling/analysis systems were addressed or in the process of being addressed at the end of the quarter. However, the above issues were the reasons there were rather limited long-term operating data during this period.

- Ammonia Injection Flow Control

Precision mass flow control valves supplied by Sierra Instrumentation were installed to control the ammonia vapor flow rates for injection into the reactors. These controllers were affected by liquid in the flow stream, pressure variations, trash in the line, and also the orientation of the controller itself. These controllers were calibrated on nitrogen and scaled to read ammonia flow. Although initial results indicated accurate flow control, subsequent measurements indicated that actual ammonia flow was 10 to 25 percent higher than the controllers were indicating. Action taken to correct this situation included installing coalescent filters on the ammonia supply lines to each control valve, reorienting the controllers, replacing the ammonia header pressure regulator, cleaning each controller, and recalibrating and verifying with other instruments.

- Low Dust Reactor Fouling

After only a few hours of operation during its first start-up after catalyst loading, the low-dust reactor experienced severe plugging of the first catalyst layer. While the large reactor bypass lines may be used to flush any ash accumulations associated with the main extraction scoop, the low dust reactor ductwork was not provided with any bypass capability. Also, the isolation damper for that line is approximately 100' downstream of the scoop allowing a deadleg for sulfate formation when the reactor is off-line. So during start-up an unusually large amount of solid material may have been introduced to the low-dust reactor. The first layer catalyst element was returned to the catalyst vendor for examination and a study undertaken to evaluate solutions to prevent recurrence of this problem. The resulting design changes to prevent recurrence of the plugging problem on the low dust reactor included the following: the reactor isolation and purge dampers should be relocated to minimize the deadleg; and the reactor heater capacity would be increased and the heater moved to just downstream of the isolation damper so the piping could be slowly warmed while drawing flue gas. These changes were to be made during the fourth quarter of 1993.

- Reactor and Air Preheater Sootblowing

The large reactors use steam supplied sootblowers for both the catalyst baskets as well as the air preheaters. Much work went into eliminating the condensate from the sootblowing steam supply piping before the sootblowers extend into the reactors, including an extra steam isolation valve on

each sootblower, using a process steam condensate trap on each reactors steam supply header, and adding warm-up vents to assure the piping is hot enough to prevent condensation. Follow up inspections reveal that the sootblowers were effective throughout this reporting period in dislodging any ash build-up on either the reactor baskets and on the air preheater baskets. The schedules and procedures for sootblowing of the reactors and air preheaters are shown below:

Sootblowing

Schedules:

Large Reactors - every 8 hours
Small Reactors - every 8 or 12 hours
Air Preheaters - every 4 hours

Procedures:

- Warmup lines by venting the top of verticals
- Condensate drains under each vertical and air preheater
- Monitoring pressure drops-before/after

- Reactor Fans

Due to the small flow, high head requirements of the test facility, the reactor fans were custom designed and not "off the shelf" models. Because of the head requirement, the fan wheels were narrow, large diameter with relatively high inertial moments that made bearing selection difficult. On the small reactor fans, the bearings were replaced twice before changing the design to ball bearings.

Because of the high speed requirement, the small reactor fans use fan belts to increase the speed. The belt tension adjustment system moved the motor, placing the motor on a thin sheet metal base that would vibrate at harmonics to the motor speed. The motor baseplate was stiffened to prevent the vibration.

Because of the possibility of ammonia slip in the flue gas, materials used in fan construction had to be compatible with ammonia. The original vane support bushings were pressed carbon and very brittle, in fact several were broken in shipment and more broken during installation. The first replacements fabricated were brass, and they were rejected due to the ammonia attack of copper alloys. The next offering was stainless steel, which galled as soon as it was installed. The latest

solution is a silicon alloyed cast iron, which has performed well over the last three months. The vane bearings were also extended off of the fan housing and new seals were also installed.

- Measurement Accuracy/Repeatability

The majority of manual measurements are made using triplicate samples. This insures the quality of the data and helps to remove operating variability from the results. Since triplicate measurements usually require several hours to complete, they also help to evaluate and insure that steady-state operation has been achieved for the particular test conditions. Each of the triplicate samples are analyzed in duplicate in the laboratory. Thus, six values are acquired for each average reported measured value. Detection limits for ammonia slip measurements are normally approximately 1 ppm with analytical repeatability to within 0.1 ppm. Intermediate ammonia detection limits are somewhat higher, namely 1 to 2 ppm with analytical repeatability to within 1 ppm. SO_2 measurements normally have detection limits of 5 ppm with analytical repeatability to within 1% of the measured value. SO_3 detection limits are normally 0.4 ppm with an analytical repeatability to within 0.4% of the measured value.

Task 1.3.2 - Process Evaluation

- Flue Gas Chemistry

The baseline concentrations of the chemical constituents of the flue gas in the Unit 5 hot-side ESP inlet and outlet ducts were measured at both high and low load conditions. The concentrations of the following gases were measured: O_2, NO_x, NH_3, HCl, SO_2 and SO_3. In addition, the concentrations of SO_2 and SO_3 were measured upstream and downstream of the in-duct heaters on one large and one small reactor to determine whether there was measurable conversion of SO_2 to SO_3 across the heaters.

- Baseline Concentrations of Gas Phase Constituents of the Flue Gas

Table 1 summarizes the measured gas-phase pollutant concentrations at the Unit 5 hot-side ESP inlet and outlet ducts for both high and low load conditions. The concentration of oxygen is shown on a percentage basis, while the concentrations of the other gases are presented on a parts per million basis. The standard deviation for each value is presented, if available.

TABLE 1 **Baseline Gas-Phase Pollutant Concentrations (@ 3% O2)**

	Unit 5 ESP Inlet Duct (High Dust Source)				Unit 5 ESP Outlet Duct (Low Dust Source)			
	84 MW (High Load)		43 MW (Low Load)		84 MW (High Load)		43 MW (Low Load)	
	Concentration		Concentration		Concentration		Concentration	
	Average ppm(v)	Std. Dev. ppm(v)	Average ppm(v)	Std. Dev. ppm(v)	Average ppm(v)	Std. Dev. ppm(v)	Average ppm(v)	Std. Dev. ppm(v)
O2	3	0.3	7.5	0.3	4.3	0.5	na	na
NOx	296	14	363	35	381	16	na	na
SO2	2383	20	1973	39	2166	97	1893	21
SO3	33	1	47	1	15	1	21	1
HCl	106	14	99	4	123	7	106	1
NH3	<0.4	na	<0.4	na	<0.4	na	<0.4	na

The concentrations of oxygen and nitrogen oxide presented in Table 1 are from the final report to Southern Company Services under SCS Contract Number 195-89-046. This report summarized the characterization of flue gases at Plant Crist Units 5 conducted in July and August 1990. Oxygen concentrations were measured with a Teledyne Analytical Instruments Model 320 Portable Oxygen Monitor. Nitrogen oxide concentrations were determined with a Thermo Electron Model 10 NO_x Monitor operating in the "NO_x mode". The tables in the report from which the O_2 and NO_x data used in Table 1 were taken can be found in Appendix A.(1)

Ammonia concentrations were determined by a manual extraction method pulling the flue gas sample through a series of bubblers filled with dilute sulfuric acid. The solution is made alkaline (converting the NH_4^+ ion to free NH_3 in solution) and the concentration is measured with an Orion Model 920A ammonia ion specific electrode.

Hydrogen chloride, HCl, was collected by drawing flue gas through a heated probe and a particulate filter and then through an air-cooled condenser and a series of bubblers filled with dilute sodium hydroxide, NaOH. The resulting solution in the bubblers containing sodium chloride, NaCl, was analyzed on a DIONEX Model DX-100 Ion Chromatograph.

Sulfur dioxide (SO_2) and sulfur trioxide (SO_3) were collected in a controlled condensation sampling train. The flue gas is sampled with a train consisting of a heated quartz-lined probe, a quartz-fiber filter supported on a frit in a heated quartz filter holder, and a quartz condensing element packed with quartz wool and maintained at 120°F to 130° F. Following the condensing element are bubblers containing an aqueous solution of hydrogen peroxide. While the SO_3 is removed in the condensing element, the SO_2 is removed in the bubblers by oxidation to H_2SO_4. In the condenser the SO_3 present begins a hydration reaction with the water vapor present making H_2SO_4. The excess water vapor also condenses to produce a condensate of concentrated aqueous H_2SO_4. Thus, two solutions of H_2SO_4 are collected -- one a very concentrated solution of limited amount containing the original SO_3 and the other a relatively weak solution in far greater amount containing the original SO_2. The concentrations of the sulfate ion are determined using ion chromatography.

The data in Table 1 show that the concentrations of SO_2 and HCl decrease between high and low load at both the ESP inlet and outlet, while the concentration of SO_3 increases. For all three species there is a somewhat smaller concentration at the ESP outlet compared to the ESP inlet. In all cases the concentration of NH_3 in the flue gas was below the detection limit. (The absence of detectable NH_3 was expected, since NH_3 is not typically found in flue gas unless it is injected

from an outside source. The injection of NH_3 to react with NO_x had not started when the analyses mentioned here were made.) As expected, the oxygen concentration was higher at low load because of the additional excess air required for proper boiler operation. It was also higher at the ESP outlet because of air inleakage across the device. The concentrations of nitrogen oxides were somewhat higher at low load and at the ESP outlet compared to high load at the ESP inlet

- Flue Gas Composition (1)

In addition to the flue gas baseline concentrations measured by Southern Research Institute, the SCR gas analyzer system was used to continuously measure several flue gas constituents at the pilot plant inlet. The following table shows these concentrations in terms of average values, normal high values, and normal low values over the reporting period. These quarterly values were determined using daily averages, daily highs, and daily lows during periods that the host boiler was on-line (operating at greater than 40 MWe).

TEST FACILITY GAS CONCENTRATIONS

	July-Sept. '93		
Constituent	Average	High	Low
Unit #5 Load (MW)	70	86	44
Inlet NO_x (ppm)	320	370	280
Inlet O_2 (%)	4.0	7.0	2.6
Inlet CO_2 (%)	11.9	17.1	9.2
Inlet CO (ppm)	47	330	7
Inlet SO_2 (ppm)	1850	2170	1560

The SCR gas analyzer system was supplied by Lear Siegler Measurement Controls Corporation (LSMCC), now Monitor Labs, Inc. of Englewood, Colorado. The system consists of thirteen (13) dilution/extraction probes for the measurement of NO_x, CO, CO_2, and SO_2. The system uses Yokagawa in-situ probes for the measurement of oxygen. There are twenty-six (26) Yokagawa oxygen probes. Normal dilution ratios on the dilution/extraction components of the system range from 30/1 to 250/1. NO_x analysis is performed using an LSMCC ML8840 chemiluminescence NO_x analyzer with a detection limit of 2 ppb resulting in a flue gas detection limit of approximately 0.25 ppm. CO is measured using a LSMCC model ML8830 infrared CO

analyzer with a detection limit of 0.1 ppm resulting in a flue gas detection limit of approximately 3 ppm. CO_2 is measured using a Siemens Ultimat 5E non-dispersive infrared CO_2 analyzer. SO_2 is measured using a LSMCC model ML8850 florescence SO_2 analyzer with a detection limit of 1 ppb resulting in a flue gas detection limit of 0.1 ppm. Oxygen is measured using in-situ zirconium oxide cell technology.

- Mass Concentration(1)

The eight high-dust reactors take their flue gas from the inlet ducting to the Plant Crist Unit 5 hot-side ESP. A major goal of the Task 1 test phase was to demonstrate that each of the eight high-dust reactors was receiving fly ash that was similar in concentration and particle size to that of the fly ash at the inlet to this ESP. To this end, Task 1 testing began by measuring the mass concentrations of the fly ash in the Unit 5 hot-side ESP inlet and outlet ducting at both high (84 MW) and low (43 MW) load conditions. All mass concentrations were determined using the EPA Method 17 technique which uses an in-situ filter. Two samples were collected at each condition. Table 2-1 summarizes the test data.

In order to verify that the mass concentration into each of the eight high-dust reactors was similar in magnitude to that measured in the main hot-side ESP inlet duct, mass concentrations were measured at the reactor inlet test ports located immediately upstream of the flow rate venturis. Initial measurements conducted on February 26-28, 1993 indicated a large disparity among the eight reactors as shown in Table 2-2. Values ranged from a high of 11.9 gr/dscr @ 3% O_2 to a low of 2.8 gr/dscf @ 3% O_2. Also shown in this table are the data for reactor J, the low-dust small reactor. The data for reactor J were well behaved and of the expected magnitude for high-load conditions. (Reactor J inlet mass concentrations were not measured at low load because of the extremely low values expected.) As a result of the large differences between the mass concentration values in the eight high-dust reactors, additional mass concentration tests were performed just upstream of the inlet transition to the eight reactors. Figure 3 shows the locations of the nine test positions in the transition piece. The test results are presented in Table 2-3. These data, together with the discovery that the original design of the inlet transition did not provide for proper isokinetic flow transition between the transition piece and the ducting to the five high-dust, small reactors, provided sufficient evidence that modification to the design of the inlet transition was required.

After modifications to the inlet transition were complete, a repeat series of tests were performed. Because of the difficulty of collecting proper samples at the inlet to the five high-dust small

TABLE 2-1 **Plant Crist Unit 5 Hot-Side ESP Mass Concentration Data**

Location Boiler Load	Inlet High	Inlet High	Outlet High	Outlet High	Inlet Low	Inlet Low	Outlet Low	Outlet Low
% Moisture	9.8	10.4	10	9.2	8.5	8.8	8.4	7.8
% Oxygen	3.4	3.2	4.2	4.0	7.7	7.3	6.8	6.5
Velocity, ft/s	47.7	48.9	39.1	40.1	30.6	30.3	22.0	21.1
Gas Temp., F	661	664	619	620	597	599	547	542
ACFM	206,000	221,000	158,000	162,000	132,000	131,000	88,800	84,900
DSCFM	86,500	87,800	68,500	70,800	59,900	59,200	42,300	40,900
WSCFM	96,000	98,000	76,100	77,900	65,500	64,900	46,200	44,400
DSCFM @ 0% O2	72,400	74,400	54,700	57,200	37,900	38,500	28,500	28,200
gr/acf @ 3% O2	1.43	1.24	0.0019	0.0019	1.26	1.20	0.0005	0.0003
gr/dscf @ 3% O2	3.40	2.98	0.0044	0.0042	2.77	2.66	0.0009	0.0005
mg/acm @ 3% O2	3,275	2,844	4.43	4.27	2,879	2,752	1.03	0.50
mg/dscm @ 3% O2	7,806	6,834	10.18	9.75	6,345	6,097	2.16	1.03
#/10^6 Btu	5.58	4.88	0.0073	0.007	4.53	4.35	0.0015	0.0007

TABLE 2-2 **Plant Crist SCR Mass Concentration Data (Reactor Inlets @ High Load)**

Location	Reactor A		Reactor B		Reactor C		Reactor D		Reactor E	
% Moisture	8.83	9.40	8.94	9.16	8.78	9.42	8.38	9.07	8.70	8.61
% Oxygen	3.2	3.3	3.6	3.2	3.2	3.3	4.2	3.5	4.3	3.2
Velocity, f/s	68.1	67.8	66.3	66.8	69.4	69.2	98.3	105.8	90.4	94.3
Gas Temp., F	711	708	700	703	697	698	766	771	747	780
ACFM	12,832	12,777	12,495	12,579	13,067	13,036	1,157	1,247	1,064	1,110
DSCFM	5,155	5,111	5,090	5,095	5,346	5,292	448	475	418	425
WSCFM	5,655	5,642	5,590	5,609	5,861	5,842	489	522	458	465
DSCFM @ 0% O2	4,292	4,255	4,213	4,315	4,528	4,456	358	396	332	360
gr/acf @ 3% O2	1.23	1.12	1.31	1.27	1.32	1.33	2.37	2.50	2.18	2.11
gr/dscf @ 3% O2	3.07	2.81	3.22	3.13	3.22	3.27	6.12	6.57	5.56	5.50
mg/acm @ 3% O2	2,829	2,575	3,011	2,911	3,025	3,042	5,439	5,739	5,008	4,830
mg/dscm @ 3% O2	7,041	6,437	7,392	7,187	7,395	7,496	14,041	15,060	12,752	12,620
#/10^6 Btu	5.12	4.65	5.28	5.13	5.28	5.35	10.03	10.76	9.11	9.02

Location	Reactor F		Reactor G		Reactor H		Reactor J	
% Moisture	8.50	9.45	9.25	8.53	8.66	6.76	8.0	8.0
% Oxygen	3.3	3.2	3.2	3.3	3.5	4.3	5.5	5.0
Velocity, f/s	93.1	93.6	94.1	92.1	93.5	90.8	84.1	83.9
Gas Temp., F	721	729	744	747	773	769	673	728
ACFM	1,096	1,102	1,109	1,084	1,102	1,069	991	988
DSCFM	441	436	434	427	421	421	415	395
WSCFM	482	481	478	467	461	452	451	430
DSCFM @ 0% O2	371	369	367	360	351	335	346	301
gr/acf @ 3% O2	3.35	3.26	4.40	4.68	2.57	2.53	0.0009	0.0008
gr/dscf @ 3% O2	8.32	8.24	11.25	11.87	6.73	6.43	0.0023	0.0020
mg/acm @ 3% O2	7,674	7,472	10,090	10,721	5,894	5,808	2.20	1.89
mg/dscm @ 3% O2	19,086	18,898	25,800	27,210	15,421	14,748	5.24	4.72
#/10^6 Btu	13.63	13.50	18.43	19.44	11.02	11.04	0.0037	0.0034

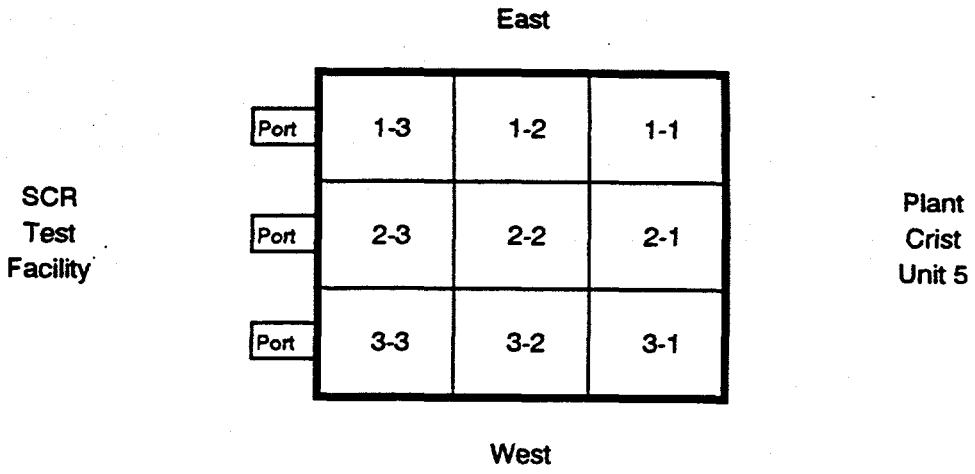

Figure 3 Identification of sampling locations at the SCR Inlet Transition.

TABLE 2-3 **Plant Crist SCR Mass Concentration Data (Special Tests at the Inlet Transition @ 70 MW)**

Port (See Figure 3-1)	1-1	1-2	1-3	2-1	2-2	2-3	3-2	3-2	3-3	Average
		Note 1		Note 1			Note 2	Note 1		
% Moisture	8.77	8.84	9.90	10.91	9.29	9.98	9.10	9.41	8.90	9.45
% Oxygen	6.4	6.4	6.4	6.4	6.4	6.4	6.4	6.4	6.4	6.4
Velocity, f/s	49.3	46.0	58.0	53.5	56.0	60.7	51.7	49.9	65.2	54.5
Gas Temp., F	662	652	670	649	664	670	648	662	668	661
ACFM	36,224	33,799	42,595	39,358	41,189	44,616	38,033	36,654	47,900	40,041
DSCFM	15,269	14,362	17,601	16,376	17,222	18,417	16,165	15,330	20,043	16,754
WSCFM	16,736	15,755	19,534	18,382	18,985	20,458	17,783	16,922	22,000	18,506
DSCFM @ 0% O2	10,593	9,964	12,211	11,362	11,948	12,778	11,215	10,635	13,905	11,624
gr/acf @ 3% O2	1.32	1.12	1.36	1.23	1.21	1.31	1.49	1.41	1.29	1.30
gr/dscf @ 3% O2	2.53	2.64	3.29	2.95	2.89	3.18	3.50	3.36	3.09	3.05
mg/acm @ 3% O2	2,447	2,571	3,122	2,818	2,772	3,009	3,408	3,226	2,964	2,926
mg/dscm @ 3% O2	5,806	6,050	7,555	6,772	6,629	7,290	8,019	7,713	7,085	6,991
#/10^6 Btu	5.12	5.34	6.66	5.97	5.85	6.43	7.07	6.80	6.25	6.17

1. Plant lost feeder and load dropped resulting in early termination of run.
2. Inadvertant repeat of point 2-3. The test point should have been 3-1.

reactors, a decision was made to repeat all of the mass concentration measurements in the eight reactors at a position downstream of the third catalyst layer. Tests were performed at both high and low load conditions. Two measurements were performed at each location. At the large reactors a nine-point matrix was traversed (three positions on each of three ports). On the small reactors a single port provided for a three point traverse. The test results are shown in Table 2-4. The mass concentrations were much more uniform after the modification to the inlet transition. However, the mass concentration data for Reactor D at high load are not of the same magnitude as the other seven reactors and should be considered not valid. In general, the mass concentrations at low load were slightly less variable compared to high load. For all reactors except Reactor D, the average high load mass concentration was 4.01 ± 0.31 gr/dscf @ 3% O_2, with a relative standard deviation of 7.7%. At low load conditions the average mass concentration for all eight reactors was 3.52 ± 0.22 gr/sdcf @ 3% O_2, with a relative standard deviation of 6.3%.

The mass concentration was measured in the economizer bypass duct at low load conditions. The test data are presented in Table 2-5. The average mass concentration, 3.60 gr/dscf @ 3% O_2, was about 33% higher than the value measured in the main Unit 5 hot-side ESP inlet duct under similar load conditions, 2.71 gr/dscf @ 3% O_2 (see Table 2-1).

- Particle Size Distribution[1]

Part of the Task 1 program was to demonstrate that fly ash characteristics (mass concentration and particle size distribution) at the inlet of each of the high-dust reactors were similar under both high-load and low-load conditions. Therefore, the fly ash samples collected during the tests to measure mass concentration (both high and low load conditions) were submitted for size analysis by laboratory technique. The instrument used to determine particle size distribution of the fly ash was a Shimadzu aerodynamic sedigraph. It is able to size the particles into approximately 25 size intervals between 0.056 and 56.2 micrometers physical diameter (or Stokes diameter, assumed spherical shape and true (actual) particle density). In addition to the fly ash tests for the eight high-dust reactors, particle size tests were also conducted on ash samples collected at the Unit 5 hot-side ESP inlet duct at high and low load conditions.

To supplement the laboratory determination of particle size and to demonstrate the accuracy of the laboratory technique to measure a particle size distribution on a redispersed ash sample (Shimadzu), cascade impactors and series cyclones were used at the Unit 5 hot-side ESP inlet duct to measure the fly ash particle size distribution in situ. Two tests were conducted at high load and two at low load for each instrument. The cascade impactors (University of Washington

TABLE 2-4 **Mass Concentrations at the 3rd Catalyst Level**

Reactor	Run Number	Date	Start Time	Unit 5 Load	Measured Oxygen (%)	Mass Concentration (gr/dscf @ 3% O2)
A	022-A3-M17-02	6/1/93	0850	High	3.0	4.01
	022-A3-M17-07	6/2/93	1325	High	3.1	3.81
	022-A3-M17-09	6/3/93	0624	Low	7.9	3.59
	022-A3-M17-11	6/3/93	0813	Low	7.8	3.60
B	022-B3-M17-01	6/1/93	0850	High	2.5	4.21
	022-B3-M17-03	6/1/93	1117	High	3.1	4.05
	022-B3-M17-12	6/3/93	1045	Low	7.5	3.41
	022-B3-M17-14	6/3/93	1238	Low	7.7	3.41
C	023-C3-M17-01	6/7/93	1021	High	2.4	3.77
	023-C3-M17-02	6/7/93	0916	High	2.5	3.91
	022-C3-M17-08	6/3/93	0628	Low	7.6	3.53
	022-C3-M17-10	6/3/93	0816	Low	7.4	3.49
D	019-D3-M17-04	5/14/93	1255	High	5.7	3.18
	019-D3-M17-06	5/14/93	1424	High	5.2	3.08
	022-D3-M17-21	6/4/93	1013	Low	9.3	3.52
	022-D3-M17-23	6/4/93	1149	Low	9.2	3.39
E	021-E3-M17-03	5/27/93	0954	High	3.3	4.31
	022-E3-M17-06	6/2/93	1122	High	4.8	4.08
	022-E3-M17-17	6/4/93	0642	Low	8.6	3.85
	022-E3-M17-19	6/4/93	0826	Low	8.4	3.90
F	021-F3-M17-04	5/27/93	0958	High	5.0	4.84
	022-F3-M17-05	6/2/93	1119	High	3.9	3.91
	022-F3-M17-16	6/4/93	0640	Low	8.7	3.67
	022-F3-M17-18	6/4/93	0823	Low	8.9	3.81
G	021-G3-M17-05	5/27/93	1320	High	4.6	3.94
	021-G3-M17-07	5/27/93	1544	High	3.9	3.81
	022-G3-M17-13	6/3/93	1041	Low	8.6	3.30
	022-G3-M17-15	6/3/93	1235	Low	8.6	3.28
H	021-H3-M17-06	5/27/93	1307	High	4.2	3.96
	021-H3-M17-08	5/27/93	1534	High	4.0	3.54
	022-H3-M17-20	6/4/93	1018	Low	8.7	3.48
	022-H3-M17-22	6/4/93	1152	Low	8.1	3.09

TABLE 2-5 **Economizer Bypass Mass Concentration Data**

Test ID #	010-MT-01	010-MT-02
% Moisture	6.6	6.6
% Oxygen	8.6	8.6
Velocity, f/s	70.1	70.8
Gas Temp., F	868	878
ACFM	5,171	5,227
DSCFM	1,911	1,917
WSCFM	2,046	2,053
DSCFM @ 0% O2	1,125	1,128
gr/acf @ 3% O2	1.35	1.30
gr/dscf @ 3% O2	3.67	3.52
mg/acm @ 3% O2	3,103	2,966
mg/dscm @ 3% O2	8,394	8,088
#/10^6 Btu	5.99	5.78

mark III (seven stage) Source Test Cascade Impactor) fractionate the fly ash into eight size ranges with stage cut points of 8.0, 5.2, 2.7, 1.4, 0.7, 0.3, and 0.16 micrometers physical diameter. The series cyclones (SRI/EPA Five-Stage Series Cyclone) fractionate the fly ash into six size ranges with stage cut points of 5.3, 3.3, 1.8, 1.19 and 0.44 micrometers physical diameter. The particle size distributions of the fly ash at the Unit 5 ESP inlet duct at high and low load are presented in Figures 4-1 and 4-2, respectively. Figures 4-1a and 4-2a present the data as a differential particle size distribution (per cent of total mass in each size range) on a linear scale. Figures 4-1b and 4-2b present the same data with a logarithmic scale. The data in Figures 4-1c and 4-2c are presented on a cumulative per cent basis (cumulative per cent less than the indicated size). The mass median diameter at high load was measured to be 13 microns with the Shimadzu, 9.5 microns with the cascade impactor and approximately 6 microns with the series cyclone. At low load the mass median diameter was 9.4 microns with the Shimadzu, 12.6 microns with the cascade impactor and 8 microns with the series cyclone. The difference in these mass median diameters is likely caused by the more detailed nature of the Shimadzu distribution (25 size fractions) compared to the particle size distributions fitted to the cascade impactor (8 size fractions) and series cyclone (6 size fractions) data. The graphs show best fit spline curves for the impactor and cyclone data.

The individual particle size distributions for the fly ash collected downstream of the third reactor level on each of the high-dust reactors are shown in Figure 4-3 (high load) and Figure 4-4 (low load). Figures 4-3a and 4-4a present the data as differential particle size distributions (per cent of total mass in the indicated size range) on a linear scale, Figures 4-3b and 4-4b present the same data on a probability scale, Figures 4-3c and 4-4c present the same data on a logarithmic scale, and Figures 4-3d and 4-4d present the cumulative percent particle size distributions. A comparison of the high and low load data show that the low load data are much more tightly grouped. Since the reactors were operating at the same conditions during each set of tests (high and low load) and the fly ash sampling techniques were identical, the more tightly grouped low load data may be caused by more favorable isokinetic flow patterns either at the inlet scoop in the main Unit 5 hot-side ESP inlet duct or in the inlet transition piece where the flow splits to the eight high-dust reactors.

The particle size distributions measured at the main duct at high and low load conditions (shown in Figures 4-1 and 4-2, respectively) are compared to the average of the eight reactor third level particle size distribution in Figures 4-5 (high load) and 4-6 (low load). The data are shown as differential particle size distributions (per cent of total mass in the indicated size rage) on three scales, linear (Figures 4-5a and 4-6a), probability (Figures 4-5b and 4-6b) and logarithmic

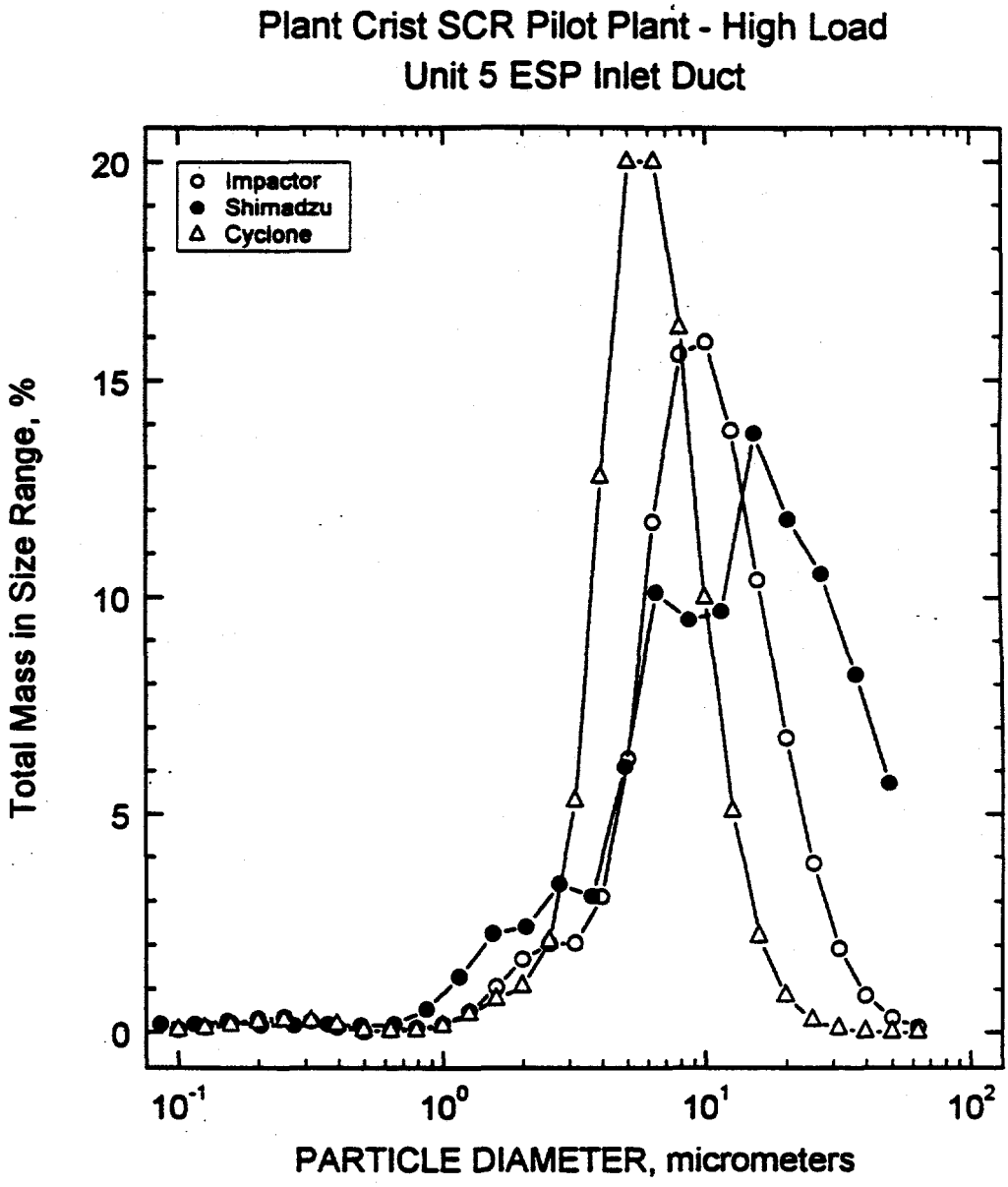

Figure 4-1a. Differential particle size distribution for fly ash at the Plant Crist Unit 5 hot-side ESP inlet during high load (linear scale).

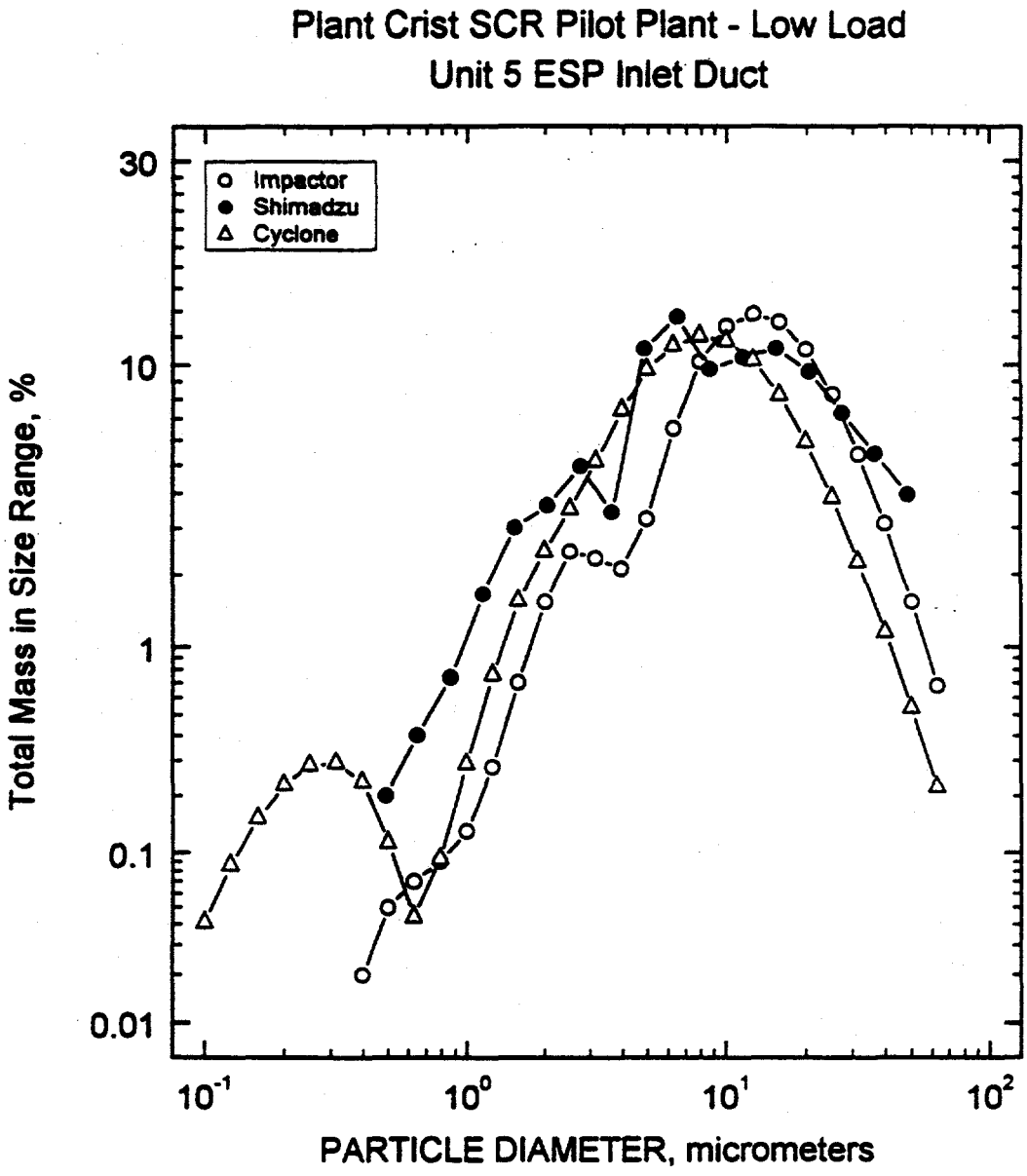

Figure 4-1b. Differential particle size distribution for fly ash at the Plant Crist Unit 5 hot-side ESP inlet during high load (logarithmic scale).

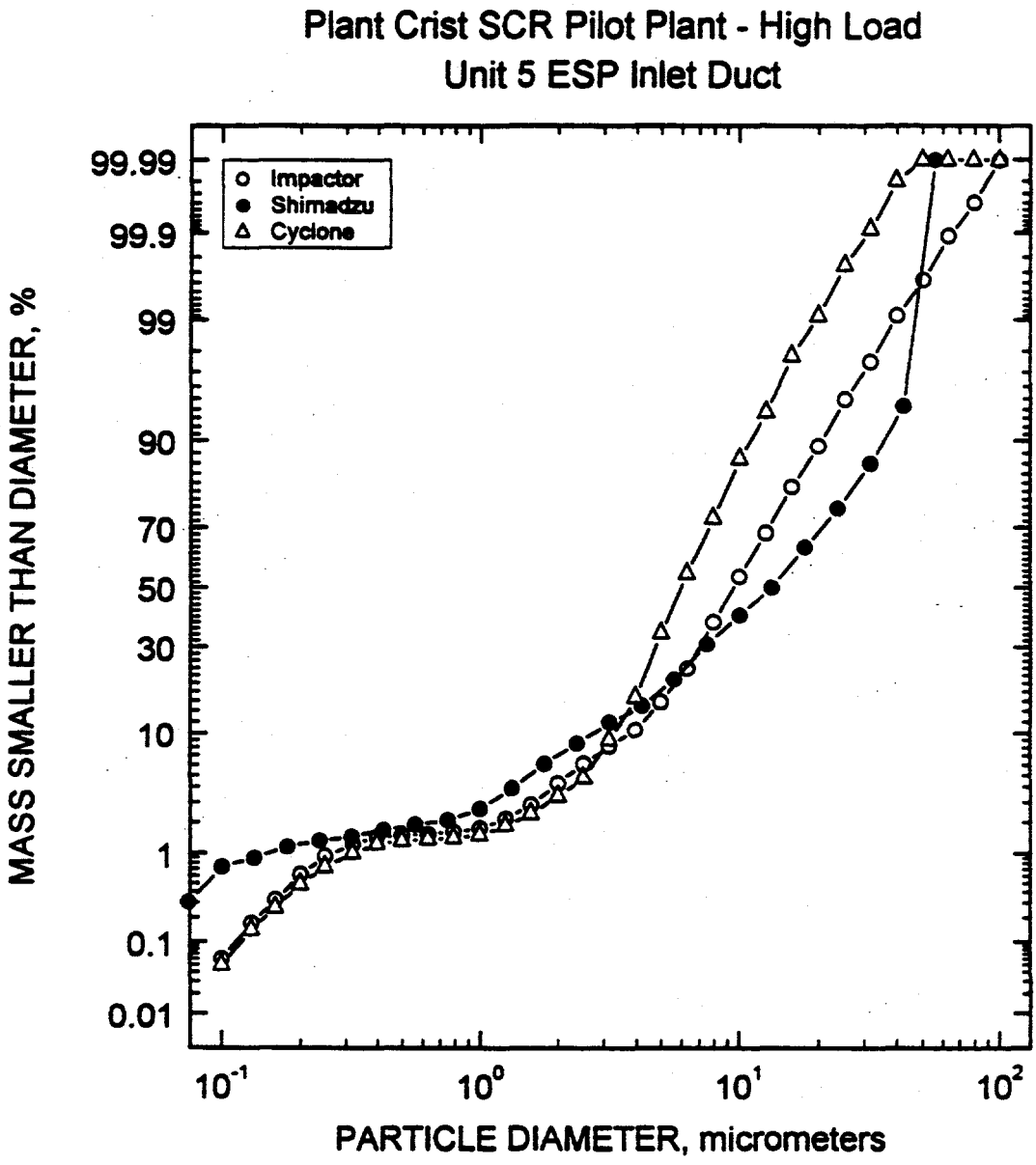

Figure 4-1c. Cumulative (percent) particle size distribution for fly ash at the Plant Crist Unit 5 hot-side ESP inlet during high load.

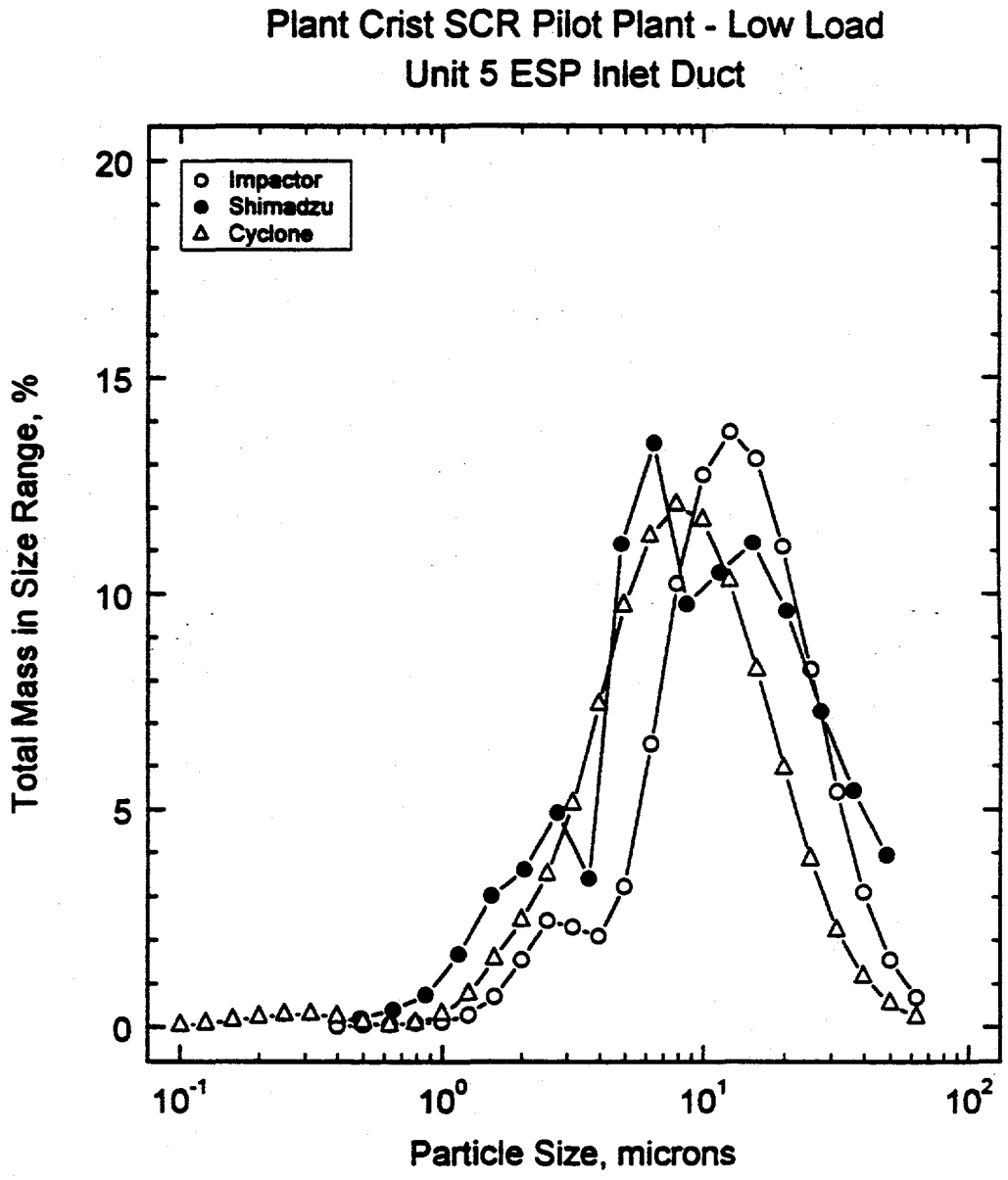

Figure 4-2a. Differential particle size distribution for fly ash at the Plant Crist Unit 5 hot-side ESP inlet during low load (linear scale).

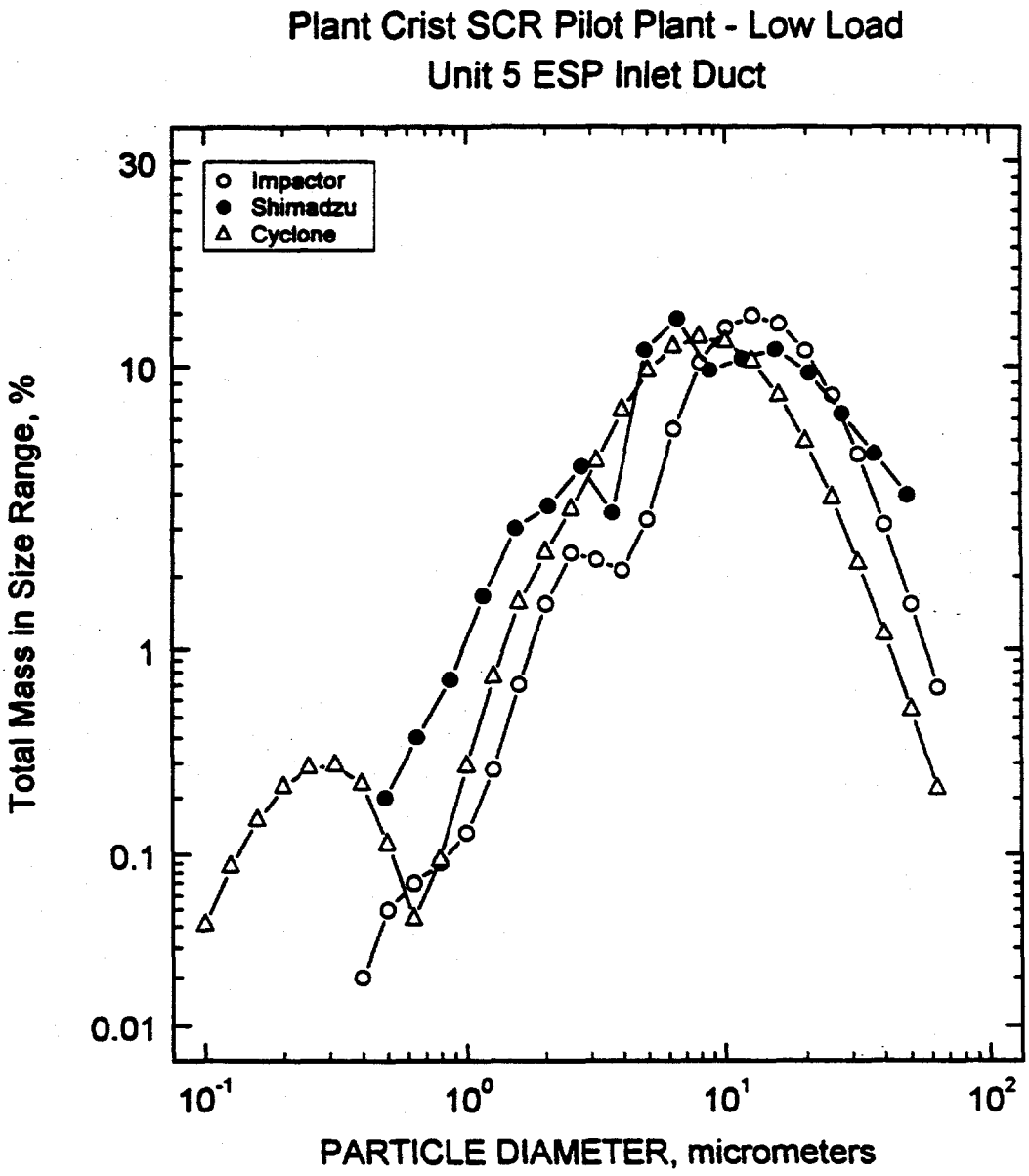

Figure 4-2b. Differential particle size distribution for fly ash at the Plant Crist Unit 5 hot-side ESP inlet during low load (logarithmic scale).

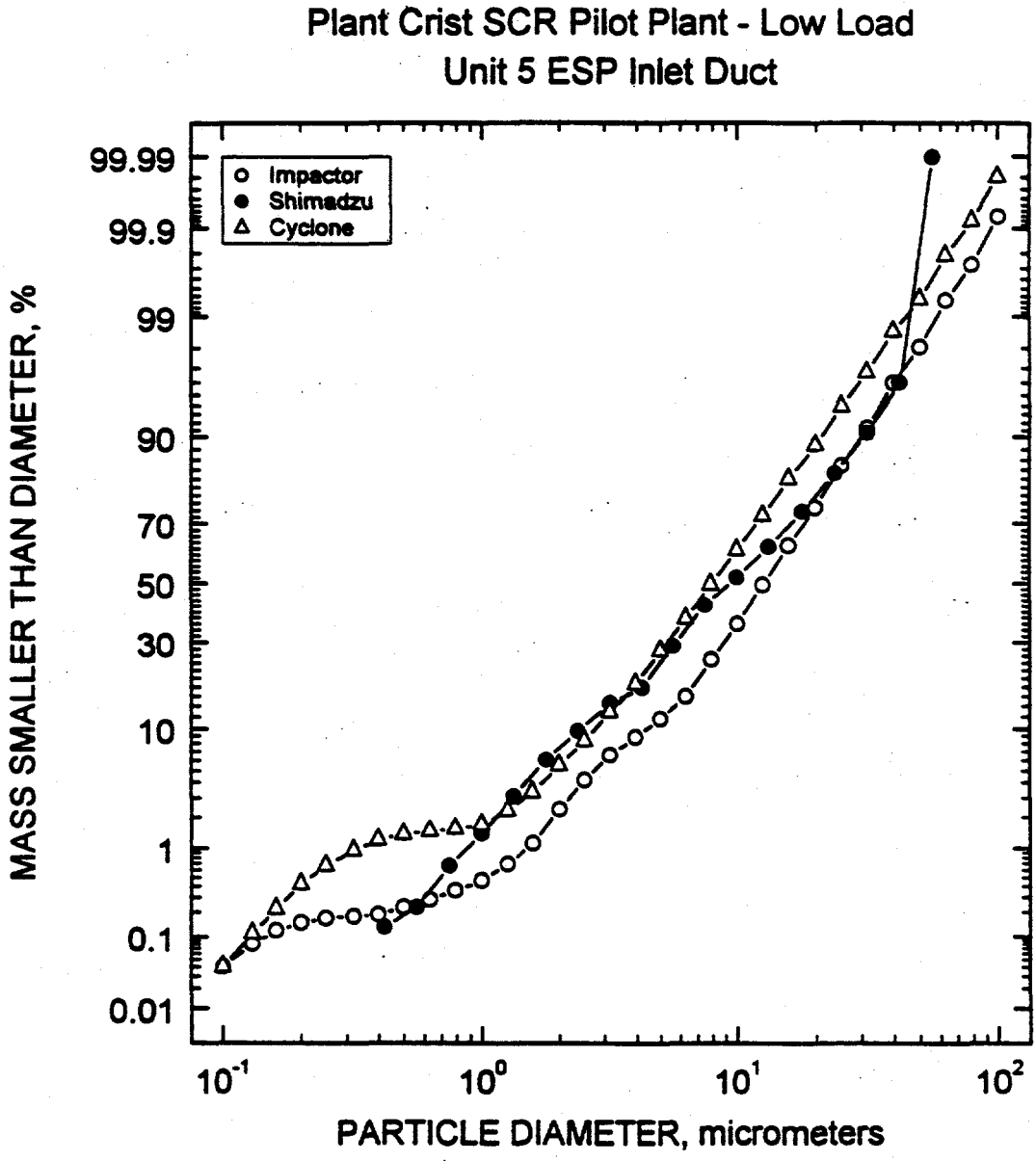

Figure 4-2c. Cumulative (percent) particle size distribution for fly ash at the Plant Crist Unit 5 hot-side ESP inlet during low load.

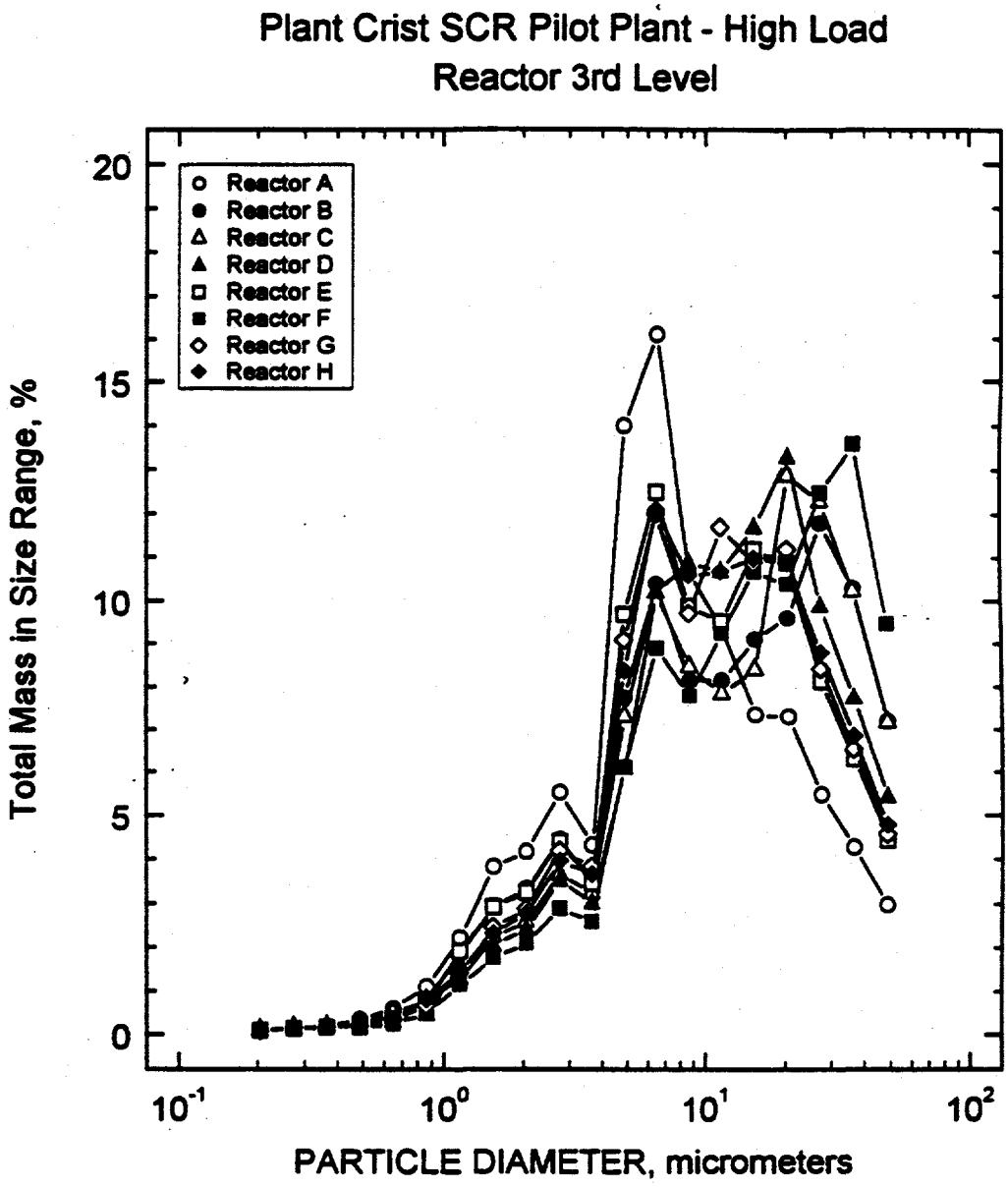

Figure 4-3a. Differential particle size distribution for fly ash downstream of the third reactor level (high dust reactors) during high load (linear scale).

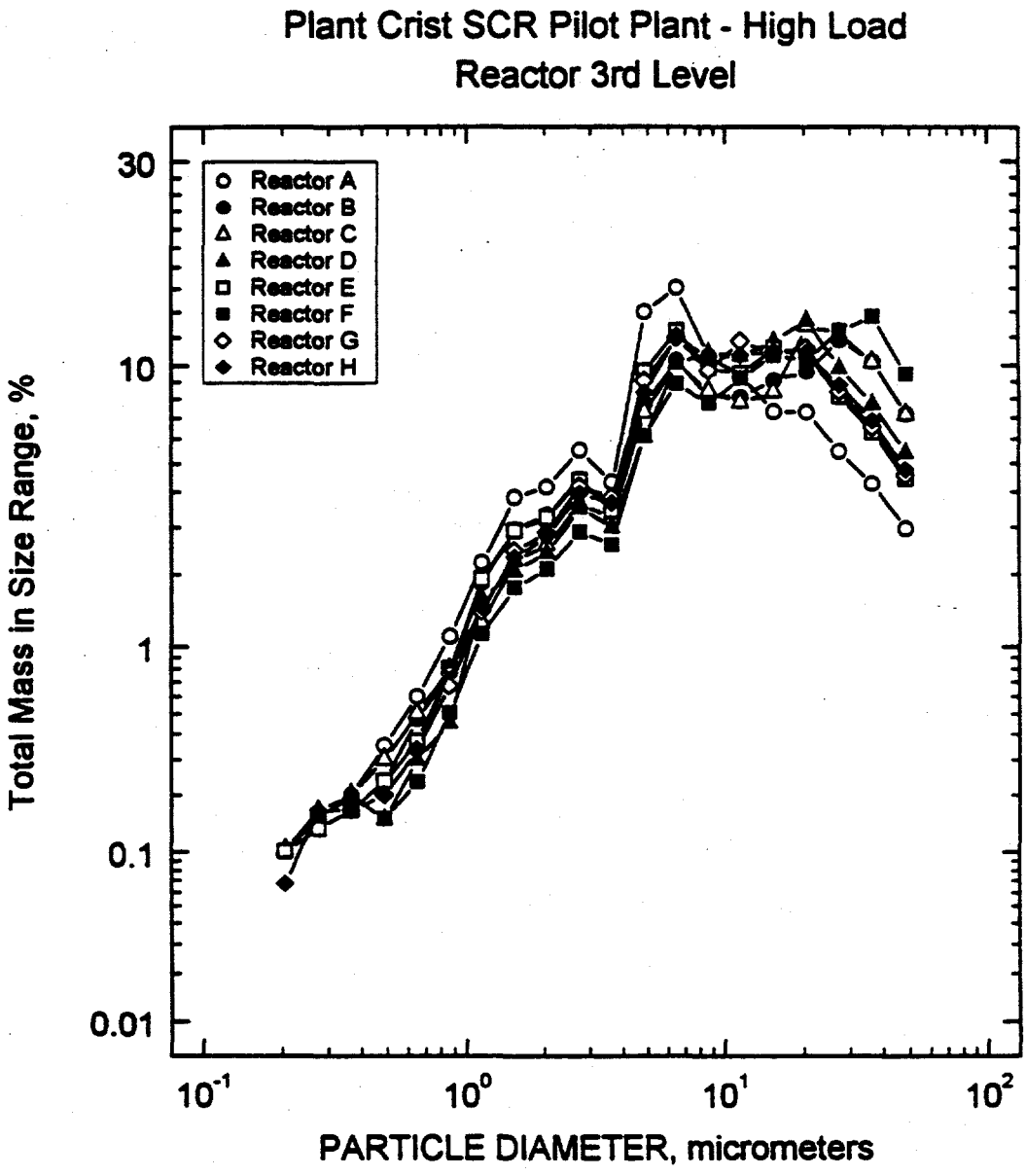

Figure 4-3b. Differential particle size distribution for fly ash downstream of the third reactor level (high dust reactors) during high load (probability scale).

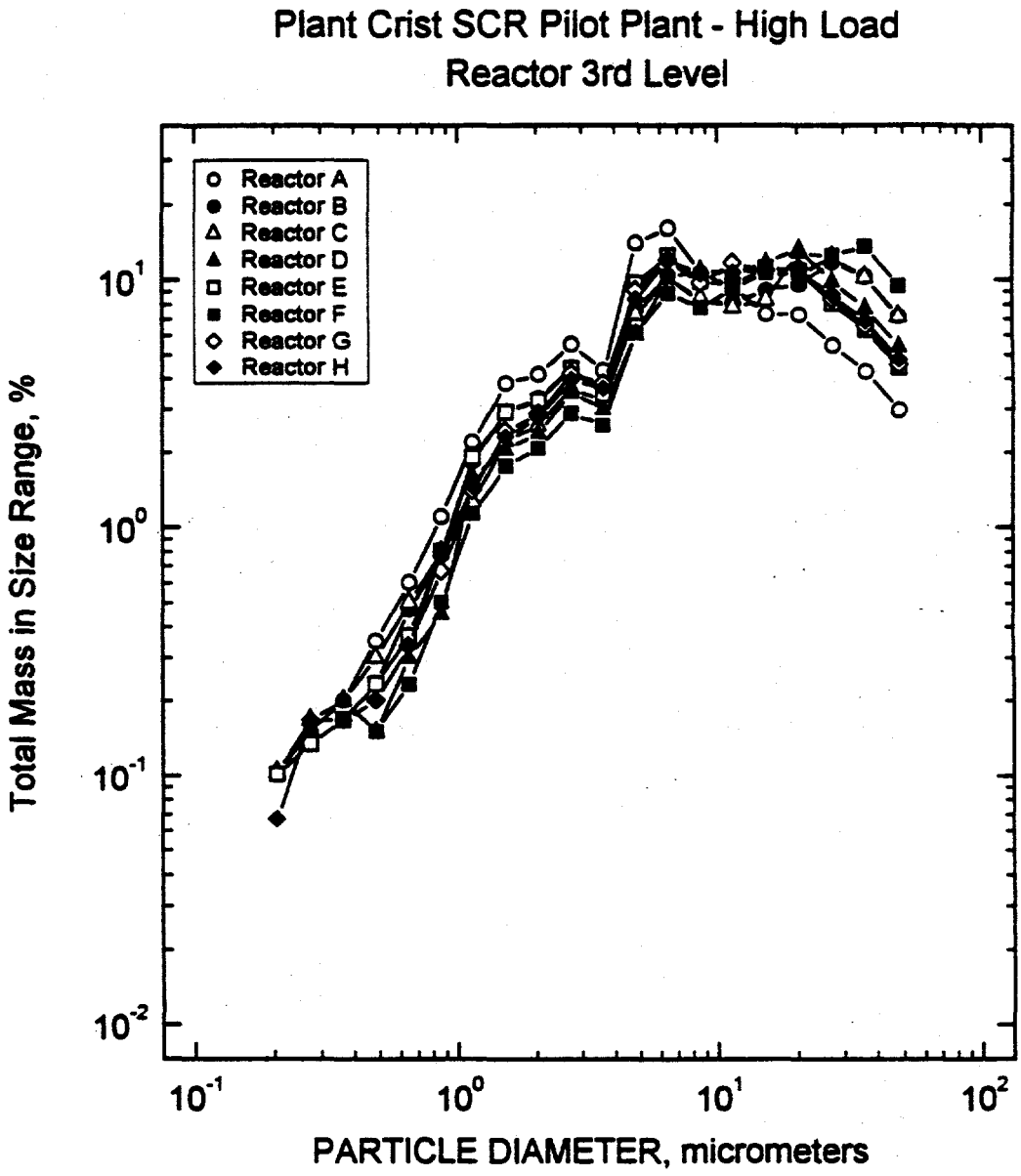

Figure 4-3c. Differential particle size distribution for fly ash downstream of the third reactor level (high dust reactors) during high load (logarithmic scale).

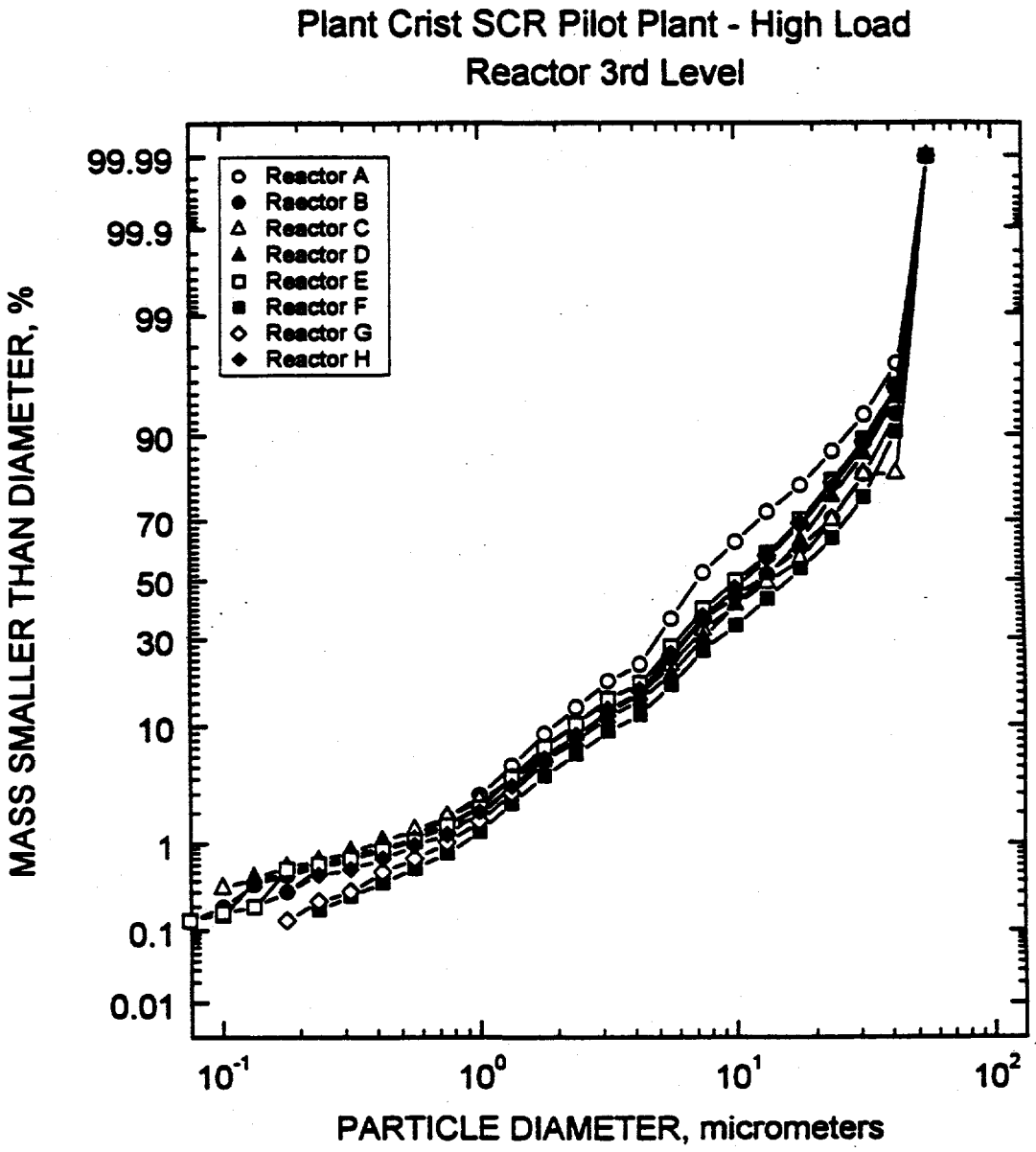

Figure 4-3d. Cumulative (percent) particle size distribution for fly ash downstream of the third reactorlevel (high dust reactors) during high load.

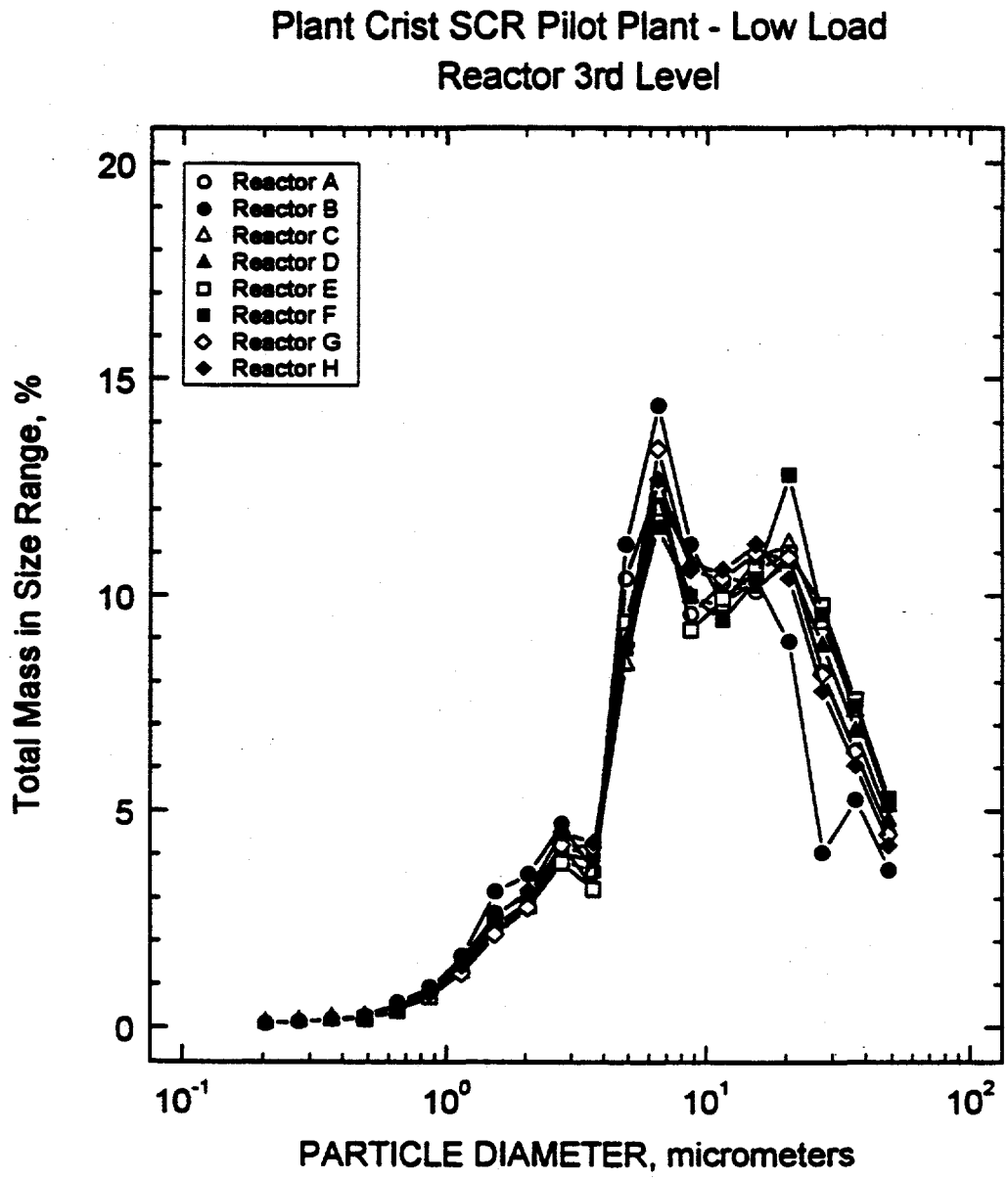

Figure 4-4a. Differential particle size distribution for fly ash downstream of the third reactor level (high dust reactors) during low load (linear scale).

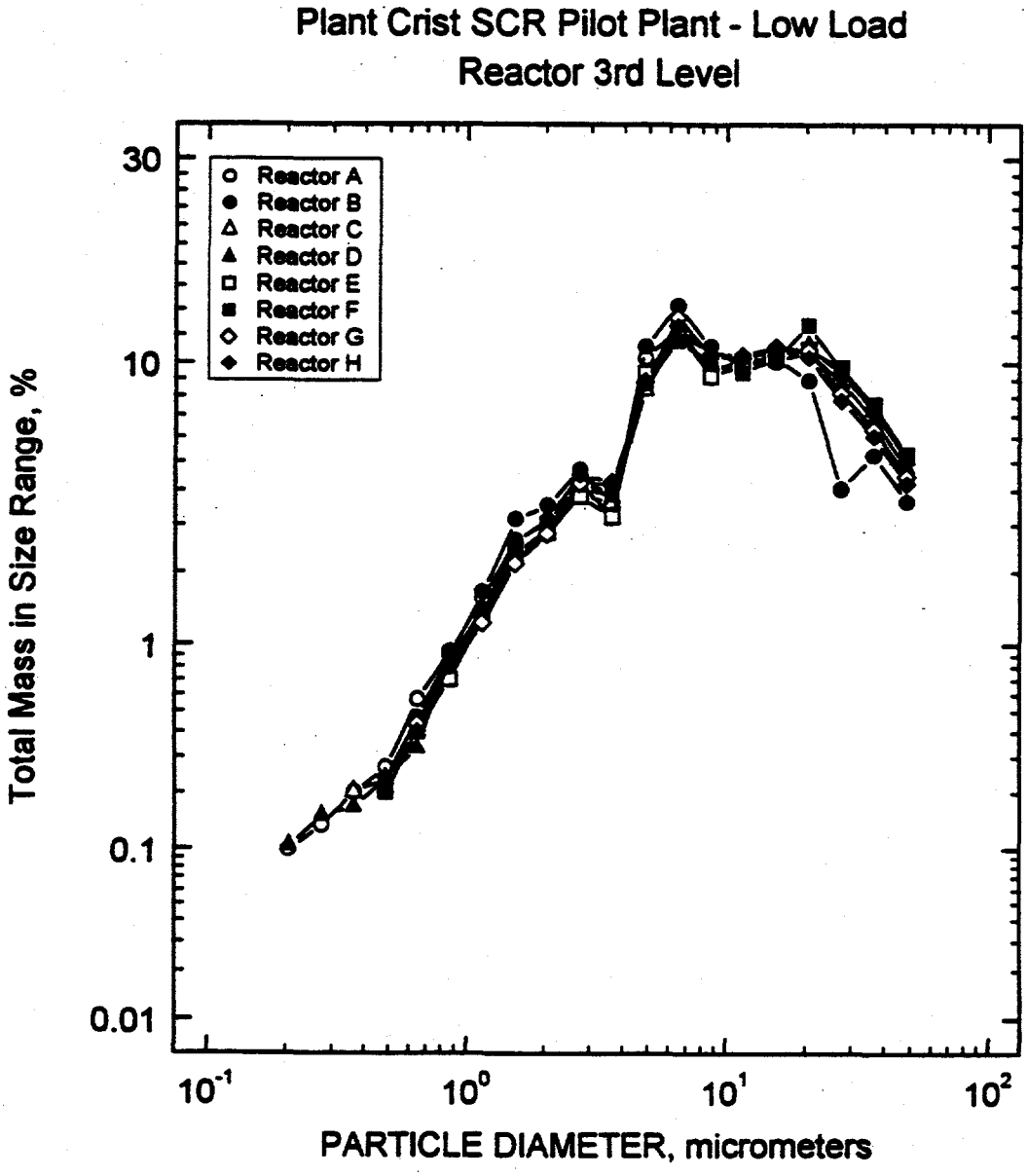

Figure 4-4b. Differential particle size distribution for fly ash downstream of the third reactor level (high dust reactors) during low load (probability scale).

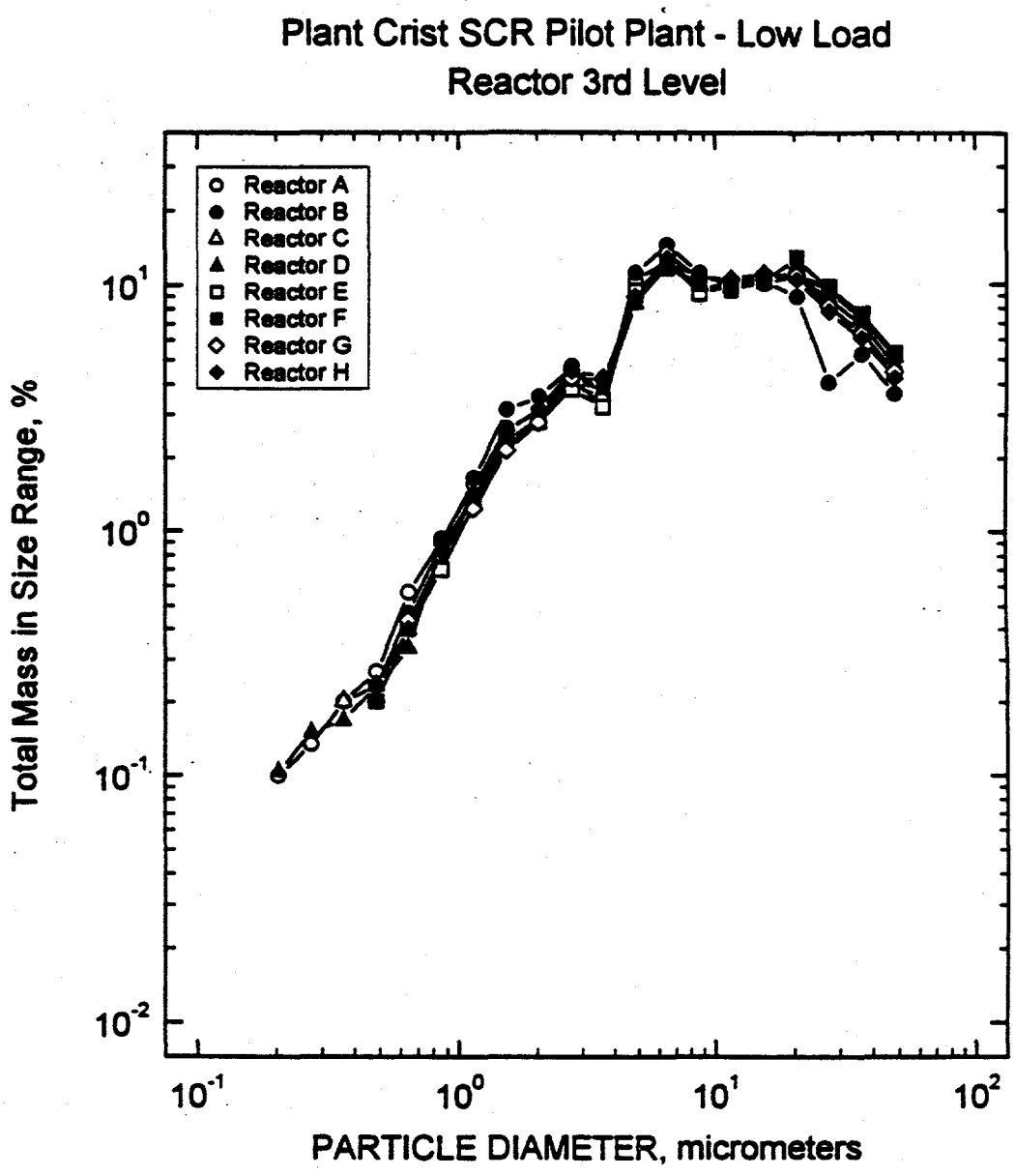

Figure 4-4c. Differential particle size distribution for fly ash downstream of the third reactor level (high dust reactors) during low load (logarithmic scale).

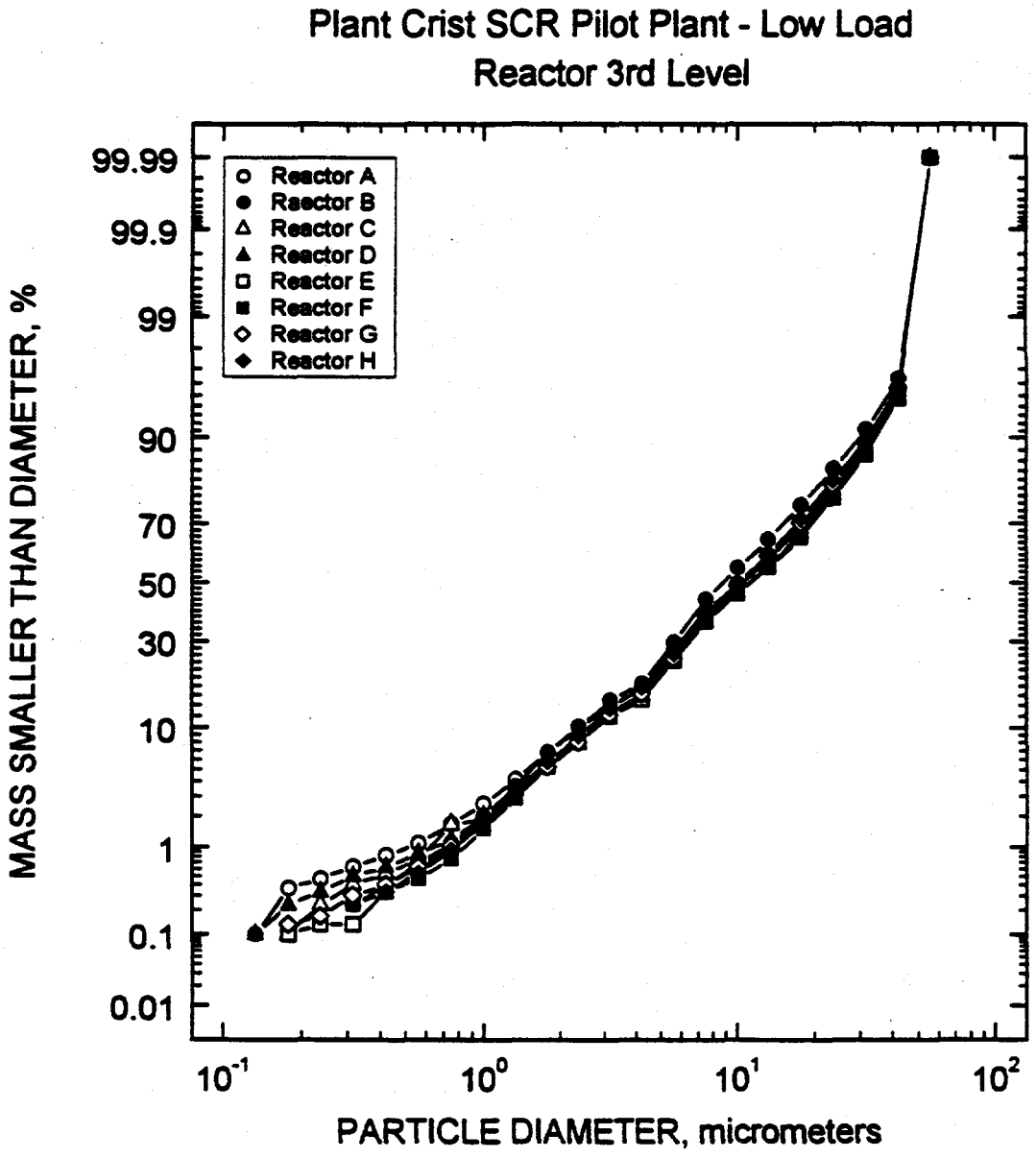

Figure 4-4d. Cumulative (percent) particle size distribution for fly ash downstream of the third reactorlevel (high dust reactors) during lowload

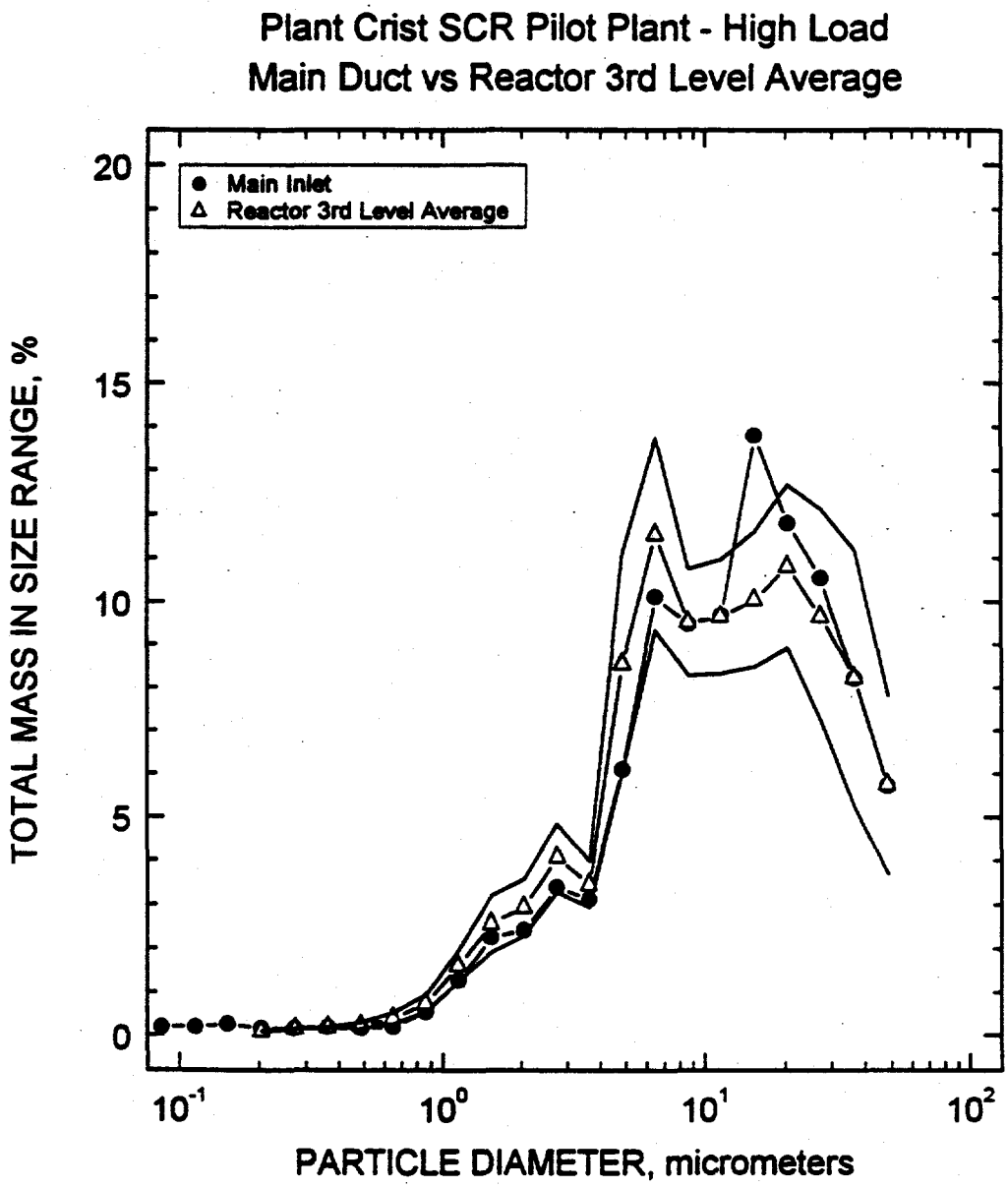

Figure 4-5a. Comparison of differential particle size distributions (linear scale): Unit 5 hot-side ESP inlet versus average of high dust reactors (downstream of third catalyst level) at high load.

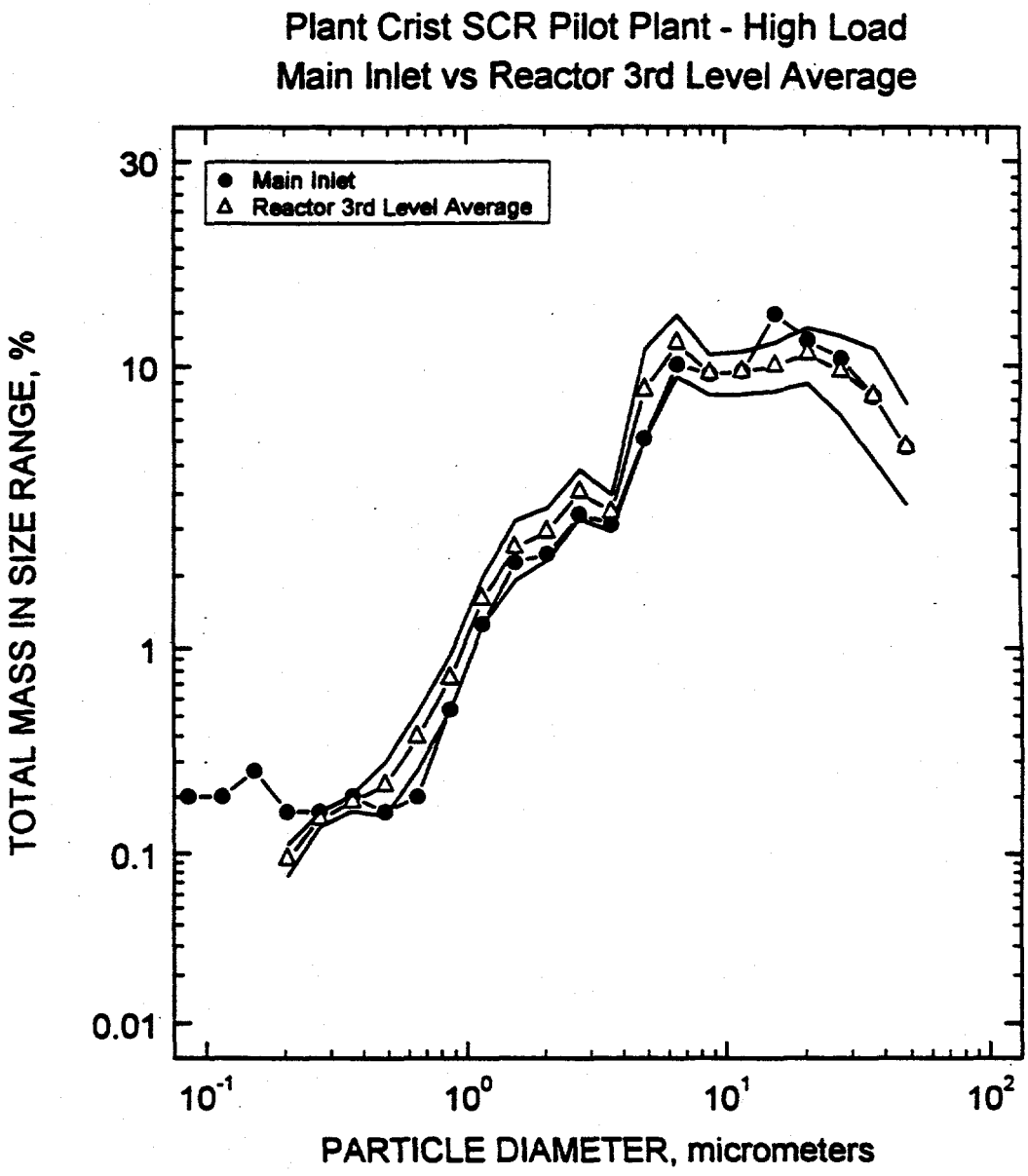

Figure 4-5b. Comparison of differential particle size distributions (probability scale): Unit 5 hot-side ESP inlet versus average of high dust reactors (downstream of third catalyst level) at high load.

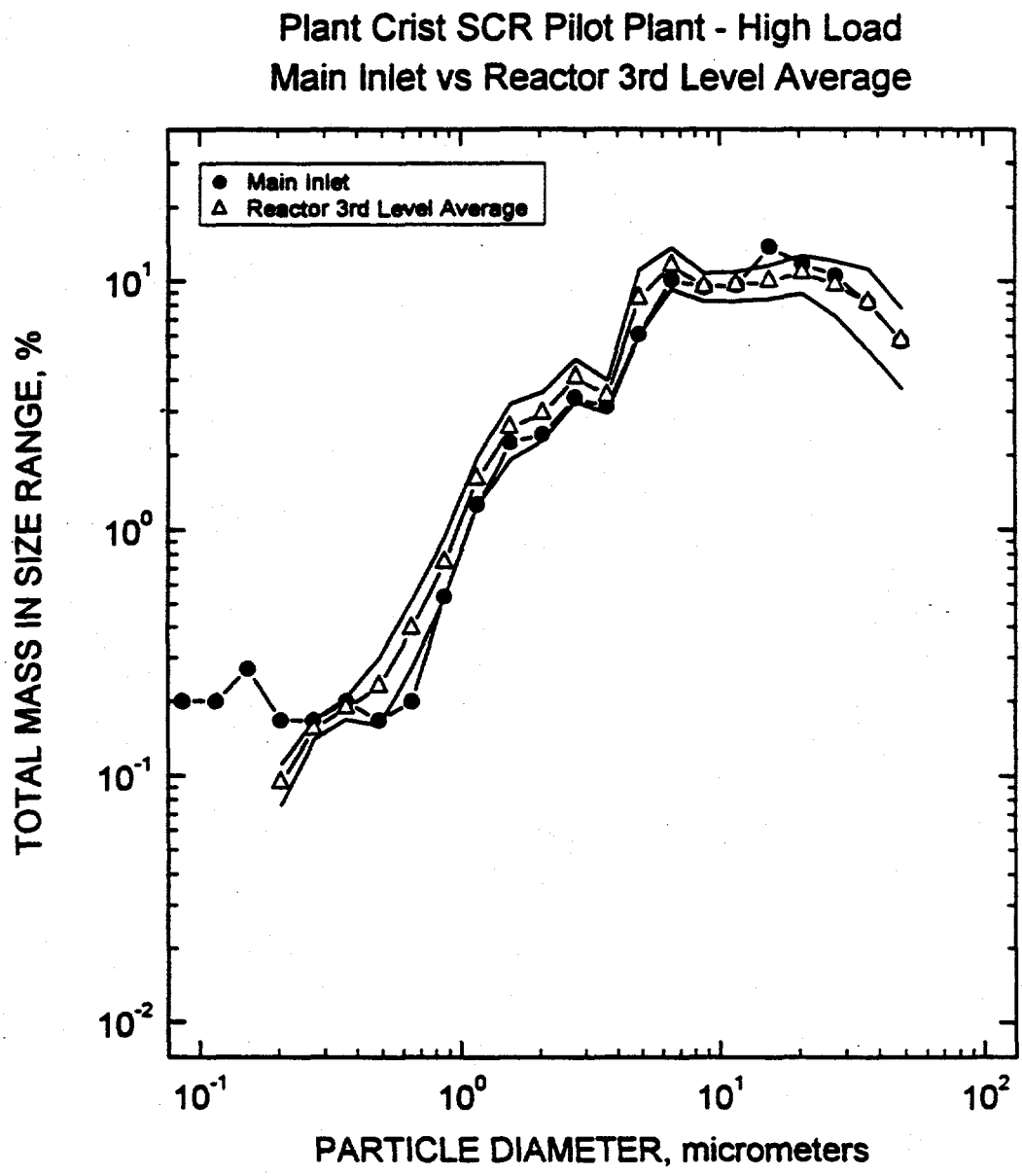

Figure 4-5c. Comparison of differential particle size distributions (logarithmic scale): Unit 5 hot-side ESP inlet versus average of high dust reactors (downstream of third catalyst level) at high load.

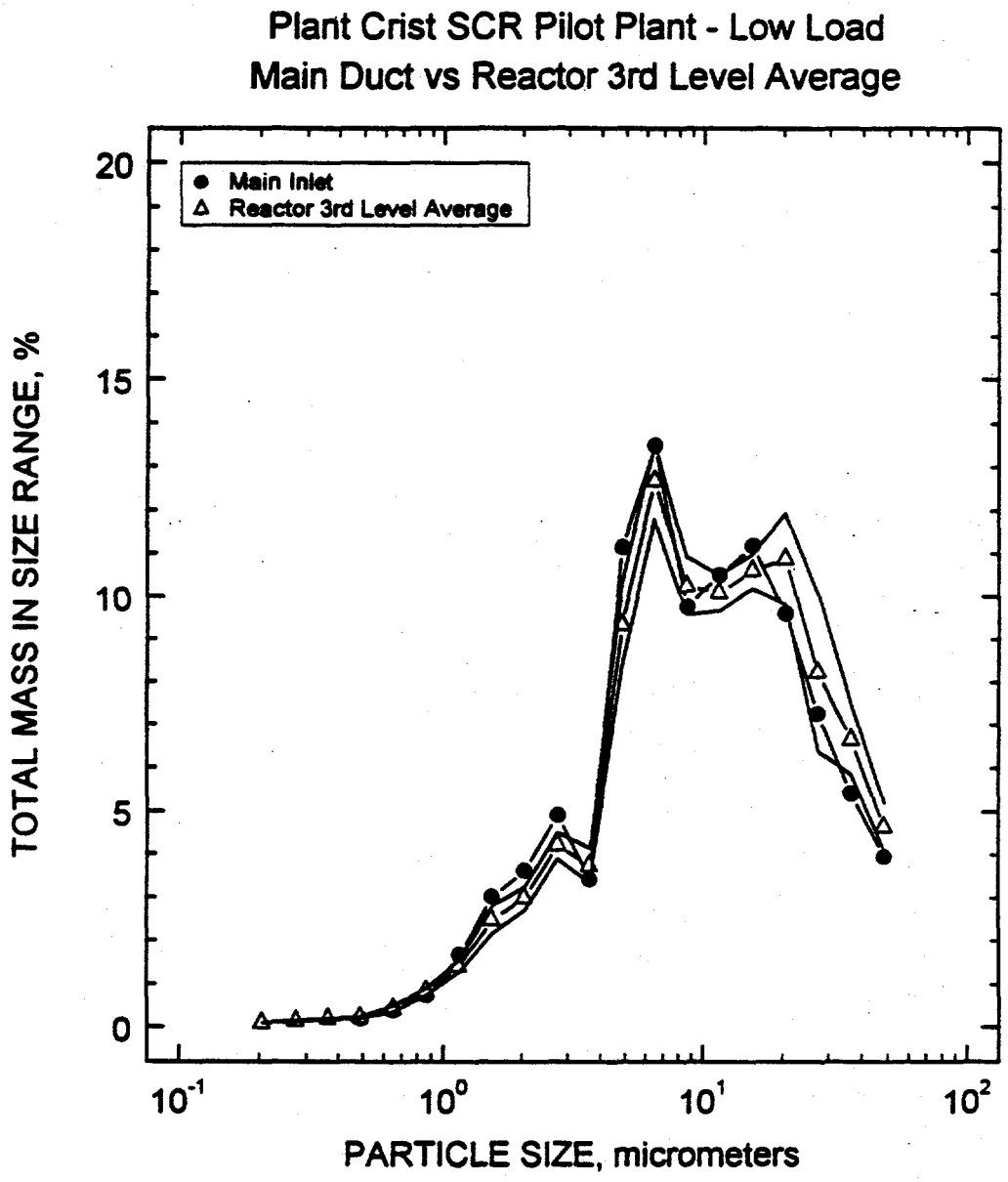

Figure 4-6a. Comparison of differential particle size distributions (linear scale): Unit 5 hot-side ESP inlet versus average of high dust reactors (downstream of third catalyst level) at low load.

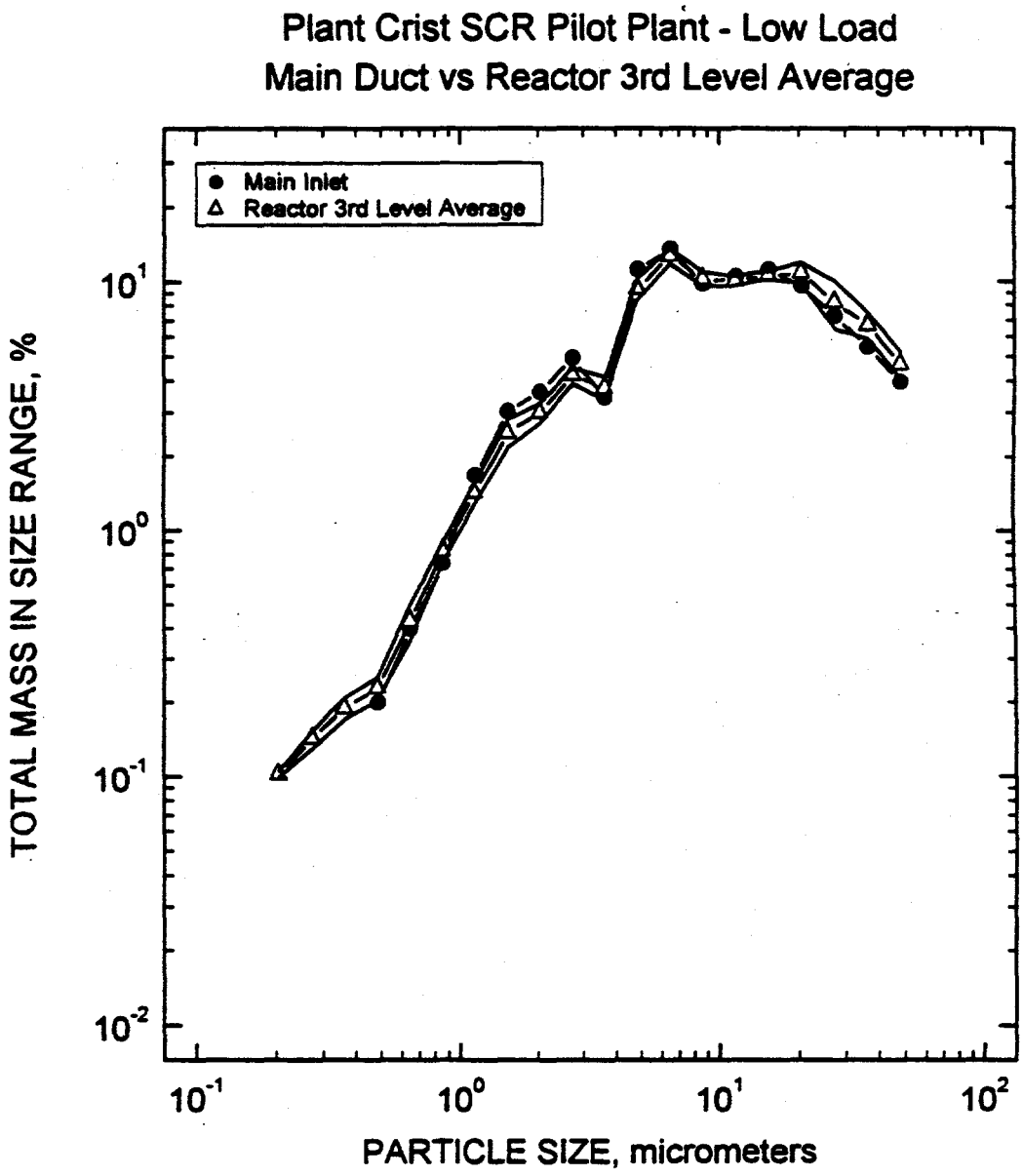

Figure 4-6b. Comparison of differential particle size distributions (probability scale): Unit 5 hot-side ESP inlet versus average of high dust reactors (downstream of third catalyst level) at low load.

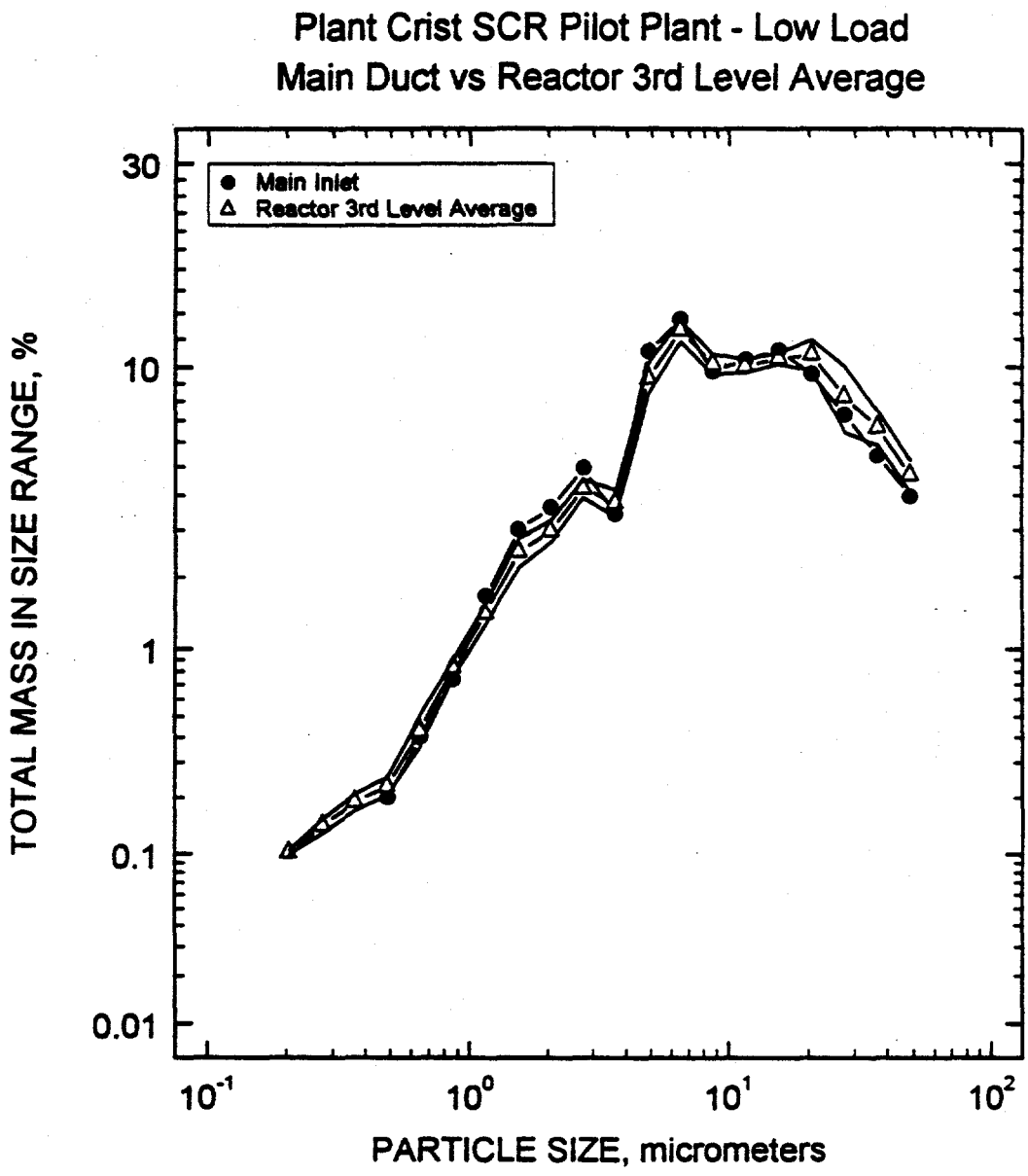

Figure 4-6c. Comparison of differential particle size distributions (logarithmic scale): Unit 5 hot-side ESP inlet versus average of high dust reactors (downstream of third catalyst level) at low load.

(Figures 4-5c and 4-6c). On each graph a pair of lines without data points are shown. They represent the range of one standard deviation about the average of the eight individual reactor size distributions. For both high and low load conditions the main inlet size distribution agrees very well with the average for the eight reactors.

- Fly Ash and Coal Chemistry, Fly Ash Resistivity[1]

- Fly Ash and Coal Chemistry

Ash mineral analyses were performed on fly ash samples collected at the Unit 5 hot-side ESP inlet at high and low load conditions. Ash mineral analyses were also performed on coal samples collected from Unit 5 corresponding to the days on which the fly ash samples were collected. The data are presented on a weight percent basis in Table 3-1. The analysis show very similar weight percents for the various chemical constituents for both high and low load conditions. These data match very well with the values for the ash generated from the ignited coal samples.

Two Plant Crist Unit 5 samples and two NIST standard coal samples were sent to the University of Missouri-Columbia Research Reactor Facility for Neutron Activation Analysis. The test results are presented in Appendix B.

Using a series cyclone sampling system, size segregated samples of fly ash were collected at the Unit 5 hot-side ESP inlet at high and low load conditions. The main purpose of this test was to determine the concentration of trace metals in each particle size range. As an additional step we requested that the concentrations of lithium, sodium, potassium be measured by Flame Atomic Emission Spectroscopy and that the concentrations of magnesium, calcium, iron and aluminum be measured using Inductively Coupled Argon Plasma (ICAP) emission spectroscopy. These test data are presented in Table 3-2. (The trace metal data can be found in Appendix C of this report.) At the top of each column the cut size of the cyclone stage is presented. An analysis of the data in the table indicates that while there seems to be an enrichment of element concentration as particle size decreases for lithium and sodium, this trend does not exist for potassium, magnesium, calcium, iron and aluminum.

- Fly Ash Resistivity

Fly ash resistivity was measured in the laboratory on a fly ash sample collected at the Unit 5 hot-side ESP at high load conditions. The technique for measuring resistivity was based on the IEEE 548 (1984) test method, commonly referred to as a descending temperature method. The atmosphere in the laboratory oven holding the sample was controlled to a moisture content of

TABLE 3-1 **Ash Mineral Analyses (weight percent basis)**

Sample Description	CRST-SCRI-1,2 Hot Side ESP Inlet Fly Ash - High Load 2/9/93	CRST-SCRI-3,4 Hot Side ESP Inlet Fly Ash - Low Load 2/10/93	Crist Unit 5 Coal As Fired 2/10/93	Crist Unit 5 Coal As Fired 2/11/93
SRI Sample No.	E1035-100-4	E1035-100-5	E1035-100-6	E1035-100-7
Li_2O	0.02	0.02	0.02	0.02
Na_2O	0.79	0.87	0.80	0.66
K_2O	2.8	2.5	2.3	2.0
MgO	0.97	0.97	0.91	0.78
CaO	4.6	4.0	4.6	2.8
Fe_2O_3	17.8	18.1	19.9	20.6
Al_2O_3	22.7	22.7	22.6	22.5
SiO_2	48.9	48.4	44.3	47.4
TiO_2	1.0	1.0	0.83	0.83
P_2O_5	0.18	0.16	0.18	0.16
SO_3	0.99	1.2	4.0	2.5
LOI	9.4	2.9	91.3 *	90.9 *
Loss on Drying @ 110 C	included in LOI	included in LOI	9.1	9.6

* : LOI performed on samples that had been dried @ 110 C.
Remainder of coal analyses performed on ignited samples.

TABLE 3-2 **Metals Concentrations in Fractionated Fly Ash Samples**

Cyclone Stage	1	2	3	4	5	Combined
High Load						
Stage Cut Point, µm	5.3	3.3	1.8	1.18	0.44	
Percent of Total Mass	62.3	29.8	6.4	1.19	0.3	100
Lithium, µg/g	63	87	113	119	364	73.9
Sodium, µg/g	0.38	0.55	0.9	1.982	3.61	0.5
Potassium, µg/g	1.59	2.01	2.61	2.72	2.08	1.8
Magnesium, µg/g	0.44	0.51	0.69	0.8	1.04	0.5
Calcium, µg/g	3.08	1.84	1.94	2.24	3.06	2.6
Iron, µg/g	13.2	7.92	8.65	9.4	12.1	11.1
Aluminum, µg/g	9.05	10.8	12.8	12.6	10.6	9.7
Low Load						
Stage Cut Point, µm	5.5	3.5	1.9	1.26	0.47	
Percent of Total Mass	69.3	17	10.1	2.8	0.85	100
Lithium, µg/g	65.8	99.1	122	130	493	81.4
Sodium, µg/g	0.53	0.88	1.13	0.96	1.08	0.7
Potassium, µg/g	1.79	2.38	3.95	2.7	3.08	2.1
Magnesium, µg/g	0.48	0.57	0.67	0.83	1.13	0.5
Calcium, µg/g	2.64	1.33	1.15	1.62	2.45	2.2
Iron, µg/g	10.3	5.34	5.1	6.29	7.6	8.7
Aluminum, µg/g	9.24	9.18	19.26	14.58	17.3	10.3

7.6%, comparable to that occurring in the actual Unit 5 flue gas. Figure 5 presents the relationship between resistivity (ohm-cm) and inverse temperature (1000/°K). This is a relatively high resistivity ash (3.9×10^{11} ohm-cm @ 293° F) and demonstrates the requirement for flue gas conditioning in cold-side ESPs treating ashes of this type, as well as the reason hot-side ESPs were selected for Crist Unit 5.

- Ammonia/NO_X Ratio

The ammonia-to-NO_X ratio is normally maintained to give approximately 80% reduction in NO_X across the reactors. This gives a theoretical required ammonia-to-NO_X ratio of roughly 0.83 assuming that the flue gas NO_X concentration consists of 5% NO_2. However, oxygen inleakage can cause an increase in ammonia-to-NO_X ratio if the NO_X values are measured upstream of the flue gas metering device. This is the case in the SCR reactors. As a result, an ammonia-to-NO_X ratio of 0.83 gives an effective ammonia-to-NO_X ratio of approximately 0.88 in the SCR reactors. Consequently, the ammonia-to-NO_X ratio is normally set at 0.74 to 0.76, resulting in an effective ammonia-to-NO_X ratio of about 0.81, giving a NO_X reduction of approximately 80% (based on 1% of the NO_X as NO_2, which is the approximate value for the SCR facility). Due to calibration problems in the ammonia injection system and calibration drift in the venturi flow measurement, the long term effective ammonia-to-NO_X ratio of the SCR reactors was approximately 0.90 during the first two quarters of testing. Parametric testing required variations in the ammonia-to-NO_X ratio. During these tests, the effective ammonia-to-NO_X ratio was varied from a high of approximately 1.2 to a low of approximately 0.7 on each reactor. These parametric tests were conducted over relatively short periods of time and represent only a small fraction of the total reactor operating time.

- Flue Gas Temperature

The SCR facility is equipped with an economizer by-pass duct. This allows for high temperature flue gas extracted upstream of the host unit economizer to be mixed with flue gas extracted downstream of the host unit economizer. By adjusting the relative flows of these two components of the pilot plant feed gas, the temperature to the pilot plant can be adjusted. Under normal operation, the flue gas temperature to the pilot plant is maintained at 650° F. This is possible when the host unit is running at relatively high loads, however, at low unit load, the pilot plant inlet gas temperature often drops below 650°F even with full use of the economizer by-pass duct. Also, under some circumstances, while the host unit is operating at very high load, the feed gas to the pilot plant may exceed 650°F even with no economizer by-pass gas being used. The average temperature of the flue gas fed to the test facility, and the daily high and low

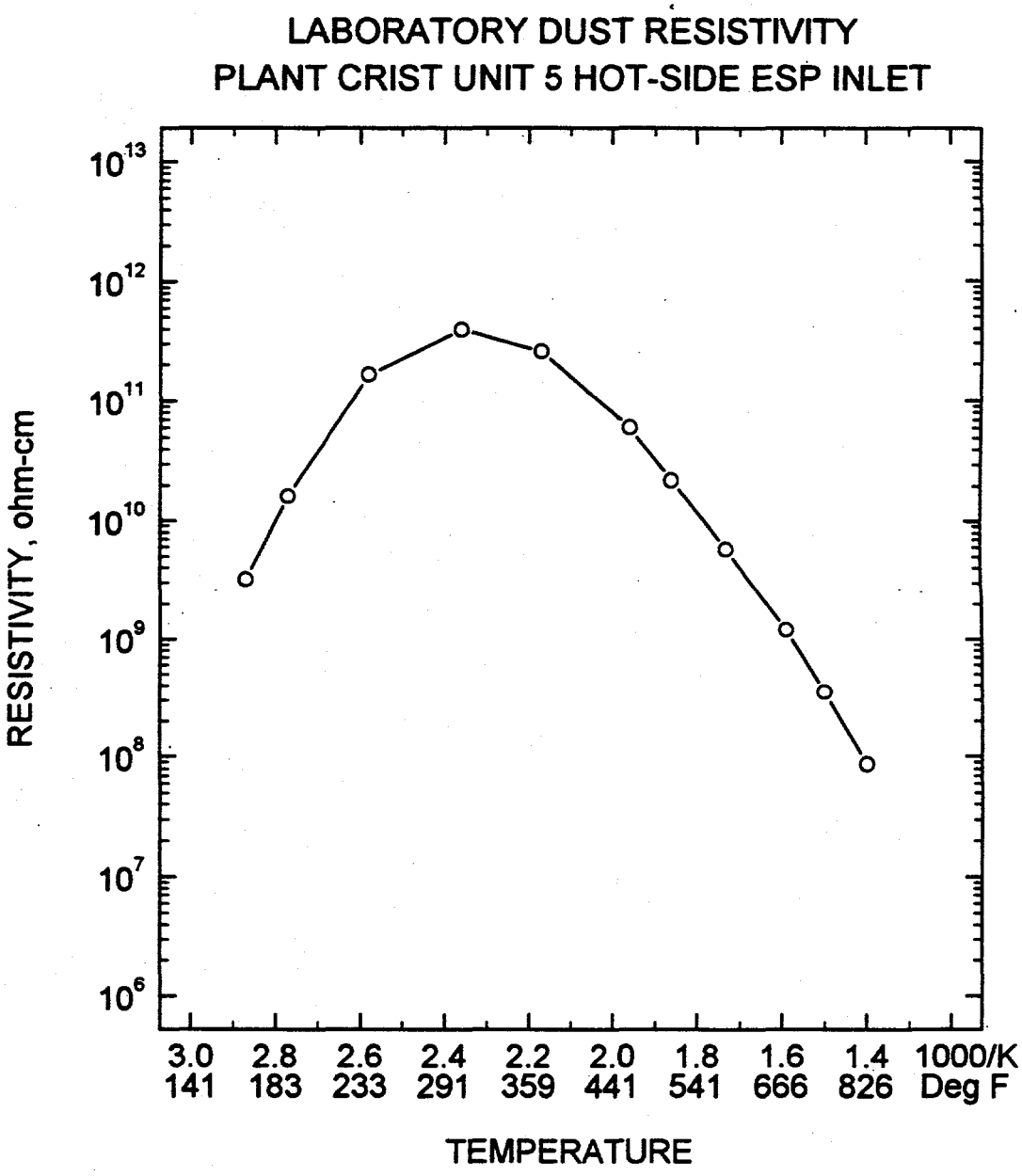

Figure 5 Resistivity of fly ash at the Unit 5 hot-side ESP inlet (high load).

temperatures are shown below for this reporting period. As with the previously shown gas concentration data, this data is constructed using daily averages, daily highs, and daily lows, during periods of on-line host boiler operation.

Test Facility Inlet Gas Temperature (° F)

July-Sept. '93

Average	High	Low
642	658	617

Each reactor is equipped with a flue gas heater which maintains strict control over the temperature of the flue gas entering the reactors. Under normal operating conditions the flue gas is maintained at 700°F at the entrance to the reactors. This requires that the gas be heated from approximately 650°F to 700°F under normal operating conditions. Of course, heat loss in the system requires some additional flue gas heating over the 50°F temperature difference noted. Under parametric conditions, the glue gas temperature to the reactors is varied from a low of approximately 620°F to a high of 750°F. Under these conditions, the economizer bypass duct flow rate may be adjusted to assist the heaters in obtaining the appropriate temperature. Under high temperature parametric conditions, heat loss through the system is more apparent, and flue gas temperatures of 780°F just downstream of the heater may be required to give 750°F at the reactor inlet. Lower temperature parametric conditions do not show as extreme a temperature loss between the heaters and the inlet to the reactors. As a result, the heater exit temperature is normally much closer to the reactor inlet gas temperature during low temperature parametric tests and normal operating conditions.

- Linear, Area, and Space Velocities

The linear, area, and space velocities for each of the reactors are shown below. In the original request for proposals for catalyst suppliers, flue gas temperatures, flow rates, NO_X reduction, and ammonia slip were all specified values. Each catalyst supplier was given the freedom of determining the necessary amounts of respective catalyst required for each reactor. As a result, each reactor has a slightly different space velocity. Area velocity differs more widely due to larger differences in the specific area values of the different catalysts. Free stream linear velocities are identical for each reactor, however, linear velocities within the various catalyst channels differs according to the open facial fraction of the particular catalyst design.

	Siemens	NSKK	Grace Noxeram	Grace Synox	Hitachi Zosen	Haldor Topsoe	Cormetech	Engelhard High Dust	Engelhard Low Dust
SV	3696	2809	2742	3579	2742	3598	3099	5772	12,830
AV	9.65	5.98	6.38	8.32	6.53	7.91	6.96	8.94	9.94
LV	2.13	2.19	2.19	2.10	2.10	2.01	2.10	2.16	2.16

SV = Space Velocity, gas flow/catalyst volume($Nm^3/m^3(hr)$).

AV = Area Velocity, space velocity/geometric surface area ($m^3/m^2(hr)$).

LV = Linear Velocity, gas flow/cross-sectional area (Nm/sec).

- Air Preheater Performance Data

The three large reactors of the SCR facility are each equipped with an air preheater. Reactor A is equipped with a trisector Lungstrum type rotary air preheater supplied by ABB Air Preheater, Inc. of Wellsville, New York. Reactor B is equipped with a bisector rotary air preheater nearly identical to the A preheater, also supplied by ABB. Reactor C is equipped with an ABB Q-pipe which is a heat pipe design utilizing toluene and naphthalene as the working fluids. The original design of the SCR facility included air preheater bypass ducting which allowed the air preheaters to be bypassed during any condition other than normal operating conditions. This was done to insure that the air preheater's long-term fouling characteristics were not skewed by extreme conditions during some of the short term parametric tests. The large reactor fan design requires relatively cool gas (less than 350°F). To accommodate this restriction, the air preheater bypass ducting was equipped with heat exchangers which were designed to cool the flue gas in place of the air preheaters. Unfortunately, the design of the by-pass heat exchangers caused immediate fouling upon use, making it unsatisfactory for the application. Consequently, the SCR facility is forced to use the three large reactor air preheaters at all times when on-line to maintain proper flue gas conditions for the large reactor fans. As a result, the air preheaters are exposed to the harsh conditions created by some of the parametric tests. However, these test periods are very short compared to the overall operating time at standard conditions, and it is assumed that overall fouling characteristics of the air preheaters are not greatly affected by the current operational requirements. The average operating parameters for the three air preheaters are shown below over this reporting period and these values include any parametric test conditions that were performed during the specific time period.

AVERAGE AIR PREHEATER OPERATIONAL PARAMETERS, JULY-SEPT 1993.

Parameter	APH A	APH B	APH C
Gas flow rate (SCFM)	4712	4778	5321
Air flow rate (SCFM)	5070	4150	5910
Inlet gas temp. (^{O}F)	643	648	659
Exit gas temp. (^{O}F)	324	309	315
Inlet air temp. (^{O}F)	100	100	100
Exit air temp. (^{O}F)	593	577	533
Gas side press. drop ("H_2O)	3.73	3.26	1.75
Air side press. drop ("H_2O)	1.66	1.51	NA
Air/Gas diff. press. ("H_2O)	0.58	0.42	NA
Inlet gas O_2 (% wet)	4.92	4.43	3.96
Exit gas O_2 (% wet)	7.07	8.73	NA

- Catalyst-Specific Performance Parameters

- Reactor A

The following table shows the performance of the catalyst at or near the design operating conditions of 0.8 ammonia-to-NOx ratio, 5,000 SCFM flow rate, and 700^{O} F reactor temperature. As can be seen in the table, the actual measured ammonia-to-NOx ratio is greater than 0.8. This is primarily the result of some miscalibrations in both flow rate and ammonia injection rate, creating a higher than desired ammonia-to-NOx ratio. This higher ratio, however, has one beneficial effect in that it creates ammonia slip values that are well within the ammonia sampling method detection range. Slip values measured at 0.8 ammonia-to-NOx ratio are expected to be near or below detection limits. Slips within the detection limits allow for more accurate comparisons between catalysts and also allow for more accurate reactor modeling to be performed. Also included in the table is the baseline SO_2 oxidation rate and the corresponding reactor conditions for the measurement. Ammonia slip and SO_2 oxidation are not typically measured simultaneously and therefore the reactor operating conditions differ slightly for the reported slip and SO_2 oxidation values.

BASELINE PERFORMANCE

Flow (SCFM)	Temp. (°F)	NOx in (ppmv)	NH3/NOx Ratio	NH_3 Slip (ppmv)	NOx Red. (%)	SO_2 Ox. (%)
4491	700	286	.92	5.7	89%	--
4372	700	239	.92	--	89%	0.22

The majority of the ammonia measurements during the preliminary parametric tests focused on concentrations downstream of the first catalyst bed. These measurements were made as part of a series of statistically designed tests which varied flow rate, temperature, and ammonia-to-NOx ratio. Each of these parameters was varied using a high and low value. Thus, eight permutations are created which correspond to the eight test conditions for this portion of the parametric tests. The results of this series of tests are shown as a plot of NOx removal across the first catalyst bed versus ammonia-to-NOx ratio in Figure 6-1. Test procedures called for the measurement of ammonia, which is used in the kinetic analyses. The reported NOx removals for the plot shown below are computed from the measured ammonia concentration using standard material balance techniques.

FIRST BED NOx RED. vs. NH3/NOx RATIO

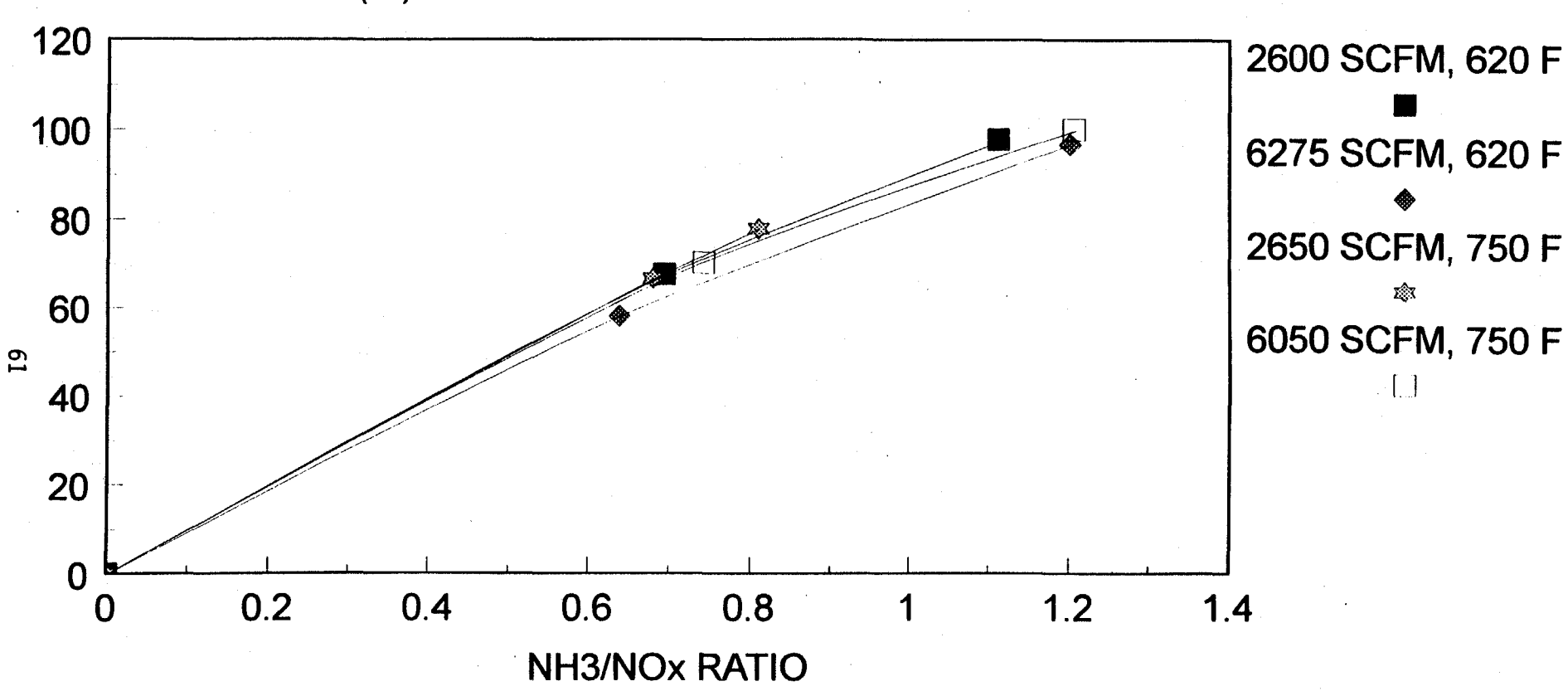

Catalyst - Grace Noxeram
Figure 6-1

The following table shows the data used to generate the previous plot. Also included is base line intermediate ammonia data. The data are presented in terms of intermediate ammonia concentrations, which is the measured parameter. All data is corrected to reactor inlet oxygen concentrations.

INTERMEDIATE AMMONIA PARAMETRIC TEST DATA

Flow Rate (SCFM)	Rxr Inlet Temp. (°F)	Inlet O_2 (%)	Inlet NOx (ppmv)	NH_3/NOx Ratio	Int. NH_3 (ppmv)
2588	620	2.914	287	0.694	5.3
2641	620	2.731	293	1.112	39.3
6637	620	4.989	356	0.638	20.6
5910	620	5.414	368	1.201	86.3
4211	700	5.765	326	0.966	14.1
2667	750	1.916	274	0.680	3.6
2619	750	1.842	374	0.810	11.9
6299	750	5.503	320	0.742	13.3
5799	750	3.191	287	1.206	31.9

Parametric tests were also performed to determine the sulfur dioxide oxidation characteristics of the catalyst. The operating parameters of the reactor were varied in an identical fashion to the intermediate ammonia parametric tests. Thus, eight specific parametric tests were performed in addition to the base line test. The data is presented in two plots, Figure 6-2 one showing the effect of flow rate on sulfur dioxide oxidation, and Figure 6-3 one showing the effect of temperature on sulfur dioxide oxidation. The flow rate effect data is based on high temperature data, with two lines shown, one for high ammonia-to-NOx ratio, and one for low ammonia-to-NOx ratio. The temperature effect is based on low ammonia-to-NOx ratio data, with two lines shown, one for high flow rate, and one for low flow rate. The plots show a definite ammonia-to-NOx ratio effect on the sulfur dioxide oxidation characteristics of the catalyst. However, this effect is not thought to be a true catalytic effect , but is actually a precipitation effect. Earlier studies with no catalyst present showed that sulfur trioxide was lost through the reactor, most likely in cold spots such as test ports, etc. The presence of ammonia may affect this precipitation phenomenon. Most likely this occurs by changing the precipitation characteristics of the sulfur trioxide through the formation of byproducts such as ammonium bisulfate in the cold spots of the reactor.

SO2 OXIDATION VS. FLOW RATE

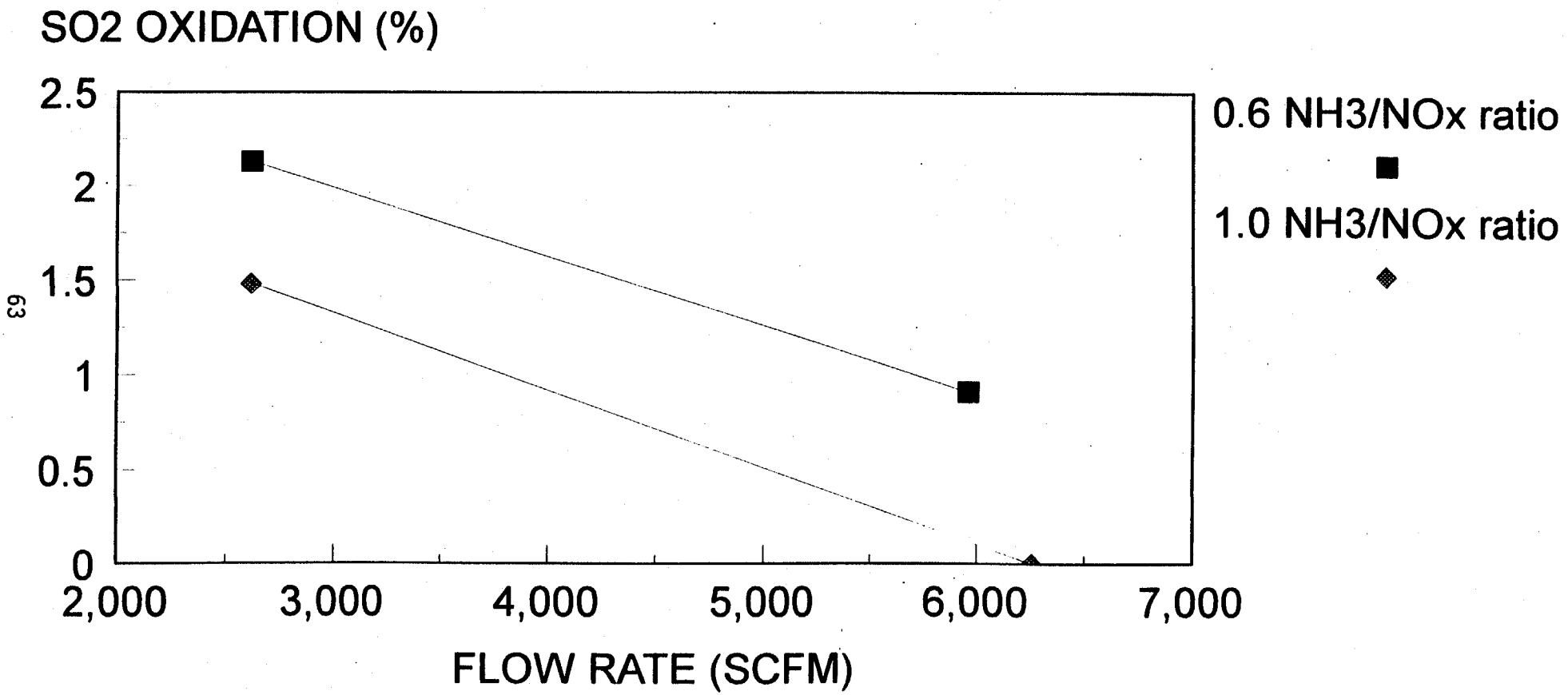

Catalyst - Grace Noxeram
Figure 6-2

SO2 OXIDATION VS. TEMPERATURE

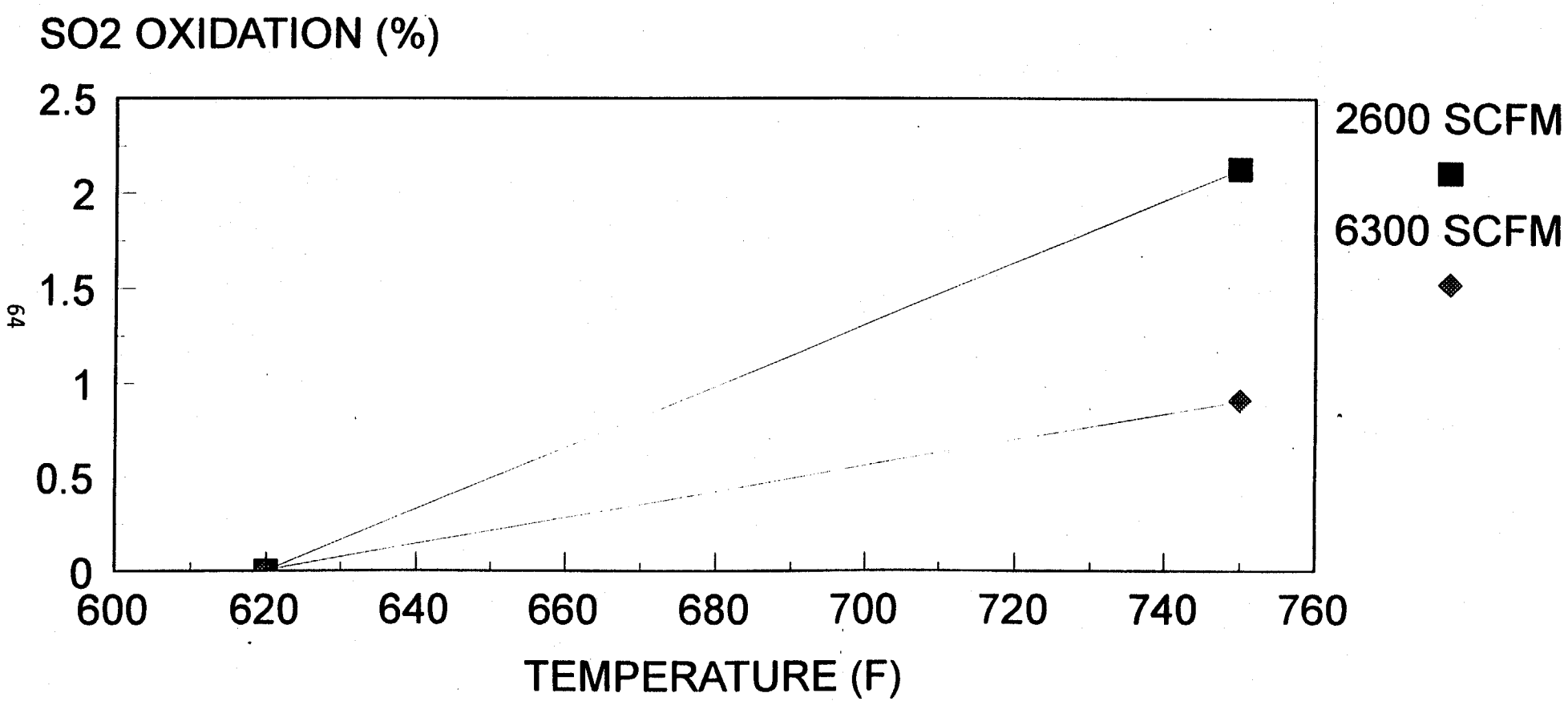

Catalyst - Grace Noxeram
Figure 6-3

Similar to the previously shown table of intermediate ammonia data, the following data shows the sulfur dioxide oxidation data for each of the parametric conditions that were tested. This data is corrected to reactor outlet oxygen concentrations. The value for sulfur trioxide produced in the reactor is based on the measured outlet sulfur trioxide concentration and estimated sulfur trioxide reactor inlet values. The reactor inlet sulfur trioxide values are estimated using past measurements of inlet sulfur trioxide based on host boiler load. In many cases, especially those involving low temperature conditions, there was no net increase in sulfur trioxide concentrations across the reactor. In fact, some operating conditions showed a loss in sulfur trioxide across the reactor in addition to the loss that normally occurs without catalyst present. In these cases, the sulfur dioxide oxidation rate is taken to be zero.

SULFUR DIOXIDE OXIDATION PARAMETRIC TEST DATA

Flow Rate (SCFM)	Rxr Inlet Temp. (%)	Outlet O_2 (%)	Inlet SO_2 (ppmv)	NH_3/ NOx Ratio	SO_3 formed (ppmv)	Predicted/ /SO_3 in (ppmv)	Measured /SO_3 out (ppmv)	Oxid. Rate (%)
2683	620	3.265	1974	0.700	-9	13.9	4.7	0
2698	620	4.633	1629	1.164	-6	13.9	7.6	0
6581	620	3.117	1955	0.714	-1	8.4	7.8	0
6560	620	2.884	1969	1.194	-5	8.0	3.1	0
2716	750	3.055	2007	0.674	43	10.5	53.3	2.13
2713	750	3.023	2008	1.111	30	10.1	39.8	1.48
5952	750	2.603	2070	0.581	19	9.3	29.1	0.91
6454	750	6.462	1239	1.089	-12	22.2	10.7	0

The pressure drop across the reactor is another important criteria for SCR usage because of its effect on fan horsepower requirements, the single largest energy need for the SCR process. Typical reactor pressure drop is shown in Figure 6-4.

FIGURE 6-4. REACTOR A PRESSURE DROP

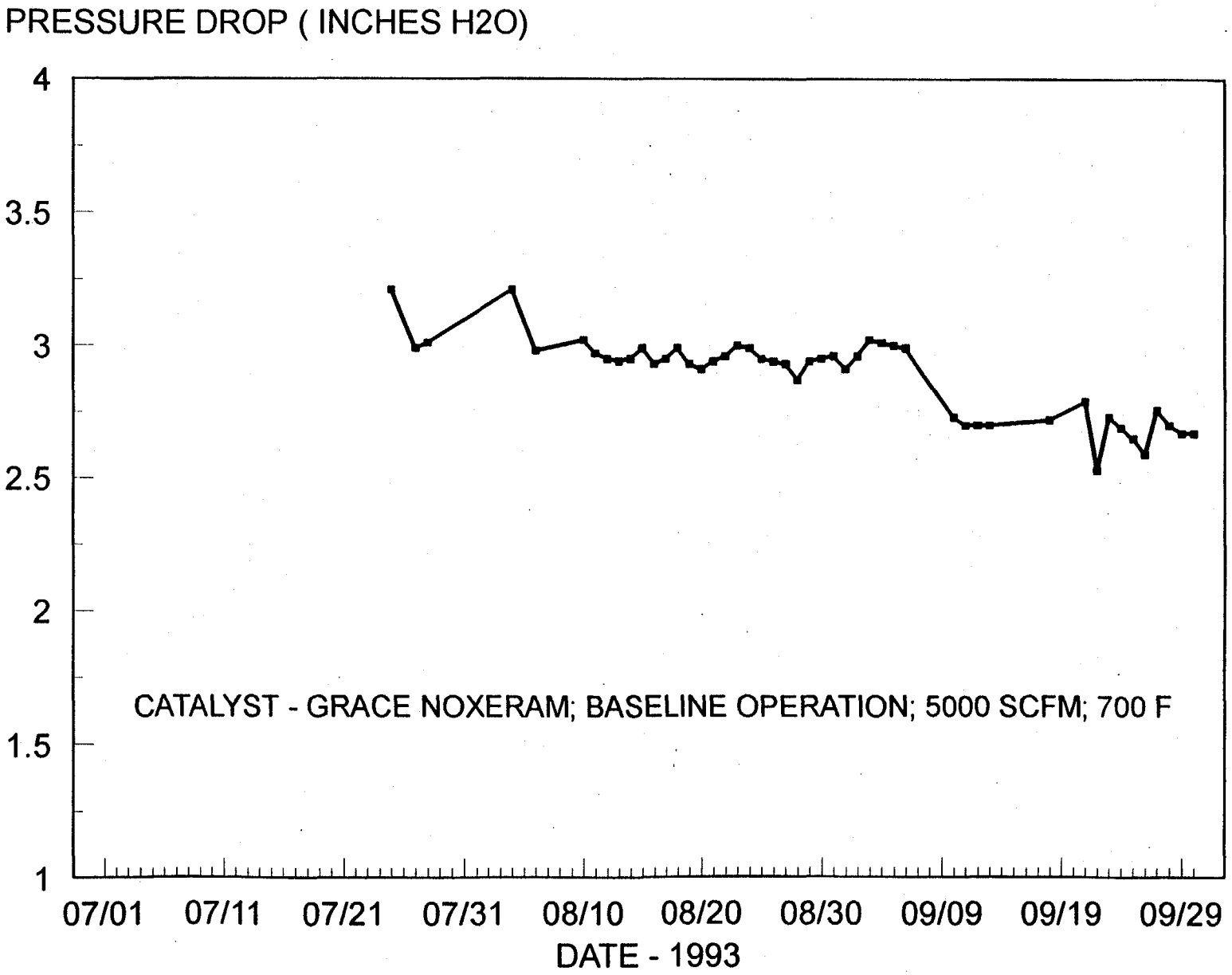

- Reactor B

The following table shows the performance of the catalyst at or near the design operating conditions of 0.8 ammonia-to-NOx ratio, 5,000 SCFM flow rate, and 700° F reactor temperature. As can be seen in the table, the actual measured ammonia-to-NOx ratio is greater than 0.8. This is primarily the result of some miscalibrations in both flow rate and ammonia injection rate, creating a higher than desired ammonia-to-NOx ratio. This higher ratio, however, has one beneficial effect in that it creates ammonia slip values that are well within the ammonia sampling method detection range. Slip values measured at 0.8 ammonia-to-NOx ratio are expected to be near or below detection limits. Slips within the detection limits allow for more accurate comparisons between catalysts and also allow for more accurate reactor modeling to be performed. Also included in the table is the baseline SO_2 oxidation rate and the corresponding reactor conditions for the measurement. Ammonia slip and SO_2 oxidation are not typically measured simultaneously and therefore the reactor operating conditions differ slightly for the reported slip and SO_2 oxidation values.

BASELINE PERFORMANCE

Flow Rate (SCFM)	Temp. (°F)	NOx IN (ppmv)	NH3/NOx Ratio	NH_3 Slip (ppmv)	NOx Red. (%)	SO_2 Ox. (%)
4208	700	307	.985	0.9	96%	--
4191	700	279	.930	--	91%	0

The majority of the ammonia measurements during the preliminary parametric tests focused on concentrations downstream of the first catalyst bed. These measurements were made as part of a series of statistically designed tests which varied flow rate, temperature, and ammonia-to-NOx ratio. Each of these parameters was varied using a high and low value. Thus, eight permutations are created which correspond to the eight test conditions for this portion of the parametric tests. The results of this series of tests are shown as a plot of NOx removal across the first catalyst bed versus ammonia-to-NOx ratio in Figure 7-1. Test procedures called for the measurement of ammonia, which is used in the kinetic analyses. The reported NOx removals for the plot shown below are computed from the measured ammonia concentration using standard material balance techniques.

FIRST BED NOx RED. vs. NH3/NOx RATIO

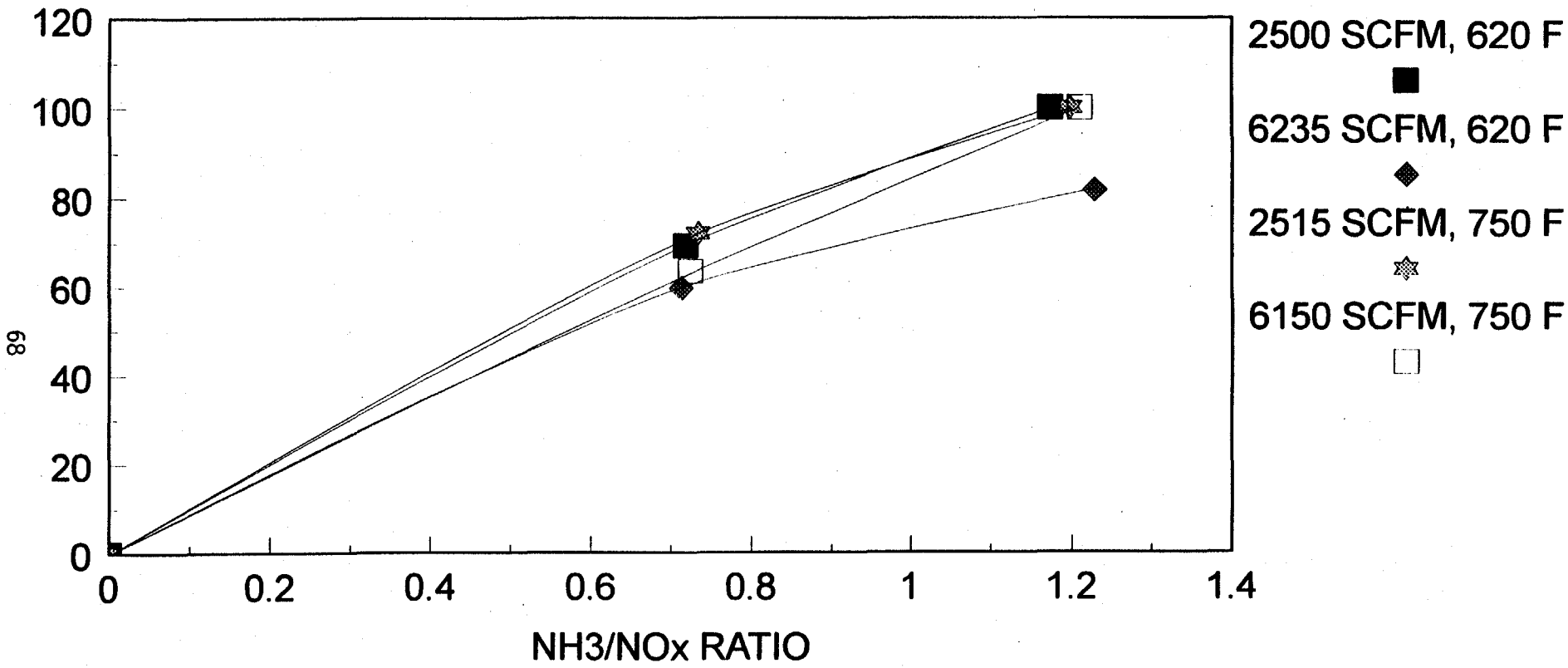

Catalyst - NSKK
Figure 7-1

The following table shows the data used to generate the previous plot. Also included is base line intermediate ammonia data. The data are presented in terms of intermediate ammonia concentrations, which is the measured parameter. All data is corrected to reactor inlet oxygen concentrations.

INTERMEDIATE AMMONIA PARAMETRIC TEST DATA

Flow Rate (SCFM)	Rxr Inlet Temp. (°F)	Inlet O_2 (%)	Inlet NOx (ppmv)	NH_3 /NOx Ratio	Int. NH_3 (ppmv)o
2562	620	2.157	290	0.718	7.7
2428	620	5.024	353	1.174	46.5
6310	620	2.752	292	0.713	34.1
6161	620	2.541	291	1.228	120.6
4211	700	4.902	357	0.896	30.4
2522	750	2.052	283	0.734	4.1
2509	750	2.080	284	1.198	13.4
6211	750	1.699	276	0.724	24.9
6084	750	2.264	281	1.210	49.7

Parametric tests were also performed to determine the sulfur dioxide oxidation characteristics of the catalyst. The operating parameters of the reactor were varied in an identical fashion to the intermediate ammonia parametric tests. Thus, eight specific parametric tests were performed in addition to the base line test. The data is presented in two plots, Figure 7-2 showing the effect of flow rate on sulfur dioxide oxidation, and Figure 7-3 showing the effect of temperature on sulfur dioxide oxidation. The flow rate effect data is based on high temperature data, with two lines shown, one for high ammonia-to-NOx ratio, and one for low ammonia-to-NOx ratio. The temperature effect is based on low ammonia-to-NOx ratio data, with two lines shown, one for high flow rate, and one for low flow rate. The plots show a definite ammonia-to-NOx ratio effect on the sulfur dioxide oxidation characteristics of the catalyst. However, this effect is not thought to be a true catalytic effect , but is actually a precipitation effect. Earlier studies with no catalyst present showed that sulfur trioxide was lost through the reactor, most likely in cold spots such as test ports, etc. The presence of ammonia may affect this precipitation phenomenon. Most likely this occurs by changing the precipitation characteristics of the sulfur trioxide through the formation of byproducts such as ammonium bisulfate in the cold spots of the reactor.

SO2 OXIDATION VS. FLOW RATE

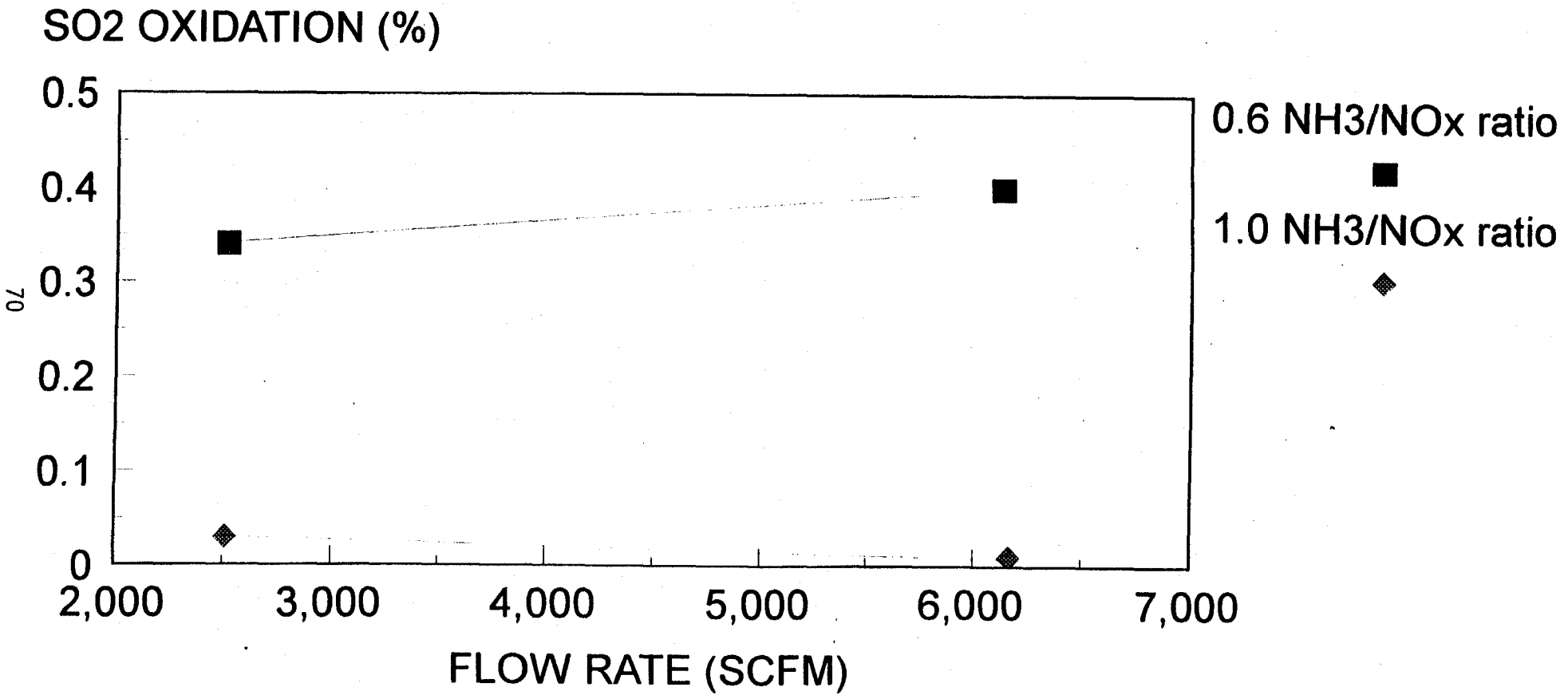

Catalyst - NSKK, 750°F
Figure 7-2

SO2 OXIDATION VS. TEMPERATURE

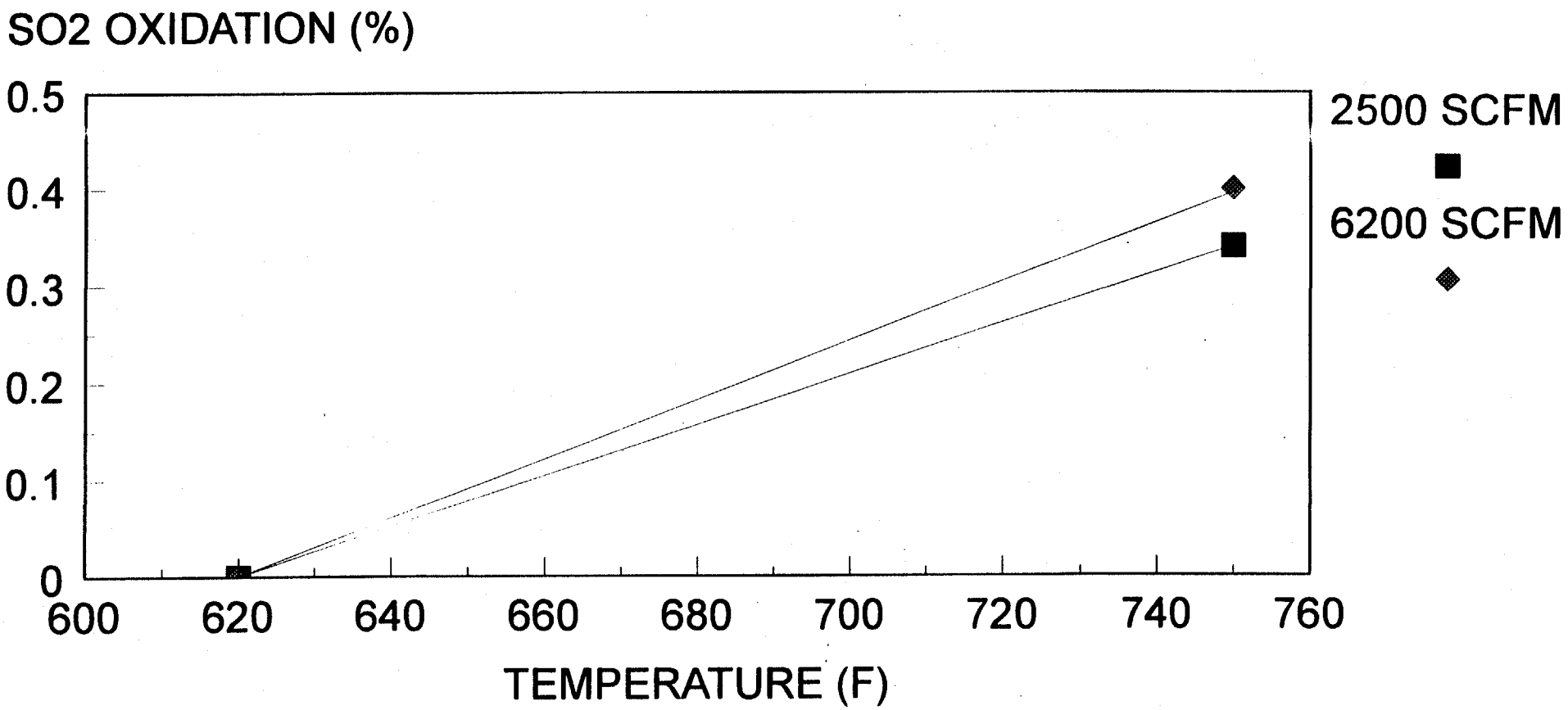

Catalyst - NSKK, 0.6 NH3/NOx Ratio
Figure 7-3

Similar to the previously shown table of intermediate ammonia data, the following data shows the sulfur dioxide oxidation data for each of the parametric conditions that were tested. This data is corrected to reactor outlet oxygen concentrations. The value for sulfur trioxide produced in the reactor is based on the measured outlet sulfur trioxide concentration and estimated sulfur trioxide reactor inlet values. The reactor inlet sulfur trioxide values are estimated using past measurements of inlet sulfur trioxide based on host boiler load. In many cases, especially those involving low temperature conditions, there was no net increase in sulfur trioxide concentrations across the reactor. In fact, some operating conditions showed a loss in sulfur trioxide across the reactor in addition to the loss that normally occurs without catalyst present. In these cases, the sulfur dioxide oxidation rate is taken to be zero.

SULFUR DIOXIDE OXIDATION PARAMETRIC TEST DATA

Flow Rate (SCFM)	Rxr Inlet Temp. (°F)	Outlet O_2 (%)	Inlet SO_2 (ppmv)	NH_3/ NOx Ratio	SO_3 formed (ppmv)	Predicted/ SO_3 in (ppmv)	Measured SO_3 out (ppmv)	Oxid. Rate (%)
2504	620	4.162	1688	0.713	-12	17.6	5.2	0
2514	620	3.572	1895	1.235	-5	8.9	4.0	0
6274	620	2.654	2002	0.729	-2	8.4	5.9	0
6282	620	2.342	2006	1.187	-6	8.0	2.2	0
2514	750	3.717	1846	0.720	6	16.8	23.1	0.34
2511	750	4.293	1697	1.221	1	14.3	14.8	0.03
6135	750	3.522	1806	0.743	7	13.5	20.7	0.40
6167	750	2.951	1970	1.245	0	8.9	9.2	0.01

The pressure drop across the reactor is another important criteria for SCR usage because of its effect on fan horsepower requirements, the single largest energy need for the SCR process. Typical reactor pressure drop is shown in Figure 7-4..

- Reactor C

The following table shows the performance of the catalyst at or near the design operating conditions of 0.8 ammonia-to-NOx ratio, 5,000 SCFM flow rate, and 700^{O} F reactor temperature. As can be seen in the table, the actual measured ammonia-to-NOx ratio is greater than 0.8. This is primarily the result of some miscalibrations in both flow rate and ammonia injection rate,

FIGURE 7-4. REACTOR B PRESSURE DROP

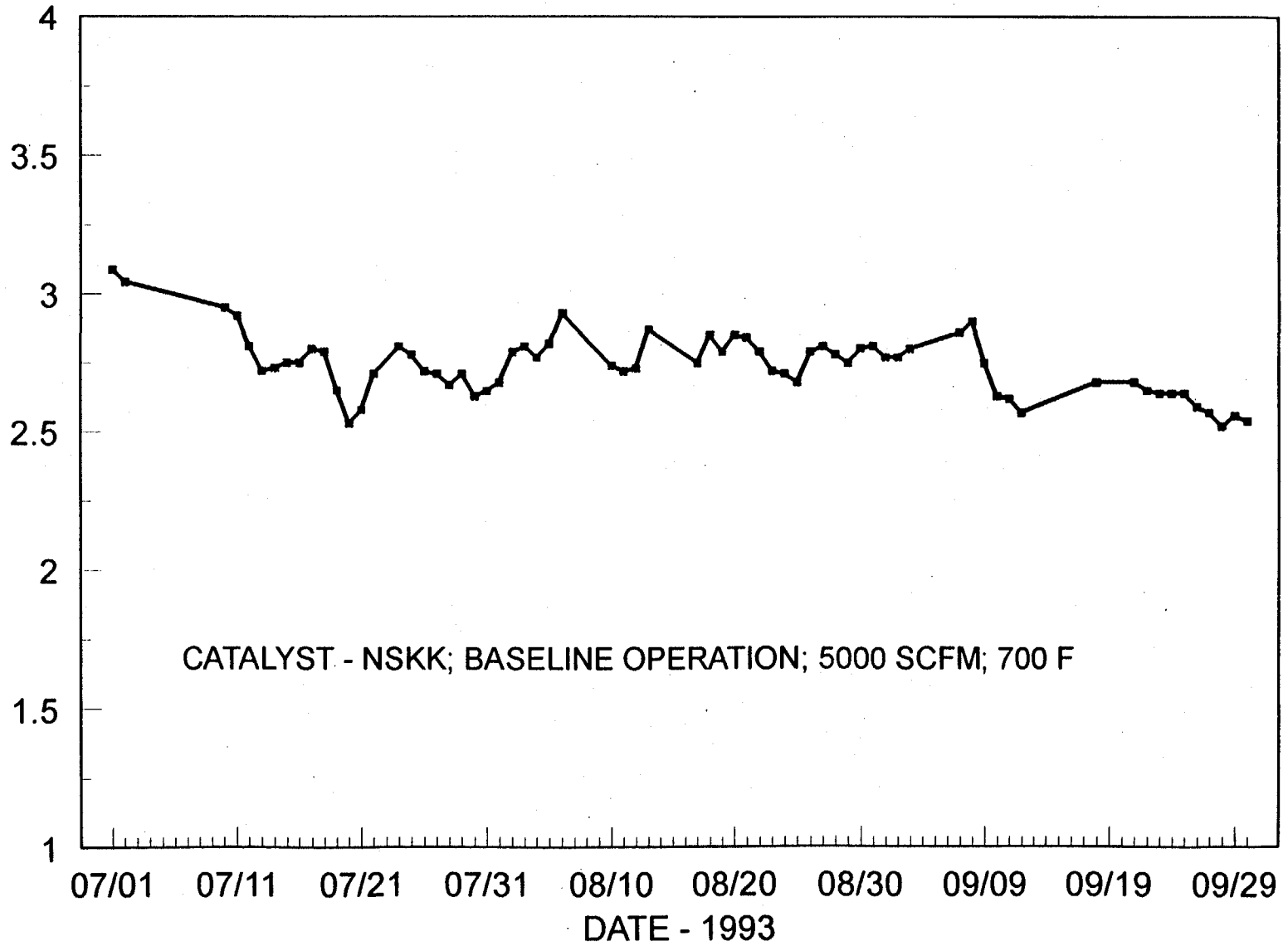

creating a higher than desired ammonia-to-NOx ratio. This higher ratio, however, has one beneficial effect in that it creates ammonia slip values that are well within the ammonia sampling method detection range. Slip values measured at 0.8 ammonia-to-NOx ratio are expected to be near or below detection limits. Slips within the detection limits allow for more accurate comparisons between catalysts and also allow for more accurate reactor modeling to be performed. Also included in the table is the baseline SO_2 oxidation rate and the corresponding reactor conditions for the measurement. Ammonia slip and SO_2 oxidation are not typically measured simultaneously and therefore the reactor operating conditions differ slightly for the reported slip and SO_2 oxidation values.

BASELINE PERFORMANCE

Flow Rate (SCFM)	Temp. (°F)	NOx In (ppmv)	NH3/NOx Ratio	NH_3 Slip (ppmv)	NOx Red. (%)	SO_2 Ox. (%)
4221	700	298	0.960	4	96%	--
4313	700	267	1.169	--	97%	1.19

The majority of the ammonia measurements during the preliminary parametric tests focused on concentrations downstream of the first catalyst bed. These measurements were made as part of a series of statistically designed tests which varied flow rate, temperature, and ammonia-to-NOx ratio. Each of these parameters was varied using a high and low value. Thus, eight permutations are created which correspond to the eight test conditions for this portion of the parametric tests. The results of this series of tests are shown as a plot of NOx removal across the first catalyst bed versus ammonia-to-NOx ratio in Figure 8-1. Test procedures called for the measurement of ammonia, which is used in the kinetic analyses. The reported NOx removals for the plot shown below are computed from the measured ammonia concentration using standard material balance techniques.

The following table shows the data used to generate the previous plot. Also included is base line intermediate ammonia data. The data are presented in terms of intermediate ammonia concentrations, which is the measured parameter. All data is corrected to reactor inlet oxygen concentrations.

FIRST BED NOx RED. vs. NH3/NOx RATIO

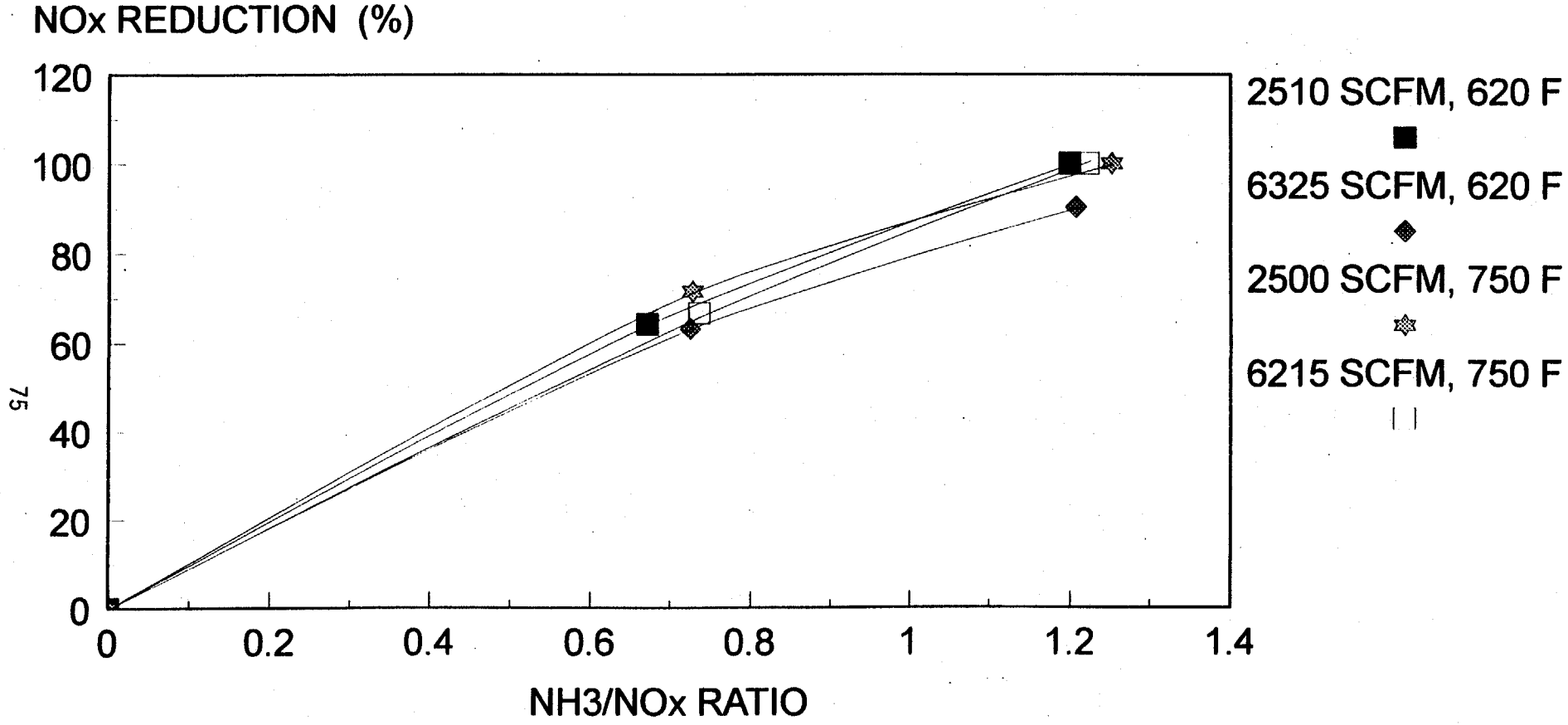

Catalyst - Siemens
Figure 8-1

INTERMEDIATE AMMONIA PARAMETRIC TEST DATA

Flow Rate (SCFM)	Rxr Inlet Temp. (°F)	Inlet O_2 (%)	Inlet NOx (ppmv)	NH_3/NOx Ratio	Int. NH_3 (ppmv)
2526	620	1.853	275	0.671	8.7
2504	620	2.697	286	1.199	55.1
6323	620	1.931	275	0.725	35.6
4195	620	2.250	280	1.207	85.5
2549	700	5.169	351	0.909	26.9
2443	750	2.320	286	0.728	6.9
6206	750	5.713	330	1.252	37.4
6228	750	2.518	284	0.736	18.8
6084	750	2.868	287	1.223	53.1

Parametric tests were also performed to determine the sulfur dioxide oxidation characteristics of the catalyst. The operating parameters of the reactor were varied in an identical fashion to the intermediate ammonia parametric tests. Thus, eight specific parametric tests were performed in addition to the base line test. The data is presented in two plots, Figure 8-2 showing the effect of flow rate on sulfur dioxide oxidation, and Figure 8-3 showing the effect of temperature on sulfur dioxide oxidation. The flow rate effect data is based on high temperature data, with two lines shown, one for high ammonia-to-NOx ratio, and one for low ammonia-to-NOx ratio. The temperature effect is based on low ammonia-to-NOx ratio data, with two lines shown, one for high flow rate, and one for low flow rate. The plots show a definite ammonia-to-NOx ratio effect on the sulfur dioxide oxidation characteristics of the catalyst. However, this effect is not thought to be a true catalytic effect , but is actually a precipitation effect. Earlier studies with no catalyst present showed that sulfur trioxide was lost through the reactor, most likely in cold spots such as test ports, etc. The presence of ammonia may affect this precipitation phenomenon. Most likely this occurs by changing the precipitation characteristics of the sulfur trioxide through the formation of byproducts such as ammonium bisulfate in the cold spots of the reactor.

Similar to the previously shown table of intermediate ammonia data, the following data shows the sulfur dioxide oxidation data for each of the parametric conditions that were tested. This data is corrected to reactor outlet oxygen concentrations. The value for sulfur trioxide produced in the

SO2 OXIDATION VS. FLOW RATE

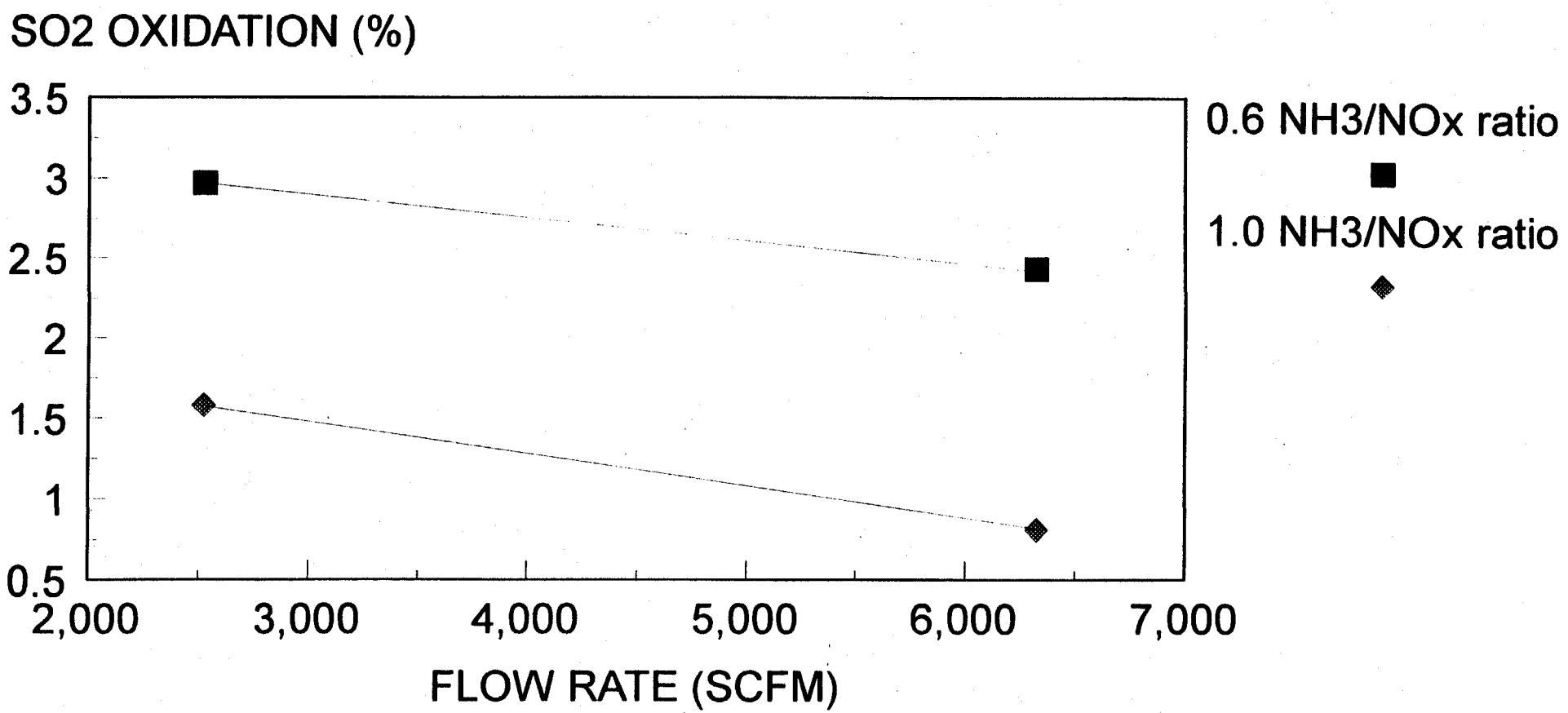

Catalyst - Siemens
Figure 8-2

SO2 OXIDATION VS. TEMPERATURE

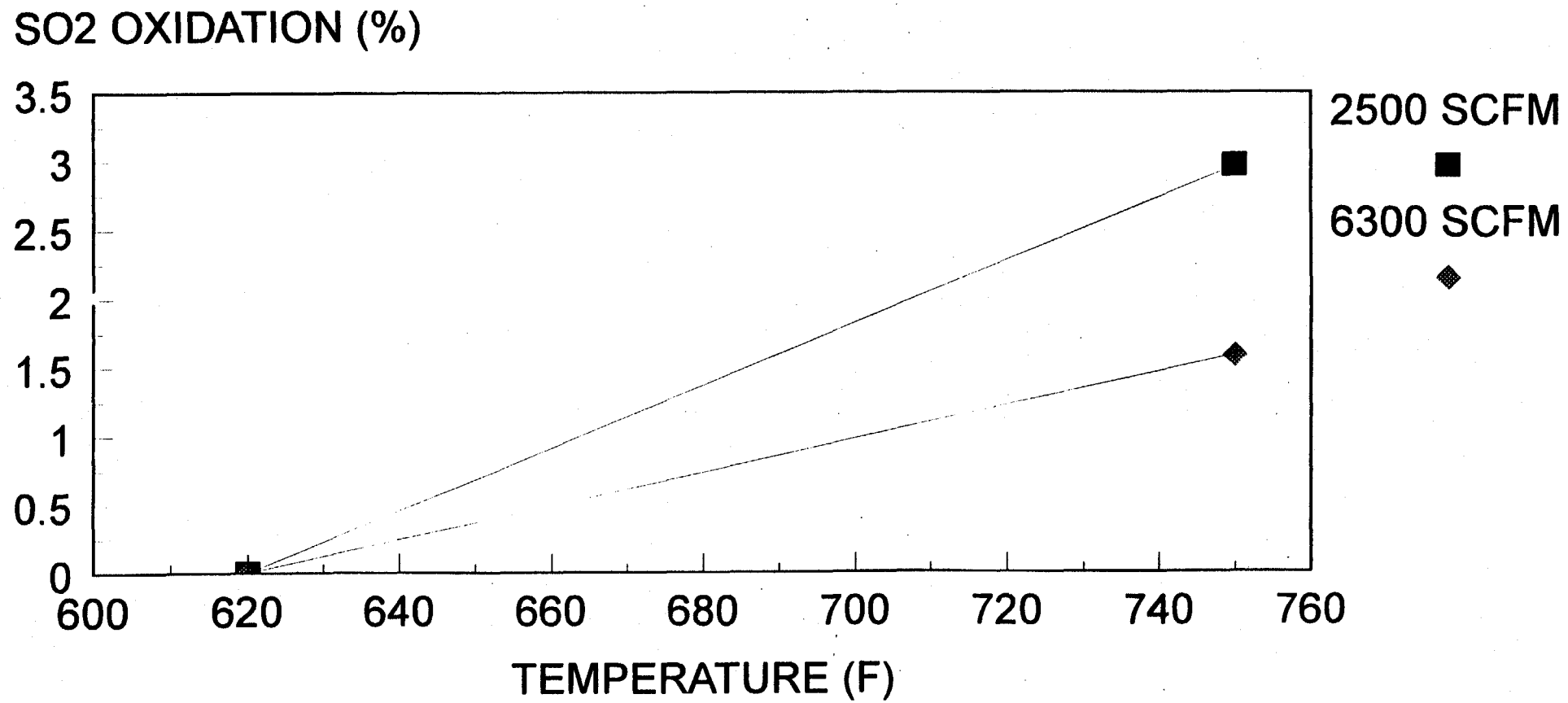

Catalyst - Siemens, 0.6 NH3/NOx Ratic
Figure 8-3

reactor is based on the measured outlet sulfur trioxide concentration and estimated sulfur trioxide reactor inlet values. The reactor inlet sulfur trioxide values are estimated using past measurements of inlet sulfur trioxide based on host boiler load. In many cases, especially those involving low temperature conditions, there was no net increase in sulfur trioxide concentrations across the reactor. In fact, some operating conditions showed a loss in sulfur trioxide across the reactor in addition to the loss that normally occurs without catalyst present. In these cases, the sulfur dioxide oxidation rate is taken to be zero.

SULFUR DIOXIDE OXIDATION PARAMETRIC TEST DATA

Flow Rate (SCFM)	Rxr Inlet Temp. (°F)	Outlet O_2 (%)	Inlet SO_2 (ppmv)	NH_3/ NOx Ratio	SO_3 formed (ppmv)	Predicted/ SO_3 in (ppmv)	Measured SO_3 out (ppmv)	Oxid. Rate (%)
2530	620	4.851	1596	0.708	-7	23.5	16.7	0
2528	620	3.259	1898	1.213	-3	9.7	6.6	0
6198	620	3.032	976	0.704	-22	25.5	2.7	0
6326	620	3.364	1919	1.197	-9	15.5	6.6	0
2527	750	4.321	1673	0.723	17	16.4	66.0	2.97
2522	750	3.134	1949	1.221	50	8.9	56.3	2.43
6326	750	2.533	2002	0.720	47	8.0	39.7	1.58
6326	750	4.468	1632	1.128	13	14.3	27.5	0.81

The pressure drop across the reactor is another important criteria for SCR usage because of its effect on fan horsepower requirements, the single largest energy need for the SCR process. Typical reactor pressure drop is shown in Figure 8-4.

FIGURE 8-4. REACTOR C PRESSURE DROP

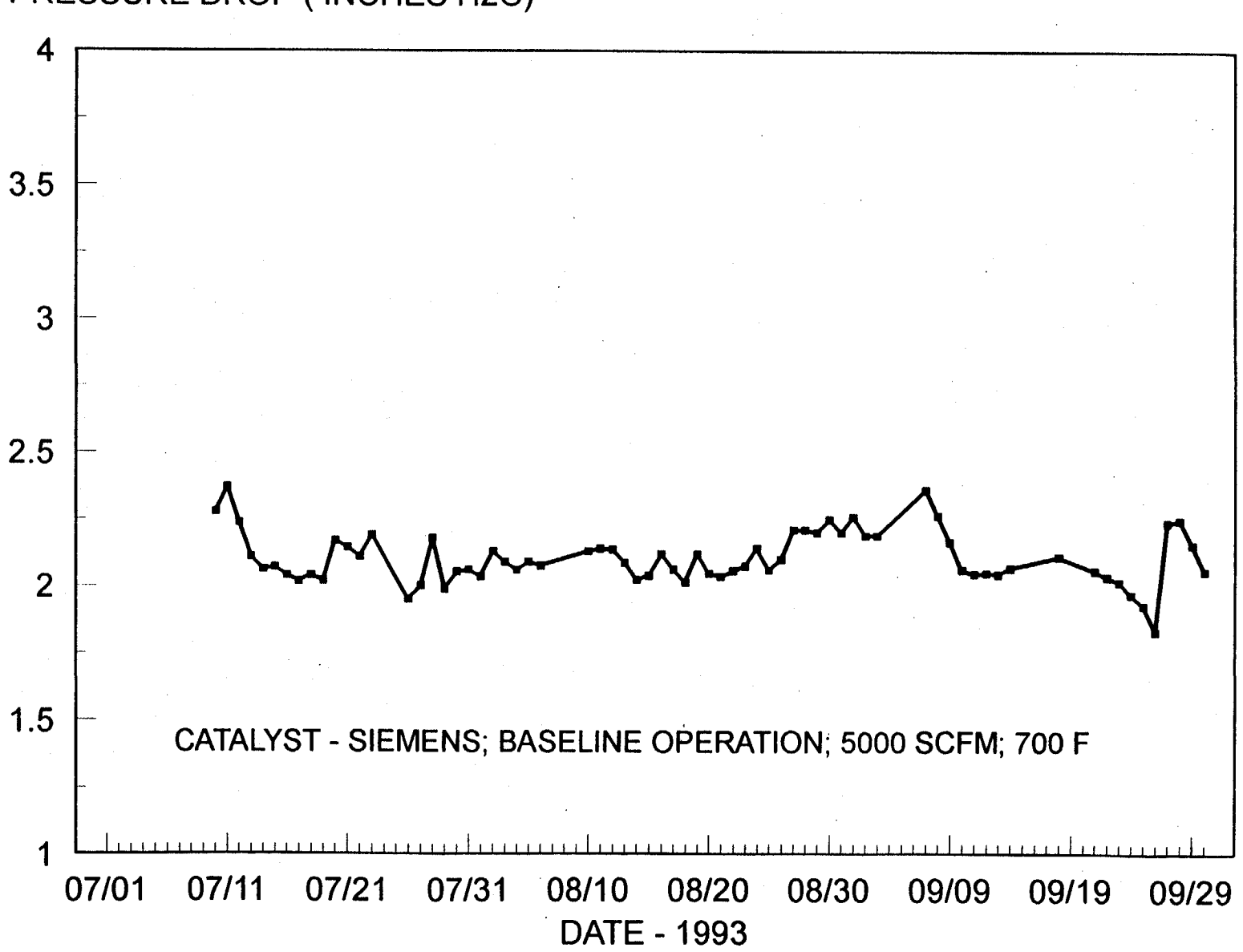

Task 1.3.6 - Project Management and Reporting

A project review meeting was held for all involved parties on September 2 at Plant Crist. A paper on the project status was presented at the Second Annual Clean Coal Technology Conference sponsored by DOE during September 7-9 in Atlanta, Georgia.

A Continuation Application and request for additional funds, which were previously submitted to DOE, continued to be considered for approval. The Continuation Application requested DOE's approval for matching funds of Budget Period 2 to continue the project to completion. Budget Period 2 provides DOE funding for Phase III, which includes operations, testing, disposition, and final report. Project cost growth was projected based on improvements to the facility design and additional funding was requested from DOE in the amount of 25% of DOE's original funding of the project. Funding from the other co-funders was also solicited to cover the entire cost growth.

Section 5

PLANNED ACTIVITIES

During the October - December, 1993 quarter, the following activities are planned:

- Complete the first set of parametric tests on all remaining reactors/catalysts not completed during this current reporting period. Meanwhile, continue operations at long term conditions for the reactors/catalysts when not undergoing parametric testing.

- Take the first set of catalyst samples and submit for laboratory analysis.

- Complete repairs for low dust reactor system.

- Continue to improve the gas analyzer system operation and ammonia flow controllers, attempt to resolve problems with the continuous NOx measuring system for the intermediate bed levels (with ammonia present).

- Hold status meeting in December.

REFERENCES

1. Testing and Analytical Services for the Innovative Clean Coal Technology Demonstration of Selective Catalytic Reduction (SCR) Technology for the Control of Nitrogen Oxide (NOx) Emissions from High Sulfur Coal, Final Report for Task 1, Commissioning without Catalysts and without Ammonia Injection, Draft.

APPENDIX A

Tables 4, 5, 11, 12 and 13 from the final report from Southern Research Institute to Southern Company Services under SCS Contract Number 195-89-046.

Table 4

CRIST UNIT 5 ESP INLET
HIGH-LOAD NO, NO_x, AND OXYGEN DISTRIBUTIONS

		NO CONCENTRATION ppm			NO_x CONCENTRATION ppm			O_2 CONCENTRATION %		
DATE	PORT	Pt 1	Pt 2	Pt 3	Pt 1	Pt 2	Pt 3	Pt 1	Pt 2	Pt 3
7/30/90	1	322	320	352	345	343	352	NA	NA	NA
	2	321	321	337	345	346	354	NA	NA	NA
	3	325	326	335	354	352	360	NA	NA	NA
	4	327	329	348	358	358	361	NA	NA	NA
	5	331	329	330	360	361	362	NA	NA	NA
	6	330	330	341	358	359	367	NA	NA	NA
	DUCT AVERAGE		331			355				
	STD DEV		9			7				
	COEFF OF VAR		0.026			0.019				
7/31/90	1	322	323	345	342	344	352	NA	NA	NA
	2	317	320	326	336	343	346	NA	NA	NA
	3	320	317	320	346	342	345	NA	NA	NA
	4	320	318	338	338	345	354	NA	NA	NA
	5	315	317	321	337	338	341	NA	NA	NA
	6	312	312	324	328	328	337	NA	NA	NA
	DUCT AVERAGE		321			341				
	STD DEV		8			6				
	COEFF OF VAR		0.025			0.019				
8/02/90	1	318	319	335	325	325	335	NA	NA	NA
	2	321	319	327	328	329	331	NA	NA	NA
	3	325	327	336	337	340	343	NA	NA	NA
	4	323	333	337	342	349	347	NA	NA	NA
	5	330	319	335	350	342	350	NA	NA	NA
	6	329	328	338	346	354	350	NA	NA	NA
	DUCT AVERAGE		328			340				
	STD DEV		7			9				
	COEFF OF VAR		0.021			0.026				
8/06/90	1	289	275	294	292	275	298	2.9	3.0	3.0
	2	277	259	317	277	285	317	2.5	2.1	2.9
	3	302	298	314	306	298	318	2.8	2.8	3.0
	4	298	290	314	298	301	321	3.0	3.2	3.4
	5	276	308	282	279	309	286	3.4	3.0	3.0
	6	289	284	296	289	284	299	3.2	3.3	2.8
	DUCT AVERAGE		292			296			3.0	
	STD DEV		15			14			0.3	
	COEFF OF VAR		0.051			0.046			0.103	

NOTES: Port 1 is at the top of the duct.
Point distance is from the West wall of the duct.
NO and NO_x are actual measured concentrations.

Table 5

CRIST UNIT 5 ESP INLET
LOW-LOAD NO, NO_x, AND OXYGEN DISTRIBUTIONS

		NO CONCENTRATION ppm			NO_x CONCENTRATION ppm			O_2 CONCENTRATION %		
DATE	PORT	Pt 1	Pt 2	Pt 3	Pt 1	Pt 2	Pt 3	Pt 1	Pt 2	Pt 3
7/28/90	1	390	390	380	400	390	380	NA	NA	NA
	2	380	390	380	400	400	390	NA	NA	NA
	3	380	390	380	390	400	400	NA	NA	NA
	4	380	380	380	380	400	390	NA	NA	NA
	5	380	380	380	400	390	400	NA	NA	NA
	6	380	380	390	400	400	400	NA	NA	NA
	DUCT AVERAGE		383			395				
	STD DEV		4			7				
	COEFF OF VAR		0.012			0.017				
7/29/90	1	300	300	310	320	310	310	NA	NA	NA
	2	310	310	310	320	320	320	NA	NA	NA
	3	320	310	310	340	330	330	NA	NA	NA
	4	320	320	330	350	340	340	NA	NA	NA
	5	330	310	320	360	350	350	NA	NA	NA
	6	330	330	330	360	360	360	NA	NA	NA
	DUCT AVERAGE		317			337				
	STD DEV		10			17				
	COEFF OF VAR		0.032			0.051				
8/07/90	1	245	227	224	248	227	224	7.6	7.9	7.2
	2	267	249	229	270	251	235	7.9	7.3	7.1
	3	271	264	260	279	269	261	7.6	7.7	7.5
	4	289	282	261	298	288	266	7.4	7.8	7.8
	5	283	281	275	295	288	284	7.4	7.7	7.6
	6	287	280	283	298	298	313	7.3	7.2	7.1
	DUCT AVERAGE		264			272			7.5	
	STD DEV		21			26			0.3	
	COEFF OF VAR		0.078			0.094			0.035	

NOTES: Port 1 is at the top of the duct.
Point distance is from the West wall of the duct.
NO and NO_x are dry and not corrected for constant O_2.

Table 11

CRIST UNIT 5 ESP OUTLET
HIGH-LOAD FLUE GAS OXYGEN DISTRIBUTIONS

		O_2 CONCENTRATION, %					
DATE	POINT	PORT 2	PORT 3	PORT 4	PORT 5	PORT 6	PORT 7
8/05/90	1	4.0	4.2	4.2	4.2	4.2	4.1
	2	4.0	4.1	4.1	4.4	4.4	4.2
	3	3.5	4.3	4.8	5.8	4.7	4.8
				DUCT AVERAGE		4.3	
				STD DEV		0.5	
				COEFF OF VAR		0.107	
8/06/90	1	5.0	4.8	4.9	4.9	5.0	5.2
	2	5.0	4.8	5.0	5.1	5.1	4.6
	3	4.8	4.9	5.1	5.1	5.8	5.0
				DUCT AVERAGE		5.0	
				STD DEV		0.2	
				COEFF OF VAR		0.048	

NOTES: Point 1 is at the top of the duct.
Port 1 is on the East side of the duct.
NO and NO_x are actual measured dry concentrations.

Table 12

CRIST UNIT 5 ESP OUTLET
HIGH-LOAD FLUE GAS NO_x DISTRIBUTIONS

		NO_x CONCENTRATION, ppm					
DATE	POINT	PORT 2	PORT 3	PORT 4	PORT 5	PORT 6	PORT 7
8/05/90	1	347	372	354	347	335	329
	2	356	383	358	352	338	335
	3	366	383	364	357	341	340
				DUCT AVERAGE		353	
				STD DEV		15	
				COEFF OF VAR		0.044	
8/06/90	1	316	305	284	305	311	320
	2	315	296	315	306	305	312
	3	311	300	326	313	317	327
				DUCT AVERAGE		310	
				STD DEV		10	
				COEFF OF VAR		0.033	

NOTES: Point 1 is at the top of the duct.
Port 1 is on the East side of the duct.
NO and NO_x are actual measured dry concentrations.

Table 13

CRIST UNIT 5 ESP OUTLET
HIGH-LOAD FLUE GAS NO DISTRIBUTIONS

		NO CONCENTRATION, PPM					
DATE	POINT	PORT 2	PORT 3	PORT 4	PORT 5	PORT 6	PORT 7
8/05/90	1	347	367	352	345	334	329
	2	357	382	353	351	337	334
	3	359	382	362	356	337	337
				DUCT AVERAGE		351	
				STD DEV		15	
				COEFF OF VAR		0.04	
8/06/90	1	315	301	282	303	310	315
	2	313	295	309	301	301	312
	3	310	298	324	306	313	327
				DUCT AVERAGE		307	
				STD DEV		10	
				COEFF OF VAR		0.03	

NOTES: Point 1 is at the top of the duct.
Port 1 is on the East side of the duct.
NO and NO_x are actual measured dry concentrations.

APPENDIX B

Report from Mr. Michael D. Glasscock of the University of Missouri-Columbia concerning Neutron Activation Analyses of Plant Crist Unit 5 and NIST standard coals. Four of the coal samples (CRST-10, CRST-20, CRST-30, and CRST-40) are pertinent to this report.

CRST-10: Plant Crist Unit 5 Coal (as fired) for February 10, 1993
CRST-20: Plant Crist Unit 5 Coal (as fired) for March 6, 1993
CRST-30: NIST Standard Coal No. 1630
CRST-40: NIST Standard Coal No. 1632b

UNIVERSITY OF MISSOURI-COLUMBIA

Research Reactor Cente

Research Pa
Columbia, Missouri 6521
Telephone (314) 882-42
FAX [314] 882-3
63

July 7, 1993

FAX No: 205-581-2875

Dr. Edward Dismukes
Southern Research Institute
P.O. Box 55305
Birmingham, AL 35355-5305

Dear Ed:

I have completed the INAA work on the ten samples of coal (five from SRI and five from SCS) as requested. The final results are enclosed on the accompanying table. The unknown samples were analyzed relative to my well-known standard of SRM-1633a Flyash. For quality control purposes, I also included three samples of SRM-1632a Bituminous Coal in this run. My analytical results for the latter are enclosed to demonstrate that my agreement with literature values is generally acceptable.

A bill for $1,250 will be submitted to your purchasing department on Purchase Order BH-40747.

Sincerely,

Michael D. Glascock

Michael D. Glascock

enclosures:

Table I. Concentrations of major and trace elements in coal samples for SRI and SCS (July 1993).

Ident.	Al(%)	As(ppm)	Ba(ppm)	Ca(%)	Ce(ppm)	Co(ppm)	Cr(ppm)	Cs(ppm)	Dy(ppm)	Eu(ppm)
Analysis of SCS coal samples:										
92-323	0.92	3.8	36	0.31	10.4	2.48	16.8	0.89	0.67	0.171
92-599	0.90	3.8	46	0.21	10.0	2.38	17.3	0.89	0.75	0.154
92-607	1.05	3.4	45	0.17	11.6	2.43	16.9	0.90	0.65	0.161
92-747	0.98	3.7	48	0.29	10.6	2.70	18.4	0.99	0.77	0.164
93-082	1.00	4.0	50	0.39	9.7	2.43	14.5	0.73	0.96	0.166
Analysis of SRI coal samples:										
CRST-10	0.92	1.5	27	0.30	11.4	2.92	12.7	1.01	0.87	0.201
CRST-20	0.97	4.1	41	0.22	10.3	3.26	15.0	0.89	0.83	0.193
CRST-30	0.49	16.5	44	0.20	10.3	2.99	5.9	0.46	0.69	0.186
CRST-40	0.94	3.5	63	0.18	9.0	2.11	10.6	0.42	0.66	0.157
CRST-50	< 0.06	0.1	5	< 0.04	0.1	0.40	0.6	0.59	< 0.45	0.005
Analysis of SRM-1632a bituminous coal for quality control:										
1632A (sam1)	2.84	9.3	100	0.25	30.4	6.42	33.2	2.25	1.86	0.482
1632A (sam2)	2.92	9.2	107	0.23	30.3	6.41	33.4	2.24	1.94	0.490
1632A (sam3)	2.95	9.1	107	0.22	29.3	6.41	33.4	2.22	2.04	0.483
mean	2.90	9.2	104	0.23	30.0	6.41	33.3	2.24	1.94	0.485
ref. value	2.95	9.2	120	0.24	29.0	6.70	34.0	2.30	2.06	0.520

Table I. Concentrations of major and trace elements in coal samples for SRI and SCS (July 1993).

Ident.	Fe(%)	Hf(ppm)	Hg(ppb)	K(%)	La(ppm)	Lu(ppm)	Mn(ppm)	Mo(ppm)	Na(ppm)	Nd(ppm)
Analysis of SCS coal samples:										
92-323	1.11	0.54	< 20	0.21	4.57	0.088	21.0	8.0	437	5.58
92-599	1.11	0.55	< 23	0.20	4.41	0.095	20.1	10.2	406	5.56
92-607	1.03	0.55	< 29	0.20	5.16	0.095	22.3	10.2	405	6.14
92-747	1.09	0.54	< 20	0.18	4.74	0.104	22.7	11.1	432	5.72
93-082	0.90	0.41	< 20	0.18	4.14	0.108	26.8	10.5	471	5.24
Analysis of SRI coal samples:										
CRST-10	0.72	0.44	< 30	0.17	5.09	0.084	44.4	6.5	527	6.55
CRST-20	1.25	0.47	< 24	0.16	4.63	0.101	28.8	10.0	364	5.26
CRST-30	0.54	0.26	< 31	0.12	4.92	0.054	5.1	1.7	334	6.86
CRST-40	0.73	0.44	< 20	< 0.05	4.00	0.052	12.3	1.3	488	4.79
CRST-50	0.02	0.03	< 20	0.34	0.04	0.001	46.3	< 0.1	218	< 0.13
Analysis of SRM-1632a bituminous coal for quality control:										
1632A (sam1)	1.07	1.63	116	0.40	13.47	0.161	30.3	2.6	800	15.59
1632A (sam2)	1.07	1.47	158	0.46	13.46	0.161	30.7	2.8	745	14.43
1632A (sam3)	1.07	1.47	132	0.40	13.41	0.158	30.2	2.4	783	13.55
mean	1.07	1.52	135	0.42	13.45	0.160	30.4	2.6	776	14.53
ref. value	1.11	1.62	136	0.41	15.00	0.170	29.0	3.9	828	12.00

Table I. Concentrations of major and trace elements in coal samples for SRI and SCS (July 1993).

Ident.	Ni (ppm)	Rb (ppm)	Sb (ppm)	Sc (ppm)	Se (ppm)	Sm (ppm)	Sr (ppm)	Ta (ppm)	Tb (ppm)	Th (ppm)
Analysis of SCS coal samples:										
92-323	< 13	12.4	1.00	2.21	0.67	0.86	< 17	0.14	0.13	1.42
92-599	< 13	12.6	1.35	2.13	0.71	0.90	< 17	0.10	0.11	1.46
92-607	< 13	12.9	1.05	2.14	0.72	0.89	< 16	0.13	0.14	1.49
92-747	< 13	14.5	1.08	2.28	0.77	1.02	< 16	0.14	0.13	1.56
93-082	< 11	10.1	0.70	1.91	0.79	0.98	10	0.10	0.13	1.27
Analysis of SRI coal samples:										
CRST-10	< 13	14.5	0.29	2.20	0.70	0.99	10	0.14	0.14	1.62
CRST-20	< 13	12.3	0.86	2.10	0.73	1.01	< 16	0.13	0.16	1.44
CRST-30	< 10	4.9	0.44	1.18	0.53	0.80	50	0.06	0.12	0.92
CRST-40	< 11	5.3	0.22	1.89	0.47	0.73	123	0.13	0.11	1.25
CRST-50	< 3	12.9	0.03	0.07	< 0.10	0.01	12	< 0.01	< 0.01	< 0.01
Analysis of SRM-1632a bituminous coal for quality control:										
1632A (sam1)	< 23	26.9	0.57	5.98	1.45	2.30	90	0.40	0.34	4.26
1632A (sam2)	< 21	27.4	0.54	5.98	1.42	2.30	89	0.39	0.36	4.24
1632A (sam3)	< 20	26.7	0.57	5.93	1.54	2.29	60	0.40	0.35	4.16
mean	< 21	27.0	0.56	5.96	1.47	2.30	80	0.40	0.35	4.22
ref. value	19	30.0	0.60	6.30	2.70	2.40	85	0.42	0.31	4.50

Table I. Concentrations of major and trace elements in coal samples for SRI and SCS (July 1993).

Ident.	Ti(%)	U(ppm)	V(ppm)	Yb(ppm)	Zn(ppm)	Zr(ppm)
Analysis of SCS coal analysis:						
92-323	0.056	1.96	52	0.43	30	27
92-599	0.061	2.47	75	0.42	46	29
92-607	0.056	2.65	59	0.48	34	29
92-747	0.068	3.24	61	0.45	36	35
93-082	0.062	4.12	47	0.47	38	34
Analysis of SRI coal analysis:						
CRST-10	0.034	1.92	27	0.51	22	17
CRST-20	0.054	3.67	33	0.50	28	36
CRST-30	0.024	0.68	11	0.40	5	8
CRST-40	0.047	0.43	13	0.37	12	19
CRST-50	< 0.030	< 0.01	< 3	0.01	2	< 3
Analysis of SRM-1632a bituminous coal for quality control:						
1632A (sam1)	0.154	1.50	46	1.19	27	41
1632A (sam2)	0.154	1.46	44	1.21	28	64
1632A (sam3)	0.168	1.38	42	1.24	30	46
mean	0.159	1.45	44	1.21	28	50
ref. value	0.163	1.26	44	1.08	27	53

Table 25. Concentrations in the National Bureau of Standards SRM-1632a Bituminous Coal

Element	Units	NBS (mean & s.d.)	Literature (mean & s.d.)
Ag	(ppb)	---	(300)
Al	(%)	(3.07)	2.95 ± 0.10
As	(ppm)	9.3 ± 1.0	9.2 ± 0.5
Au	(ppb)	---	(3)
B	(ppm)	---	53 ± 2
Ba	(ppm)	---	120 ± 15
Br	(ppm)	---	41 ± 2
C	(%)	---	64.4 ± 3.9
Ca	(ppm)	---	2410 ± 170
Cd	(ppb)	170 ± 20	178 ± 23
Ce	(ppm)	(30)	29 ± 2
Cl	(ppm)	---	756 ± 30
Co	(ppm)	(6.8)	6.7 ± 0.4
Cr	(ppm)	34.3 ± 1.5	34 ± 2
Cs	(ppm)	(2.4)	2.3 ± 0.2
Cu	(ppm)	16.5 ± 1.0	15.9 ± 0.8
Dy	(ppm)	---	2.06 ± 0.14
Er	(ppm)	---	(0.91)
Eu	(ppb)	(540)	520 ± 40
F	(ppm)	---	160 ± 50
Fe	(%)	1.11 ± 0.02	1.11 ± 0.03
Ga	(ppm)	(8.49)	8.0 ± 0.4
Gd	(ppm)	---	2.6 ± 0.6
Ge	(ppm)	---	(2.5)
H	(%)	---	4.1 ± 0.4
Hf	(ppm)	(1.6)	1.62 ± 0.15
Hg	(ppb)	130 ± 30	136 ± 19
Ho	(ppb)	---	(360)
I	(ppm)	---	1.80 ± 0.15
In	(ppb)	---	38 ± 2
K	(ppm)	---	4110 ± 200
La	(ppm)	---	15 ± 2
Li	(ppm)	---	39 ± 6
Lu	(ppb)	---	170 ± 15
Mg	(ppm)	---	1150 ± 225
Mn	(ppm)	28 ± 2	29 ± 2
Mo	(ppm)	---	(3.85)
N	(%)	---	1.25 ± 0.04
Na	(ppm)	---	828 ± 77
Nb	(ppm)	---	(4.0)

Table 25. Concentrations in the National Bureau of Standards SRM-1632a Bituminous Coal (continued)

Element	Units	NBS (mean & s.d.)	Literature (mean & s.d.)
Nd	(ppm)	---	12 ± 2
Ni	(ppm)	19.4 ± 1.0	18.5 ± 2.0
O	(%)	---	18.8 ± 0.8
P	(ppm)	---	250 ± 40
Pb	(ppm)	12.4 ± 0.6	12.2 ± 1.4
Pr	(ppm)	---	(3.2)
Rb	(ppm)	(31)	30 ± 2
S	(%)	(1.64)	1.55 ± 0.05
Sb	(ppb)	(580)	600 ± 45
Sc	(ppm)	(6.3)	6.3 ± 0.3
Se	(ppm)	2.6 ± 0.7	2.7 ± 0.2
Si	(%)	---	5.87 ± 0.22
Sm	(ppm)	---	2.4 ± 0.3
Sn	(ppm)	---	4 ± 4
Sr	(ppm)	---	85 ± 6
Ta	(ppb)	---	420 ± 40
Tb	(ppb)	---	311 ± 17
Te	(ppb)	---	(500)
Th	(ppm)	4.5 ± 0.1	4.5 ± 0.2
Ti	(ppm)	(1750)	1630 ± 130
Tl	(ppm)	---	< 1
Tm	(ppb)	---	(390)
U	(ppm)	1.28 ± 0.02	1.26 ± 0.08
V	(ppm)	44 ± 3	44 ± 2
W	(ppb)	---	880 ± 90
Y	(ppm)	---	9.2 ± 0.8
Yb	(ppm)	---	1.08 ± 0.09
Zn	(ppm)	28 ± 2	27.2 ± 1.4
Zr	(ppm)	---	53 ± 5

Literature Reference(s): Gladney et al. (1987)

APPENDIX C [1]

TRACE METAL CONCENTRATION

Trace metal concentrations were measured at the Unit 5 hot-side ESP inlet (high and low load), at the reactor A inlet (high and low load), at the Unit 5 hot-side ESP outlet (high load only) and at the economizer bypass duct (low load only). For collecting trace metals, the U.S. EPA has sanctioned the use of a Method 5 filtration device and back-up impingers - two filled with nitric acid and hydrogen peroxide and two filled with potassium permanganate and sulfuric acid. This test method is commonly referred to as Method 29 - Determination of Metals Emissions from Stationary Sources. This is a proposed method and has not been formally promulgated. We used Method 29 to collect samples at the locations described above. The combination of a particulate filter and the back-up impingers provides a convenient way to collect the trace elements in fly ash and flue gas that are of paramount concern. The trace elements that occur as components of the fly ash are collected on the filter, except for the fractions of certain metals (such as arsenic and selenium) that may occur partly in the vapor state. These partly volatile metals are collected in the HNO_3/H_2O_2 impingers. Mercury is usually completely in the vapor state at temperatures above 300°F and is collected both in the HNO_3/H_2O_2 and $KMnO_4/H_2SO_4$ impingers.

Analysis was performed separately on the fly ash (front end) and impinger (back end) samples. The ash was dissolved completely in concentrated mineral acids and the screening analysis was performed by Inductively Coupled Argon Plasma Emission Spectroscopy (ICAP). ICAP required auxiliary determination of arsenic and selenium by atomic absorption with the elements converted to hydrides for improved sensitivity. Cold vapor atomic absorption was used for mercury determination.

The concentrations of the following elements were determined with Method 29: antimony (Sb), arsenic (As), barium (Ba), beryllium (Be), cadmium (Cd), cesium (Cs), chromium (Cr), cobalt (Co), copper (Cu), lead (Pb), manganese (Mn), mercury (Hg), molybdenum (Mo), nickel (Ni), rubidium (Rb), selenium (Se), strontium (Sr), tin (Sn), vanadium (V), and zinc (Zn). Analysis of the Method 29 samples was conducted at SRI laboratories in Birmingham.

Finally, trace element concentrations were determined for size segregated fly ash samples collected at the Unit 5 hot-side ESP inlet at high and low load. The samples were collected using a five-stage series cyclone sampling system. These ash samples were analyzed by ICAP in our Birmingham laboratory.

Additional tests for mercury (elemental) were performed with iodated carbon mercury vapor traps. Tests were conducted at the Unit 5 hot-side ESP inlet (high and low load), reactor A inlet (high and low load), the Unit 5 hot-side ESP outlet (high and low load) and the economizer bypass duct (low load only). These traps were analyzed by Brooks Rand, Ltd. of Seattle, Washington.

Trace Elements Determined By Method 29 and Series Cyclones

The concentrations of metal species determined by the Method 29 Multiple Metals Train are presented in Tables 7-1, 7-2, and 7-3. Table 7-1 gives the metal concentrations as weight fractions (ug/g) of the total solids collected in the probe and on the filter (front half). Table 7-2 presents cumulative data for the metal concentrations in the front half and in the impingers (back half), also as weight fractions (ug/g) of the total solids. Table 7-2 reflects differences from Table 7-1 due only to the amounts of some elements that were in the vapor state. The third table, Table 7-3, expresses the total of each element (front and back halves) as a concentration in the gas stream (ug/Nm^3); it also includes values for total solids in the gas stream (last line of the table). The right-hand column in each table shows the average and the standard deviation of all of the tests, except the one at the ESP outlet at high load (next to last column). To calculate averages when data are reported only as upper limits, the true value was assumed to be half the limit.

As a first approximation, all of the runs except that at the ESP outlet at high load were expected to show the same metal concentrations in either ug/g or ug/Nm^3. All tests except that at the ESP outlet were made at sampling locations that were uneffected by the ESP (ESP inlet, Reactor A inlet, and economizer bypass). Conceivably, stratification of the gas and particulate matter could have made compositions different at these three sampling locations. Also, differences could be attributed to the different dates when the tests were performed and the differences in boiler load during each test. Nevertheless, any variations at these locations would have been expected to be relatively subtle. (No significant effect is evident between high and low load at the same sampling location.) The ESP outlet data, however, are very different from all of the other data. The test results show much higher values on a ug/g basis as a general rule. This is expected, since the outlet dust is finer in particle size and contains a higher concentration of any metal that at some time existed as a vapor that underwent condensation or adsorption onto existing particle nuclei. On a ug/Nm^3 basis, however, Table 7-3 shows much lower values for the ESP outlet since most of any metal not in the vapor state has been collected in the ESP.

Table 7-4 compares data precision for all runs except the test at the ESP outlet on the basis of concentrations as ug/g and ug/Nm^3. The comparison suggests that variability was due more to imprecision in analyses than to imprecision in the determination of total particulate concentrations, although there was considerable variation in the latter.

Tables 7-5 and 7-6 present the metal concentrations in the dust fractions obtained from the five-stage series cyclone at high and low load, respectively. The tables show the cut points for each stage and give the percentage of the total mass on each stage. By use of the metal concentrations and the weight percentages on each stage, it is possible to calculate the apparent metal concentration in the total ash sample. The results of these calculations are given in the final column in each table.

The data in Tables 7-5 and 7-6 suggest that increasing concentration of an element in the solid (ug/g) as particle size decreases is more the rule than the exception. There were very few elements where this did not occur. It suggests that nearly all of the elements, if not exactly all, were in the vapor state at some time in the time-temperature history of the flue

Table 7-1. Volatile Metals Concentrations (µg/g)
Multiple Metals Trains (Front Half Only)

	ESP inlet 2/9/93 High load Run 1	A inlet 3/6/93 High load Run 7	ESP inlet 2/11/93 Low load Run 5	ESP inlet 2/11/93 Low load Run 6	A inlet 3/6/93 Low load Run 9	Econ.B.P. 3/6/93 Low Load Run 10	ESP outlet 2/9/93 High load Run 3	Avg. ± s.d. except Run 3
Sb	9	6.1	2.9	<3.6	8.3	<3.8	<180.0	5.0± 3.2
As	139	51.3	69.7	97.9	47.2	38.5	110	73.9± 38.2
Ba	298	302	377	563	259	261	339	343.0±116.0
Be	11.3	9.6	14.5	21	10.3	9	<35.0	12.6± 4.5
Cd	5.9	4.6	10.3	20	7.2	55.4	39.1	17.2± 19.5
Cs	85.5	72.9	74.6	<80.0	69.9	<76.0	<3500.0	63.5± 19.7
Cr	124	132	148	152	124	125	241	134.0± 13.0
Co	23	27.4	30.6	30.7	22.8	22.8	<70.0	26.2± 3.9
Cu	71.6	66.2	86.4	93.2	65.4	63	215	74.3± 12.5
Pb	221	227	286	404	239	223	426	267.0± 72.0
Mn	152	225	172	174	169	163	226	176.0±25.0
Hg	0.35	0.12	0.13	0.21	0.18	3.6	<7.0	0.76± 1.39
Mo	72.9	82.6	77	85.7	74.6	88.5	880	80.2± 6.3
Ni	86.5	100	104	106	89.5	87.3	<180.0	95.5± 8.8
Rb	134	132	126	125	123	119	<1800.0	126.0± 6.0
Se	99.3	1.37	8.02	13.7	7.1	9.9	514	23.2± 37.4
Sr	186	188	237	252	175	172	228	202.0± 34.0
Sn	26.8	21.5	27.6	22.7	20	19.2	<180.0	23.0± 3.5
V	683	467	458	428	531	565	577	522.0± 94.0
Zn	311	436	647	1118	353	336	3320	534.0±311.0

Table 7-2. Volatile Metals Concentrations (µg/g) Multiple Metals Trains (Front Half plus Back Half)

	ESP inlet 2/9/93 High load Run 1	A inlet 3/6/93 High load Run 7	ESP inlet 2/11/93 Low load Run 5	ESP inlet 2/11/93 Low load Run 6	A inlet 3/6/93 Low load Run 9	Econ.B.P. 3/6/93 Low Load Run 10	ESP outlet 2/9/93 High load Run 3	avg.±s.d. except Run 3
Sb	9	6.1	2.9	<3.6	8.3	<3.8	<180.0	5.0±3.2
As	141	51.7	69.7	98.6	49	39.2	154	74.9±38.6
Ba	298	303	377	563	264	261	339	344±115
Be	11.3	9.6	14.5	21	10.3	9	<35.0	12.6± 4.5
Cd	6.1	4.6	10.4	20.2	7.4	55.4	356	17.4±19.5
Cs	85.5	72.9	74.6	<80.0	69.9	<76.0	<3500.0	63.5±19.7
Cr	124	132	148	153	126	125	310	135± 3
Co	23	27.4	30.6	30.7	23.3	22.8	<70.0	26.3±3.8
Cu	71.8	66.7	86.6	93.5	67.4	63.8	286	75.0±12.2
Pb	221	227	286	404	239	223	426	267± 72
Mn	152	226	172	174	174	164	226	177± 25
Hg	1.41	1.4	0.74	1.53	2.38	2.58	285	1.67±0.69
Mo	72.9	83	77	85.7	76.9	88.5	880	80.7± 6.0
Ni	86.8	100	104	106	91.8	87.3	<180.0	96.0± 8.5
Rb	134	132	126	125	123	119	<1800.0	126± 6
Se	102.6	3.41	10.1	15.8	9	13.6	197.5	25.8±37.9
Sr	186	189	237	252	177	172	228	202± 34
Sn	30.7	40.6	31.1	27.7	25.3	23.5	<180.0	29.8± 6.0
V	683	468	458	428	544	565	577	524± 94
Zn	314	439	648	1120	362	337	3545	537±311

Table 7-3. Volatile Metals Concentrations (µg/Nm3) Multiple Metals Trains (Front Half plus Back Half) Solids Concentrations (g/Mn3)

	ESP inlet 2/9/93 High load Run 1	A inlet 3/6/93 High load Run 7	ESP inlet 2/11/93 Low load Run 5	ESP outlet 2/11/93 Low load Run 6	A inlet 3/6/93 Low load Run 9	Econ. B.P. 3/6/93 Low Load Run 10	ESP outlet 2/9/93 High load Run 3	avg.±s.d. except Run 3
Sb	71.2	68	32.3	<23.0	80	<36.0	<4.0	34.5±20.9
As	1120	574	768	640	473	375	3.98	658±264
Ba	2370	3360	4150	3650	2550	2500	7.72	3100±730
Be	89.8	106	160	136	98.9	86	<0.8	113± 29
Cd	48.7	50.5	115	131	69.9	530	9.24	158±186
Cs	680	810	822	<460.0	674	<730.0	<80.0	597±244
Cr	989	1470	1640	988	1220	1200	5.48	1250±260
Co	183	304	337	199	182	219	<1.6	237± 67
Cu	571	741	954	606	650	611	6.5	689±142
Pb	1760	2530	3160	2620	2300	2130	9.7	2420±480
Mn	1210	2500	1890	1130	1670	1566	5.16	1660±500
Hg	11.2	15.6	8.2	10.2	22.9	24.7	6.48	15.5± 6.9
Mo	580	922	858	555	730	848	20	749±154
Ni	690	1120	1150	687	886	836	<4.0	895±202
Rb	1070	1460	1380	809	1190	1140	<40.0	1170±230
Se	816	37.9	112	103	86.4	130	45	214±296
Sr	1480	2100	2607	1630	1710	1650	5.2	1860±420
Sn	244	451	343	179	244	225	24.1	281±99
V	5430	5200	5050	2770	5250	5410	13.1	4850±1030
Zn	2500	4870	7140	7240	3490	3230	80.7	4740±2040
Solids	7.952	11.111	11.019	6.48	9.646	9.576	0.0228	9.297±1.800

Table 7-4. Data Precision for Metals Concentration

	Relative std. dev (%)	
	Table 7-2 (µg/g)	Table 7-3 (µg/Nm3)
Sb	64	60
As	52	40
Ba	33	24
Be	36	26
Cd	112	118
Cs	31	41
Cr	2	21
Co	14	28
Cu	16	21
Pb	27	20
Mn	14	31
Hg	50	45
Mo	7	21
Ni	9	23
Rb	5	20
Se	147	138
Sr	17	23
Sn	20	5
V	18	21
Zn	58	43

Table 7-5. Particle Size Dependent Concentrations (µg/g) (High Load)

Stage	1	2	3	4	5	ALL
cut point, µm	5.5	2.3	1.8	1.2	0.43	
% of mass	62.3	29.8	6.4	1.19	0.3	100
Sb	40.9	44.5	92	173	24	46.8
As	8.84	26.6	22.2	42.7	38.2	15.5
Ba	496	420	669	917	1484	492
Be	15.1	20.4	33	41.4	59.3	18.3
Cd	7.37	11.1	37	59.9	153	11.5
Cs	no data available					
Cr	148	195	312	412	606	177
Co	23.9	24.8	37.7	36.9	33.1	25.2
Cu	68.7	89.8	147	175	212	81.7
Pb	212	473	1060	1378	1703	363
Mn	170	127	200	260	375	363
Hg	no data available					
Mo	50.8	122	222	287	286	86.5
Ni	98.9	121	206	274	461	116
Rb	111	114	137	<398	<1400	<121
Se	1.04	1.2	1.33	<4.98	<20	<1.21
Sr	198	199	293	339	412	207
Sn	10.1	15.7	14.5	<5	<5	<12.0
V	565	577	1024	1451	1856	612
Zn	372	797	1950	2825	6116	646

Table 7-6. Particle Size Dependent Concentrations (µg/g) (Low Load)

Stage	1	2	3	4	5	ALL
cut point, µm	5.5	3.5	1.9	1.26	0.47	
% of mass	69.3	17	10.1	2.8	0.85	100
Sb	<1.0	<1.0	<2.0	<6.0	<25.0	na
As	1.97	0.87	6.45	7.44	62.1	2.9
Ba	340	418	504	531	670	378.1
Be	11.1	18.3	23.9	27.4	32.5	14.3
Cd	13.2	9.48	14.3	20.4	29.4	13.0
Cs	115	529	475	1378	6600	312.3
Cr	168	324	253	323	337	209.0
Co	27.6	36.5	47	59.7	<100	<32.6
Cu	68.2	107	144	198	264	87.8
Pb	78.4	218	356	426	462	143.2
Mn	195	181	211	257	346	197.4
Hg	<0.2	<0.4	<0.7	<2.5	<10.0	na
Mo	176	379	559	703	761	269.0
Ni	103	193	196	280	341	134.7
Rb	122	144	167	<221	<985	<140
Se	0.74	1.08	<2.0	<6.0	<25.0	<1.28
Sr	245	291	272	348	392	259.8
Sn	19.6	20.4	26.6	<60	<250	<23.5
V	434	492	628	801	1067	479.3
Zn	246	624	1016	1350	2830	441.0

gas and became enriched more in the small particles than the larger ones, because of the greater ratios of surface area to mass in the smaller particles. This explanation, however, is contrary to the widely held belief that some metals partition evenly between bottom ash and fly ash and are not volatile. Therefore, some alternative explanation - perhaps problems in analysis or better digestion of small particles - accounts for some of the apparent trends. We are continuing our analysis of these data.

Two of the metals shown in Tables 7-5 and 7-6, mercury and selenium, are volatile. This fact may account for the relatively poor concentrations of these metals. The concentrations of some metals appear to increase with decreasing particle size even though the data given are only limits. Limits that increase in magnitude as particle size decreases do not imply that actual concentrations increase; they merely signify that the sample amount decreases with particle size and thus the detection limit increases.

There are some differences between the high-load and low-load data in Tables 7-5 and 7-6 that are difficult to associate with just the difference in load conditions. For example, Sb, As, Pb, and Mn appear at higher concentrations in the high-load samples, and Mo was high at low load. Conceivably, there was a change in coal composition accounting for these differences, but there may have been unknown problems in the analytical laboratory that account for the differences.

Table 7-7 compares specific concentrations in the solids (concentrations on the ug/g basis) for samples from the Method 29 Multiple Metals Train and samples from the cyclones (high load only). The data for the metals train are from Table 7-1, Column 9. The data for the cyclones are from Table 7-5, Column 7. There are outstanding differences for four elements: Sb, As, Se, and Sn. The first three of these are known to be relatively volatile. As and Se follow a logical pattern; they are more concentrated in the solids collected on the filter of the metals train (at 250°F) than they are in the solids collected in the cyclones (at temperatures exceeding 600 - 700°F). In other words, they show evidence of having been absorbed at the lower collection temperature. Sb seems not to have followed this pattern. Sn shows evidence of being relatively volatile. Sn, like As and Se, appears to have been removed from the vapor state in the filtration step.

Table 7-8 attempts to show the proportions of the elements in the particulate and vapor states as they existed in the Method 29 Multiple Metals Train. This table lists the ratios of front-half-only concentrations (Table 7-1, Column 9) to front-and-back-half concentrations (Table 7-2, Column 9). Most of the ratios are close to unity. The major exceptions occur with Hg (R = 0.455), Se (R = 0.899), and Sn (R = 0.772). These are all elements with expected or suspected volatility. As is not in the group, but As has shown evidence in the past of not being volatile in the sampling train (lower temperatures).

Table 7-9 lists ratios of ESP outlet concentrations to ESP inlet concentrations (in ug/g, the single ESP outlet test compared to the average of the other tests). The smaller the ratio the more the element is indicated as a matrix element with low volatility. All of the elements with ratios below 2 are plausible as matrix elements; the element with the highest ratio, Hg, is the one expected to be the most volatile. Some of the other elements seem misplaced; for

Table 7-7. Comparison of Specific Concentrations (µg/g) in Particulate From Metals Trains and Cyclones

	Metals train Table 7-1, Column 9	Cyclones Table 7-5, Column 7
Sb	5	46.8
As	73.9	15.5
Ba	343	492
Be	12.6	18.3
Cd	17.2	11.5
Cs	63.5	(no data)
Cr	134	177
Co	26.2	25.2
Cu	74.3	81.7
Pb	267	363
Mn	176	161
Hg	(disregard)	(no data)
Mo	80.2	86.5
Ni	95.5	116
Rb	126	<121
Se	23.2	<1.21
Sr	202	207
Sn	23	<12.0
V	522	612
Zn	534	646

Table 7-8. Ratios of ESP Inlet Front-Half Concentrations to Total Concentrations (Front and Back Halves) Data from Tables 7-1 and 7- 2, Column 9 in each

	Ratio
Sb	1.000
As	0.987
Ba	0.997
Be	1.000
Cd	0.989
Cs	1.000
Cr	0.993
Co	0.996
Cu	0.991
Pb	1.000
Mn	0.994
Hg	0.455
Mo	0.993
Ni	0.994
Rb	1.000
Se	0.899
Sr	1.000
Sn	0.772
V	0.996
Zn	1.000

Table 7-9. Ratios of ESP Outlet Concentration to Average ESP Inlet Concentrations
Data from Table 7-2, Columns 3 and 9

	R<2	R<5	R<10	R<100	R<1000
Sb				<36	
As		2.06			
Ba	0.985				
Be		<2.78			
Cd				20.5	
Cs				<55.1	
Cr		2.3			
Co		<2.66			
Cu		3.81			
Pb	1.6				
Mn	1.28				
Hg					171
Mo				10.9	
Ni	<1.88				
Rb				<14.3	
Se			7.66		
Sr	1.13				
Sn			6.04		
V	1.1				
Zn			6.6		

example, Zn seems to be in the wrong place in the company with Se and Sn. Cd and Mo give evidence of being relatively volatile, although we would not expect this.

Mercury Concentrations (Elemental) Determined From Iodated Carbon Traps

The concentration of elemental mercury in the flue gas at the Plant Crist SCR Test Facility was also measured by sampling flue gas through iodated carbon mercury vapor traps. Tests were performed at both the Plant Crist Unit 5 hot-side ESP inlet and outlet ducts at high and low load conditions. Tests were also performed at the Reactor A inlet at high and low load and in the economizer bypass duct at low load conditions. For the purpose of material balance calculations, both Plant Crist Unit 5 and NIST certified coal samples were submitted for determination of elemental mercury concentration. The carbon traps and coal samples were analyzed by Brooks Rand, Ltd. of Seattle, WA. The test results are summarized in Table 7-10.

The mercury concentration in each trap was measured and reported at nanograms per trap. Based on the volume of flue gas sampled through each trap, we calculated the mercury concentration in the flue gas as nanograms per standard dry liter corrected to 3% oxygen. The values generally fell in the range of 9 to 14 nanograms per liter. In two cases (CRST-Hg-2 and CRST-Hg-7) Brooks Rand performed triplicate analyses to provide a level of quality assurance. For CRST-Hg-2 the relative standard deviation (rsd) was 2% and for CRST-Hg-7 the rsd was 5%. Another quality assurance test was to spike blank samples with a known quantity of mercury. (For each test two iodated carbon traps are run in series. The second trap is analyzed and treated as a blank. The murcury concentration measured in the blank trap is then used to adjust the concentration measured in the first trap. Generally the blank mercury concentration averages approximately 1 nanogram per trap.) Mercury spiking was done on two samples, CRST-Hg-3 and CRST-Hg-7. The recovery was 102% and 91%, respectively.

Two coal samples were submitted for analysis. Brooks Rand, as part of their normal service, also tested NIST certified coal samples. The NIST certified value is 0.13 ug/g. In both cases this value was recovered. The mercury concentration in the Plant Crist coal samples differed significantly between the two dates, 0.11 ug/g for 2/10/93 and 0.081 ug/g for 3/6/93. A triplicate of tests was performed on the 3/6/93 sample. The rsd was 4%. Using the mercury concentration values for the coal, the approximate coal feed rate for Unit 5 at high and low load conditions, and the measured flue gas flow rate at the hot-side ESP inlet (the number was doubled to account for the two inlet ducts), the predicted mercury vapor concentration in the flue gas was calculated. The values, ranging from 9.7 to 14.6 nanograms per dry standard liter @ 3% oxygen, agree well with the range of values measured by the iodated carbon mercury vapor traps (9.2 to 14.1 nanograms per dry standard liter @ 3% oxygen).

Table 7-10. Mercury (Elemental) Concentrations Determined from Iodated Carbon Traps

Sample ID #	Date	Location	Load	Hg Concentration (nanograms/trap)	Flue Gas Temperature (F)	Flue Gas Sampled St. Dry Liters @ 3%O2	Hg Concentration in Flue Gas (nanograms/liter) St. Dry Liters @ 3% O2	Comments
Iodated Carbon Traps								
CRST-Hg-2	2/9/93	ESP Inlet	High	220 + 4.4	663	24.0	9.2	A
CRST-Hg-3	2/10/93	ESP Outlet	High	224	620	20.4	11.0	
CRST-Hg-4	2/10/93	ESP Outlet	Low	140	544	20.3	6.9	
CRST-Hg-6	2/11/93	ESP Inlet	Low	308	598	21.8	14.1	
CRST-Hg-7	3/6/93	Reac. A Inlet	High	265 + 13.3	733	21.6	12.3	A
CRST-Hg-8	3/6/93	Reac. A Outlet	Low	187	738	16.6	11.3	
CRST-Hg-9	3/6/93	Econ. Bypass	Low	149	870	15.0	9.9	
Coal Samples								
				(micrograms/gram)				
Crist Unit 5	2/10/93			0.11				
NIST-1630 Coal				0.13				B
Crist Unit 5	3/6/93			0.081 + 0.0032				A
NIST-1630 Coal				0.13				B
Predicted Mercury Vapor Concentration in Flue Gas								
	2/10/93		High				14.6	C
	2/10/93		Low				13.2	C
	3/6/93		High				10.8	C
	3/6/93		Low				9.7	C

A: Test performed 3 times to provide level of uncertainty

B: NIST-1630 certified value is 0.13 micrograms per gram

C: Based on coal feed rate (42 tons/h @ high load & 20 tons/h @ low load) and measured flue gas flow rate at Unit 5 hot-side ESP inlet